THE UNIVERSITY OF OKLAHOMA

GRADUATE COLLEGE

LOCALIZED FAILURES OF ARCHITECTURAL SANDWICH COLUMNS HAVING FOAMED-PLASTIC CORES

A DISSERTATION

SUBMITTED TO THE GRADUATE FACULTY

in partial fulfillment of the requirements for the

degree of

DOCTOR OF ENGINEERING

BY

BILLY JOE HARRIS

Norman, Oklahoma

1967

LOCALIZED FAILURES OF ARCHITECTURAL SANDWICH COLUMNS

HAVING FOAMED-PLASTIC CORES

APPROVED BY

[illegible]

[illegible]

Charles W. Bert

Fulton K. Fears

[illegible]

DISSERTATION COMMITTEE

ACKNOWLEDGMENTS

The author wishes to express his appreciation to Dr. Gene M. Nordby for his guidance during this program in which he served as major professor. Thanks also go to Dr. Charles W. Bert, III, and to W. C. Crisman for their assistance and counsel which were extended on many occasions.

Thanks must also go to several authorities in other research organizations who contributed invaluable suggestions and technical information. These include David Countryman of The American Plywood Association, Donald G. Masterson of Plywood Fabricators Service, Edward W. Kuenzi of Forest Products Laboratory, A. I. Poms of Koppers Company, and Howard A. Spalt of Masonite Corporation.

Appreciation is extended to the companies that generously supplied most of the materials required in this research. Dow Chemical Company contributed all of the required Styrofoam and Dorvon plastic foams, Masonite Corporation contributed pressedwoods, and Koppers Company fabricated and contributed special Dylite sandwich panels.

TABLE OF CONTENTS

LIST OF TABLES

LIST OF ILLUSTRATIONS

Figure		Page

LIST OF SYMBOLS AND NOMENCLATURE

A = Total amplitude, $A_b + A_o$, in.

A_c = Effective core shear area, in^2.

A_b = Maximum amplitude of additional bending displacements, in.

A_o = Maximum amplitude of initial displacements, in.

a = Midspan amplitude, in.

B = Depth of marginal zone, in.

C = Integration constant, also Euler column constant for given end conditions.

C_f = Shear strain energy form factor.

C_Δ = General representation of core shear coefficient.

Ca = Core shear coefficient for bowing.

C_δ = Core shear coefficient for end displacement.

C_e = Core shear coefficient for eccentric loads.

d = Column end displacement, in.

E = Bending modulus, psi.

E_c = Core extensional modulus, psi.

E_f = Facing bending modulus, psi.

e = Load eccentricity, in.

F = Core strength, psi.

F_e = Smallest of core compression, core tension, or bond strength, psi.

F_s = Core shear strength, psi.

f = Facing compressive stress, psi.

G_c = Average core shear modulus, psi.

I = Moment of inertia about neutral axis, in.^{4}

I_b = Moment of inertia of the facings taken about the sandwich elastic axis, in^4.

I_f = Moment of inertia of facing about its own center, in^4.

k = Linear spring constant, psi; also used as buckling parameter.

L, ℓ = Column length; also wave length, in.

L_{cr} = Critical buckling wave length, in.

$M, M(x)$ = Bending moment, in-lb.

N = Shearing force normal to the deflected axis, lb.

n = Integer, 1,2,3,...

P = Axial compressive load, lb.

P_b = Axial compressive buckling load, lb.

P_{cr} = Critical buckling load, lb.

P_e = Euler buckling load, lb.

P_s = Engesser buckling load, lb.

p = Facing compressive stress, psi.

p_{cr} = Critical facing stress, psi.

Q = Shearing force component normal to the deflected axis under exact shear deformations, lbs.

$q, q(x)$ = Local beam lateral load, lb/in.

t_c = Core thickness, in.

t_f = Facing thickness, in.

U = Total strain energy, in-lb.

U_b = Bending strain energy, in-lb.

U_c = Total core strain energy, in-lb.

U_e = Extensional strain energy, in-lb.

U_k = Energy stored in deflected spring, in-lb.

U_γ = Shear strain energy, in-lb.

u = Displacement in longitudinal x direction, in.

V,V(x) = Transverse shear force normal to x axis, lb.

W = External work, in-lb.

w = Displacement of facing in normal y direction, in.

w_b = Additional displacement of facing due to bending, in.

w_o = Initial displacement of facing, in.

x = Longitudinal coordinate, in.

y = Normal coordinate; also beam deflection, in.

z = Lateral coordinate, in.

α = Wrinkling parameter.

δ = Deflection, in.

ϵ_y = Normal core extensional strain, in/in.

γ = Core shearing strain, in/in.

θ = Angle between the initial normal to the beam axis and the normal to the deflected axis when load is applied, rad.

Subscripts:

c = Core, also complimentary solution.

L = Left face of deformed element.

o = Initial condition.

p = Particular solution.

R = Right face of deformed element.

LOCALIZED FAILURES OF ARCHITECTURAL SANDWICH COLUMNS HAVING FOAMED-PLASTIC CORES

CHAPTER I

INTRODUCTION

Sandwich type structural components are making a major impact upon building construction. In the words of Dr. A. G. H. Dietz,[1] Professor of Building Engineering, M.I.T., "Sandwich construction has become so widespread in building, and its development is being pressed hard by so many diverse organizations that it is difficult to keep in touch with current progress."

A. Sandwich Definition

A structural sandwich is a layered construction formed by bonding two thin facings to a thick core. The basic concept is to space the strong, thin facings far enough apart with a thick core to assure that the construction will have adequate bending stiffness, will provide a core that is strong enough to hold the facings flat through a bonding medium such as an adhesive layer, and which also has sufficient shear resistance. The structural sandwich is analogous to an I-beam, with the facings carrying direct compression and tension loads, as do

I-beam flanges, and the core carrying shear loads, as does the I-beam web.[2]

To clarify the meaning of a structural sandwich, the American Society for Testing Materials adopted the following standard definition:[3] "Structural Sandwich Construction: A laminar construction comprising a combination of alternative dissimilar simple or composite materials assembled and intimately fixed in relation to each other so as to use the properties of each to attain specific structural advantages for the whole assembly."

A typical load bearing sandwich wall panel is illustrated in Figure 1-1.

B. Application of Sandwich Construction

Sandwich construction has been pioneered primarily by the aircraft industry with the first extensive application of sandwich materials being in British aircraft in World War II. In the post World War II period was witnessed the first serious entry of sandwich construction into architectural applications. The structural efficiency and consequently the potential economy of sandwich structures has attracted the attention of the prefabricated house industry. Fabricating problems caused temporary obstacles to the development of architectural sandwich panels but these growing pains are quickly disappearing as the technology improves and the volume of sales increases.

Recent applications of structural sandwiches have been mostly in roof and floor panels under bending loads. Increasing numbers of

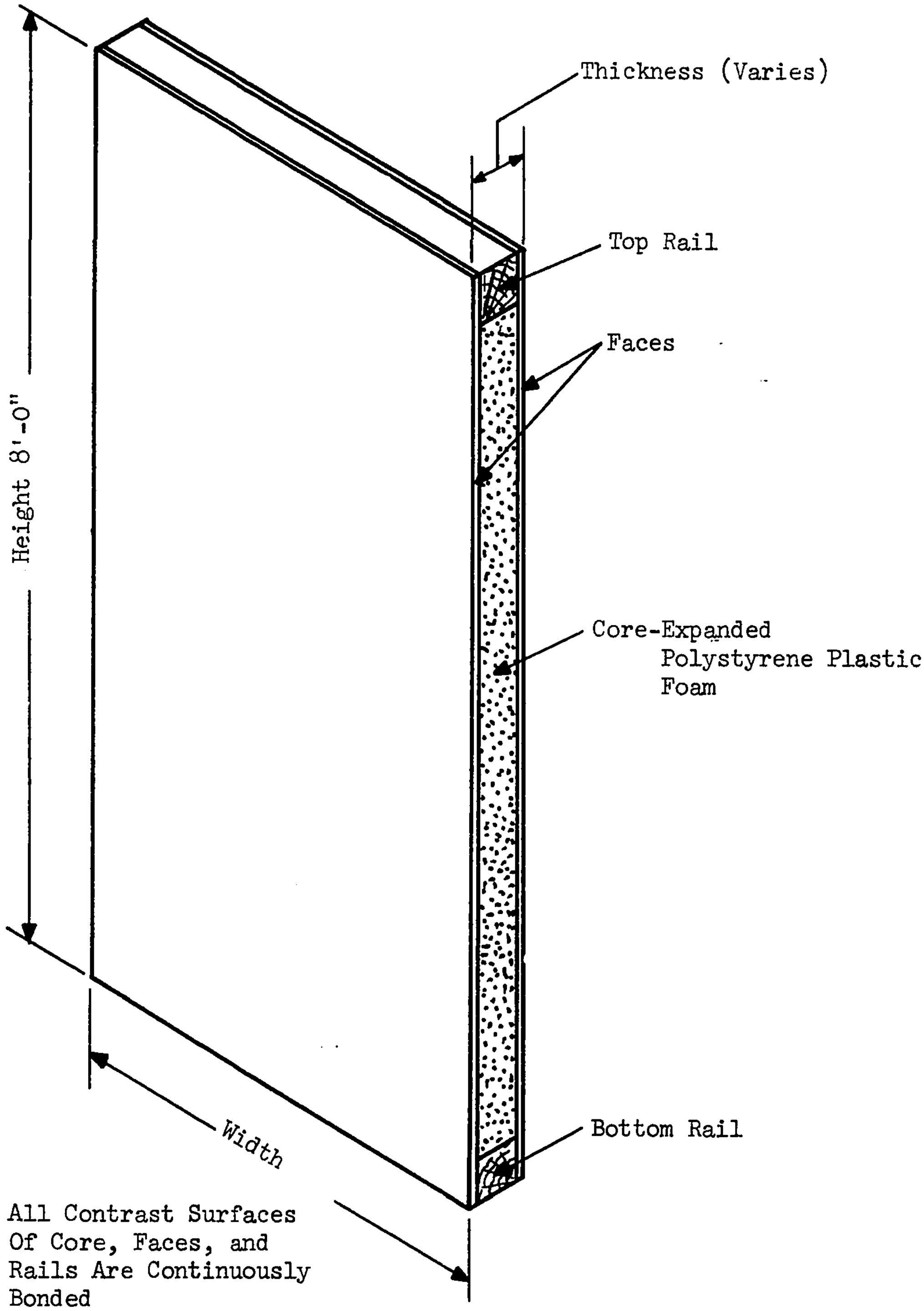

Figure 1-1. Typical Load Bearing Sandwich Wall Panel With Plastic Foam Core.

architects are specifying sandwich panels for curtain walls in offices, schools, and many types of commercial buildings such as that shown in Figure 1-2. However, the curtain walls have not been utilized to take advantage of their full strength. As pointed out by Parkinson,[4] "Some inherent strengths of sandwich structures, such as edge compression strength, are not being used. When means are devised for attachment of panels so that this surplus strength can be utilized to bear the building loads, we shall have a revolutionary means of construction with tremendous potentials."

C. Plastic Foams as Core Materials

In recent years there have been many advances in the development of plastic foams. There are many advantages in using plastic foams as core materials in sandwich panels and it appears that the competition in the chemical industry is bringing the price down.[5] The need for research in plastic foams in sandwich panel construction is reflected in the words of Ferrigno,[5] "Insulation and flotation apolication for foams are comparatively well understood, whereas the most promising field of construction requires intense concentration upon primary needs. One such need is for engineering standards and information regarding plastics in construction." When the combination of structural efficiency and excellent thermal resistance are desired, plastic foam filled sandwich panels are the most attractive structural elements available today. Expanded polystyrene and polyurethane are the major plastic foams on the market. Polystyrene is by far the most

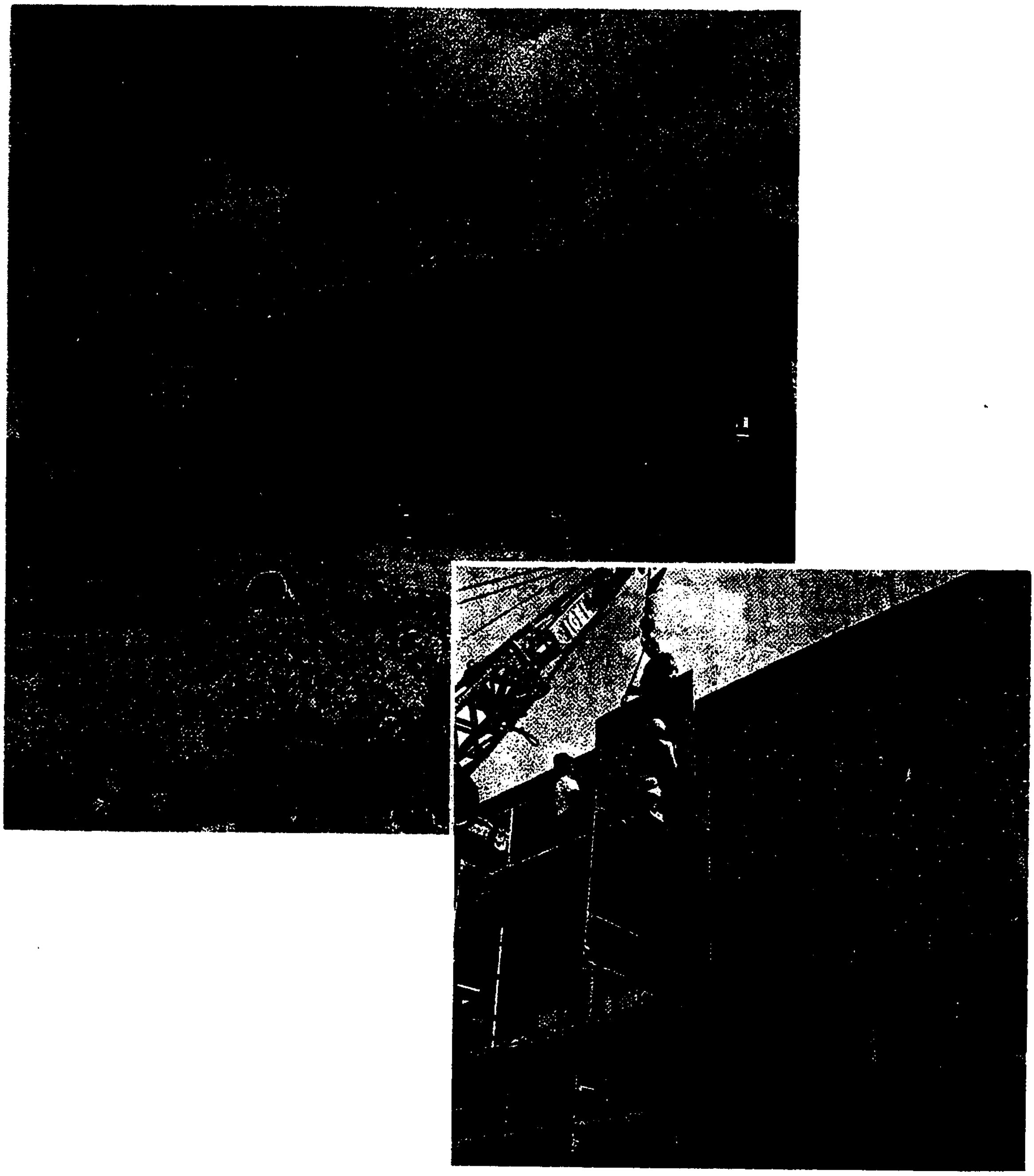

Figure 1-2. Sandwich Panels Used As Curtain Walls.

economical, however, polyurethane possesses the characteristic of being easily foamed in place.

D. Sandwich Buckling

Past experience with aircraft type structural sandwiches reveals that failure of column-loaded structural sandwiches can occur as an overall Euler column (or panel) type instability or by a localized failure resulting from face wrinkling, shear crimping, or direct compressive failure. In correspondence with the major suppliers, or research organizations which deal in some respect with architectural sandwich panels, there were only three studies reported which provide data for column design of plastic-foam-filled sandwich panels. These were studies conducted by Rensselaer Polytechnic Institute for Koppers Company, on long, rib-stiffened Dylite panels,[6] studies by the American Plywood Association on long panels,[7] and proprietary tests by the Masonite Corporation on long, rib-stiffened panels. None of the studies reported treated the specific problem of localized instabilities.

E. Research Introduction

The purpose of the research reported herein is to contribute needed knowledge, both theoretical and experimental, in understanding general and local instabilities of plastic-foam-filled sandwich columns. The major emphasis is on the development of local instability theories based on extensive experimental observations. However, the need arose also to develop theoretical general instability equations since present theories were found to be totally inadequate. The resulting studies produced an integrated analysis procedure for determining failure stresses in all modes of column instability, specifically applicable to foam-filled sandwiches.

The following chapters outline the general problem of column instability, sandwich experimental programs, analytical development of face wrinkling theories, analytical development of general instability equations, including shear crimping, and integrated design analysis procedures.

CHAPTER II

STABILITY OF SANDWICH COLUMNS

The instability failures of sandwich panels, loaded as columns with in-plane axial stresses, can generally be described by one of the following four failure modes:

(1) Overall panel buckling (general instability)

(2) Shear crimping

(3) Face wrinkling

(4) Intracellular buckling (dimpling)

These four failure modes are illustrated in Figure 2-1. An additional failure mechanism, not an instability, is direct compressive failure, or crushing.

It is, perhaps, a misnomer to list overall panel buckling and shear crimping as separate failure modes. The usual understanding of overall panel buckling is that it results when compressive loads exceed theoretical limits predicted by Euler's column formulas which are functions of facing material properties only. It is assumed at failure that internal restoring moment is exceeded by the applied moment at some critical point in the column and the column becomes unstable. When the shearing rigidity of the core is small, the overall buckling load is reduced due to increased lateral deflections brought on by shear deformations. Engesser[8] developed a simple buckling relationship

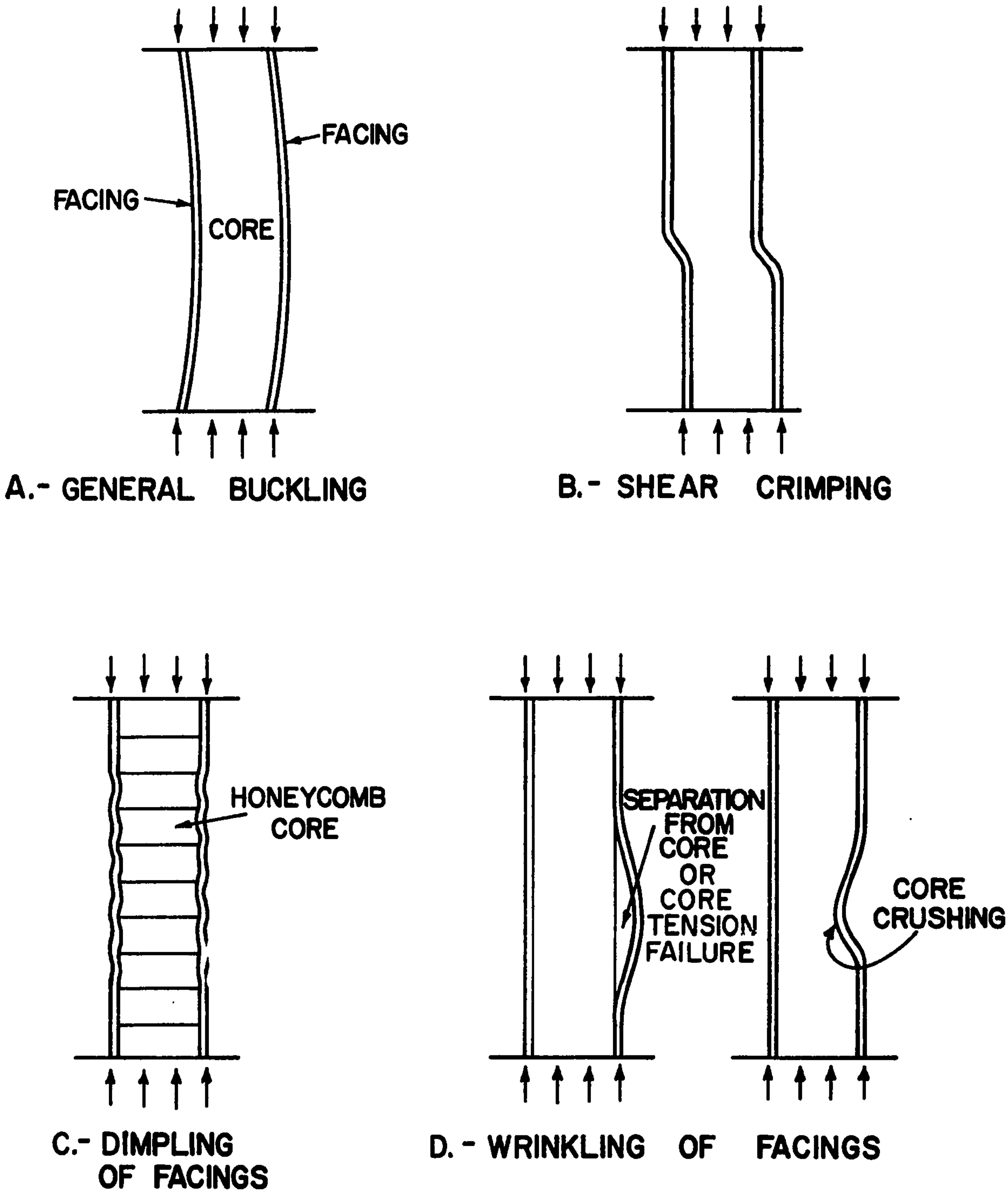

Figure 2-1. Modes of Failure of Sandwich Construction Under Edgewise Loads.

accounting for shear in terms of the non-shear Euler buckling load. His equation is often given in the form

$$P_s = \frac{P_{cr}}{1 + \frac{P_{cr}}{A_c G_c}} \tag{2-1}$$

where P_{cr} is the Euler buckling load without shear deformations considerations, G_c the average core shear modulus, and A_c the effective area in shear.* It will be shown in a later chapter that the Engesser equation is totally invalid for application to foam core sandwich columns. When overall buckling equations include effects of core shear deformation, the shear instability failure mode associated with very weak cores will be checked automatically.[9]

The shear instability mode calculated by the overall buckling equation assumes that strains in the core and facing remain linear with load until failure results from unrestrained deflection. However, failure of the core under transverse shear load could occur prematurely if the panel has surface irregularities or if the ends are displaced laterally with respect to the load plane. This can be a serious problem in sandwiches having foam core densities in the 1.0 pcf range. This problem is treated in depth in Chapter VI.

---

*The effective area in shear is the core cross sectional area for a sandwich composite in which the extensional modulus of the core is very small compared with that of the facings. This results from the fact that shear stress is negligible across the faces and is practically constant across the core. This assumption is in accord with the unity shear form factor commonly used in sandwich analysis. See Appendix A for a discussion of the shear form factor.

Face wrinkling is a localized failure identified as either (a) separation of the facing from the core by bond tension, (b) local core crushing, or (c) local transverse shear failure. Face wrinkling has been observed in tests of sandwiches with metallic and thin fiberglass facings. Previous studies at the University of Oklahoma have contributed extensively in this area.[10,11] Kuenzi[9,12] stated that the problem of wrinkling has not been solved in spite of various theoretical and experimental attempts. He also stated[9] that face wrinkling should be expected in sandwiches with very weak foam cores. Development of face wrinkling theories and review of present methods are treated in Chapter V.

Direct compressive failure may result if the column is free of eccentricities and surface irregularities, and possesses large bending stiffness. The failure would occur when the compressive stresses exceed the strength of either the facing or the core.[13] This failure mode might have the post-buckling appearance of shear crimping, however, it would be expected to occur rather explosively.

Intracell buckling,[14] commonly known as "dimpling," is found only in sandwiches with honeycomb, or similar cellular cores. It is a local buckling effect isolated to individual cells and is believed to precipitate face wrinkling. This failure mode would not occur in tests on sandwiches with plastic foam cores.

As this research progressed it became apparent that not only local instability analysis techniques were inadequate for foam type sandwiches but also that theoretical general instability results were not available to predict behavior of foam type columns under various end conditions, artificial displacements, surface irregularities, and eccentric loads. For this reason these items were added to the research and are included in Chapter VI. This addition complements the local instability results in that an integrated analytical study into all modes of column instability of foam filled sandwiches is presented in one volume. However, cognizance must be taken of the fact that experimental verification of the general instability equations has not been attempted. This is a critical area in need of considerable experimental investigation.

CHAPTER III

SELECTION OF SANDWICH MATERIALS

A. Introduction

This chapter presents general information regarding properties and influencing factors involved in the selection of sandwich facings, cores, and adhesives.

In 1960 the Building Research Institute held a workshop on sandwich panel design.[16] General design criteria for load-bearing sandwich walls were adopted at this meeting and they included the following material selection considerations:

<u>Face sheets</u>

Strength and stiffness

Bowing and dimensional stability

Puncture resistance

Durability

Fire resistance

Cost

Appearance

<u>Core materials</u>

Moisture resistance and retention

Thermal insulation

Fire resistance

Adhesive

Must insure mutual interaction between core and facings. It primarily determines the durability and aging characteristics, and insures the design strength and stiffness of a panel.

These considerations are quite general but serve as a good base reference when comparing materials for possible use in sandwich design.

B. Facing Materials

In selecting facing materials for this research a large list of materials was available. In order to keep the research program within manageable bounds it was decided to study only the facing materials which appear most likely to be used in economical load-bearing wall applications. Suggestions by manufacturers and material suppliers led to the selection of plywoods, pressedwood wall boards, and cement asbestos for the sandwich facing materials to be used in this research. Obvious omissions include fiberglass and metals. Thin metals are not considered compatible with plastic foam cores due to fire safety requirements. Plastic foams lose strength at temperatures above 175 ^{o}F, therefore, metal facings which would quickly transmit heat to the core would be totally unacceptable in load-bearing applications. A similar problem would exist with thin fiberglass facings.

Plywood--Plywood is by far the most widely used facing material used in sandwich and stressed skin construction in the building industry. This popularity stems from the fact that plywood bonds well to core materials, is light weight and easily fabricated, and can provide bending stiffness and strength, as well as a variety of finished surfaces.[17] Plywood has good dimensional stability in most climates. In areas where high moisture content is common, surface treatments, such as acrylic plastic spraying, act to moistureproof the plywood and avert moisture bowing. Delamination of sandwich faces due to moisture could not be tolerated, therefore, exterior grade plywood is recommended for sandwich column applications since it is laminated with waterproof glues.

An extensive accelerated exposure testing program was conducted by Dow Chemical Company and Douglas Fir Plywood Association.[18] Temperature and humidity were varied in a manner that was described as substantially worse than any which would occur within the United States during a winter season. No deterioration of construction or structural strength was noted in these tests.

Pressedwoods--The class of pressedwoods used in this research may be more technically defined as fibrous hardboards. These materials are often referred to as "Masonite" hardboards, although this is quite a misnomer since many companies produce fibrous hardboards. Structurally, pressedwoods are attractive since they offer increased strength over that of layer laminated plywood. Strengths up to 12,000 psi are advertised for tempered pressedwoods.

As described in the Wood Handbook,[19] fibrous hardboards are made from refined or partially refined vegetable fiber, principally from wood, although fiber from bagasse, waste paper, straw, licorice root, and cornstalks is used to some extent. Binding agents and other materials are added during manufacture to increase strength, resistance to moisture, fire, or decay. Among the materials added are rosin, alum, asphalt, paraffin, various cements, preservative and fire-resistant chemicals, synthetic resins, and drying oils.

Fibrous hardboard is distinguished from particle board which is composed of visibly distinct particles bonded together in a flat sheet with a synthetic resin. Most of the fibrous boards are manufactured by an adaptation of a papermaking process; that is, the fiber raw material is reduced to a pulp and formed into a mat from a water slurry on the screen of a paper machine. The wet mat is then dried in a continuous drier or simultaneously compressed and dried into a compact sheet. In a modification of the conventional wet-felting process, known as the semidry process, the fibers are carried in an air suspension into the mat.

Hardboard manufactured by the conventional process is characterized by one smooth face and one face with a screen impression. In the air suspension process a board with two smooth faces is produced. Thin panels having one screen impression side may exhibit lower elastic moduli than panels with both sides smooth.

Hardboards are classified as untreated or treated. The untreated hardboards will be referred to in this research as "standard pressedwood." The treating process consists of impregnating pressed boards in drying oils and then baking them in ovens. This treatment increases the strength and water resistance above that of untreated hardboard. The treated hardboards will be referred to in this research as "tempered pressedwood."

The pressedwoods are extremely appealing to architects since they may be readily manufactured in highly decorative forms with prefinished paints and plastic coverings. The principal objection to the use of pressedwoods is their vulnerability to moisture penetration. This presently limits their use in sandwich columns to interior applications unless special moistureproofing is possible.

Cement Asbestos--Cement asbestos continues to win favor with builders and architects based on its established qualities. This durable and now attractive colored and textured material will not rot, burn, corrode or rust. It is weatherproof, fireproof, and wearproof.[20]

All asbestos-cement products now on the market consist essentially of a mixture of asbestos fibers, silica, and Portland cement.

Cement asbestos appears to be an excellent facing material for foam-filled sandwich columns. It is best known in sandwich construction for its resistance to fire. Flame spread, a measure of the flame propagation, rates the fire hazard classification of a composite. The nature of the facings essentially determines this rate. A common flame spread rate, described in ASTM E84-50T is based on a flame spread index with cement asbestos board rated zero on a scale where red oak is rated 100. This test also rates the smoke density factor, a most important fire performance characteristic.

Cement asbestos has other attractive characteristics enhancing its potential for use in sandwich construction. It is very strong in compression and affords much greater bending stiffness than plywood or pressedwood. Cement asbestos withstands atmospheric exposures without surface treatment. Acoustically, cement asbestos is superior to plywood and pressedwood, by virture of its much higher density.

C. Core Materials

Since the purpose of this research was to study the behavior of foam filled sandwiches, the choice of core materials was isolated to plastic foams.

Foamed plastics, sometimes called expanded, cellular, or sponge plastics, are a group of low-density, high-quality materials which can be engineered to meet specific end requirements of density, cell size, flame spread, etc.[21,22] Thermoplastic or thermosetting resins are expanded in volume by means of a gas to produce a cellular structure which resembles a fine honeycomb or a mass of tiny hollow spheres fused together.

Foaming can be accomplished by many processes, the most basic being 1) mechanical frothing, 2) dissolving a gas or a low-boiling-point liquid in the resin, or 3) incorporating a foaming or blowing agent which will release an inert gas in the resin when the temperature is increased.

Although there are some eight or more plastic foams on the market only polyurethane and polystyrene are presently economically feasible for use in architectural sandwiches. Choosing between these two materials was difficult because each has certain superior characteristics when compared with the other.

Urethane foams have the advantage of a higher service temperature of 250 ^{o}F compared with 175 ^{o}F for polystyrene.[5] This is a serious consideration in industrial buildings where summer static temperatures might exceed 200 $^{\circ}F$. Urethane and polystyrene foams are both excellent thermal insulators. However, urethane is much superior since it has a thermal conductivity of 0.13-0.16 $\frac{\text{BTU-in}}{\text{hr-ft}^2\text{-}^{o}\text{F}}$ compared with 0.25 for polystyrene foam. In subfreezing temperatures polystyrene maintains constant mechanical properties.[23] Both foams are excellent vapor barriers.

Urethane may be purchased in board form but it has the unique advantage of being foamed-in-place. It may be poured as a liquid which then expands approximately 30:1. It may be applied in a frothed form so that the material leaves a special mixing head in a partially expanded form such as shaving cream from an aerosol can. The advantages of frothing are that foaming pressures are reduced 75 percent over poured or sprayed liquid systems, and lower overall densities may be obtained.[24]

Polyurethane has widely varying density within a panel, therefore, the physical properties are extremely complex and variable. This complicates the analysis in column design requiring the use of overly conservative safety factors. Urethane foam is specified by average density within the panel. Presently, urethane foam is available at minimum densities of approximately 1.9 pounds per cubic foot (pcf).[24]

Polystyrene foam is commercially available in board stock. Extruded expanded polystyrene foam is available at a minimum density of 1.9 pcf. Molded expanded polystyrene is available at a density of 1.0 pcf. Koppers Company markets a foam which is produced by a patented foamed-in-place method but the equipment is not available commercially.

Although polyurethane foam may possess certain physical advantages over polystyrene foam, it is also more costly. For example, in 1965 urethane foam insulation cost 40 percent more than the same size polystyrene foam.[25] This cost differential is reduced somewhat when the urethane is foamed in place, thereby eliminating the adhesive.

The foams selected for this research were the low-density polystyrene foams from Dow Chemical Company. Extruded "Styrofoam" densities selected were 1.9, 2.5, and 3.3 pcf. The lowest density polystyrene foam selected was the 1.0 pcf molded "Dorvon" foam. In addition to the "Styrofoam" and "Dorvon" foams, Koppers Company provided completed sandwich panels filled with a polystyrene foam by their special method of expanding polystyrene beads.

D. Adhesives

An adhesive is a substance capable of holding materials together by surface attachment. The resulting bond may be one of mechanical adhesion, specific adhesion, or a combination of both. Mechanical adhesion may best be described as an interlocking action between the adhesive and the materials being bonded. Specific adhesion might be termed a chemical attraction involving primary or secondary valence forces of the adhesive and the materials being bonded.[26]

Adhesives may be classified into three basic groups according to the method by which they ultimately reach the bonded state: drying adhesives, setting adhesives, and hot melt adhesives.

The drying adhesives reach the bonded state by the evaporation of a liquid such as water or organic compounds.

The setting adhesives, which reach the bonded state by means of a chemical reaction, include water reactive inorganic compounds such as Portland cement and plaster of Paris, and organic compounds such as phenolics, ureas, and epoxies. Organic adhesives require the addition of a suitable catalyst to initiate the chemical reaction or polymerization by which these adhesives cure or harden.

Hot melt adhesives require softening with heat before use. They are applied in a molten state with the bond resulting as the adhesive cools and hardens to its original solid state. Certain asphalts and waxes are of interest in the bonding of foam materials.

Drying adhesives are not recommended for one-stage glueing of foam core sandwiches for two reasons:

(1) The foam core and facing materials are considered vapor impervious thereby preventing drying of the adhesive within reasonable curing times.

(2) The better drying adhesives have organic evaporation liquids which react as solvents on the plastic foam.

The pressure-sensitive adhesives are classified as drying adhesives but are actually set up in two stages which permits open time to allow evaporation of most of the liquid vehicle before effecting the bonds.

Setting adhesives are most popular in foam type sandwiches because of their superior performance under moderately high temperatures, resistance to creep, and general durability.[23] Resorcinol, phenolic, and phenol-resorcinol adhesives effect excellent bonds between Styrofoam cores and faces of plywood, hardboard, particle board, and cement asbestos board.[23] Epoxy adhesives are considered superior for bonds between plastic foams and all facing materials, however, the cost of epoxies is not competitive with other adequate adhesives.

Upon the recommendations of Dow Chemical Company and U. S. Plywood Corporation waterproof resorcinol adhesive was selected for use in this research program.

CHAPTER IV

EXPERIMENTAL INVESTIGATIONS

A. Introduction

There are two essential purposes for this experimental investigation. First, the short column buckling behavior of foam-filled sandwiches has never been confirmed experimentally, to the writer's knowledge, therefore, a void exists in basic knowledge which must be answered. Secondly, the prediction techniques for local failures appear dependent on semi-empirical correlation factors. This means that experimental data, covering the spectrum of projected architectural foam-filled sandwich combinations, should be available in sufficient quantities to allow a meaningful statistical analysis.

Due to the range of facing materials plus four densities of polystyrene plastic foam, a large amount of preparatory testing of individual materials was necessary before composite sandwich tests could be performed. Manufacturer's published data were available for comparison with many of the tests. Agreement was excellent in most cases, as will be shown.

Facings tests are for compression only. Compression testing is more difficult than tension testing because of the problem of avoiding bending, buckling, and delamination.

Core specimens were required to be tested in tension, compression, and shear. Again, compression is difficult due to bowing. Shear is always difficult to determine; however, a cantilever concept was applied which appears to have given reasonable results.

Facing and core tests will be discussed in separate sections, followed by a section on composite sandwich tests. The final section will present a special study on debonding (unbonded regions).

B. Facing Material Tests

Materials--Compression tests were conducted on the following facing materials:

1/4" Douglas fir plywood (from Dylite panels, grade unknown)

1/8" Ash plywood

1/4" Ash plywood

3/16" Standard pressedwood (Masonite)

3/16" Tempered pressedwood (Masonite)

1/8" Cement asbestos

Specimen size:

Nominal length = 2.0"

Nominal width = 1.0"

Nominal thickness:

Douglas fir = 2 x nominal sheet thickness

All others = 3 x nominal sheet thickness

The specimens were glued together to improve their column stability. Two sheets of plywood were glued; three sheets for each of the other materials. The adhesive used was resorcinol. The specimens were clamped under heavy pressure to minimize the thickness of the adhesive layer.

Testing Machine--The equipment used in this study consisted of a basic axial loading machine and auxiliary measuring equipment.

The testing machine was a 5000 pound "Cal-Tester," Model TH-5, distributed by Pacific Scientific Company. This machine is equipped with two load gages. One gage has a range of 0 to 1000 pounds, and the other has a range of 0 to 5000 pounds. The rate of load application cannot be controlled accurately with the manual hydraulic valve, therefore, load was applied gradually and deflection readings were taken after gage stabilization. Figure 4-1 shows the "Cal-Tester" equipped with a compression attachment set up with a foam specimen.

Strain Measurement--The large strains common to the materials tested allowed the use of dial indicators. Ames and Lufkin gages (0.0001 in.) were installed in pairs such that end rotations would be detected, and axial deflection would be the average of the two readings. This arrangement is shown in Figure 4-2 where a pressedwood specimen is being tested.

Test Results--Compression tests appear to have given quite reasonable results. These results are presented in Figures 4-3 through 4-8. As noted in these figures, it was not possible to obtain exactly zero initial conditions. This was due to creeping hydraulic pressure and imperfect ends on specimens. Average linear stress-strain relationships were determined for each set of tests and then shifted to an initial zero value. This adjusted average is shown as a dotted line in each of the figures. This same adjustment procedure was also followed in the core material tests.

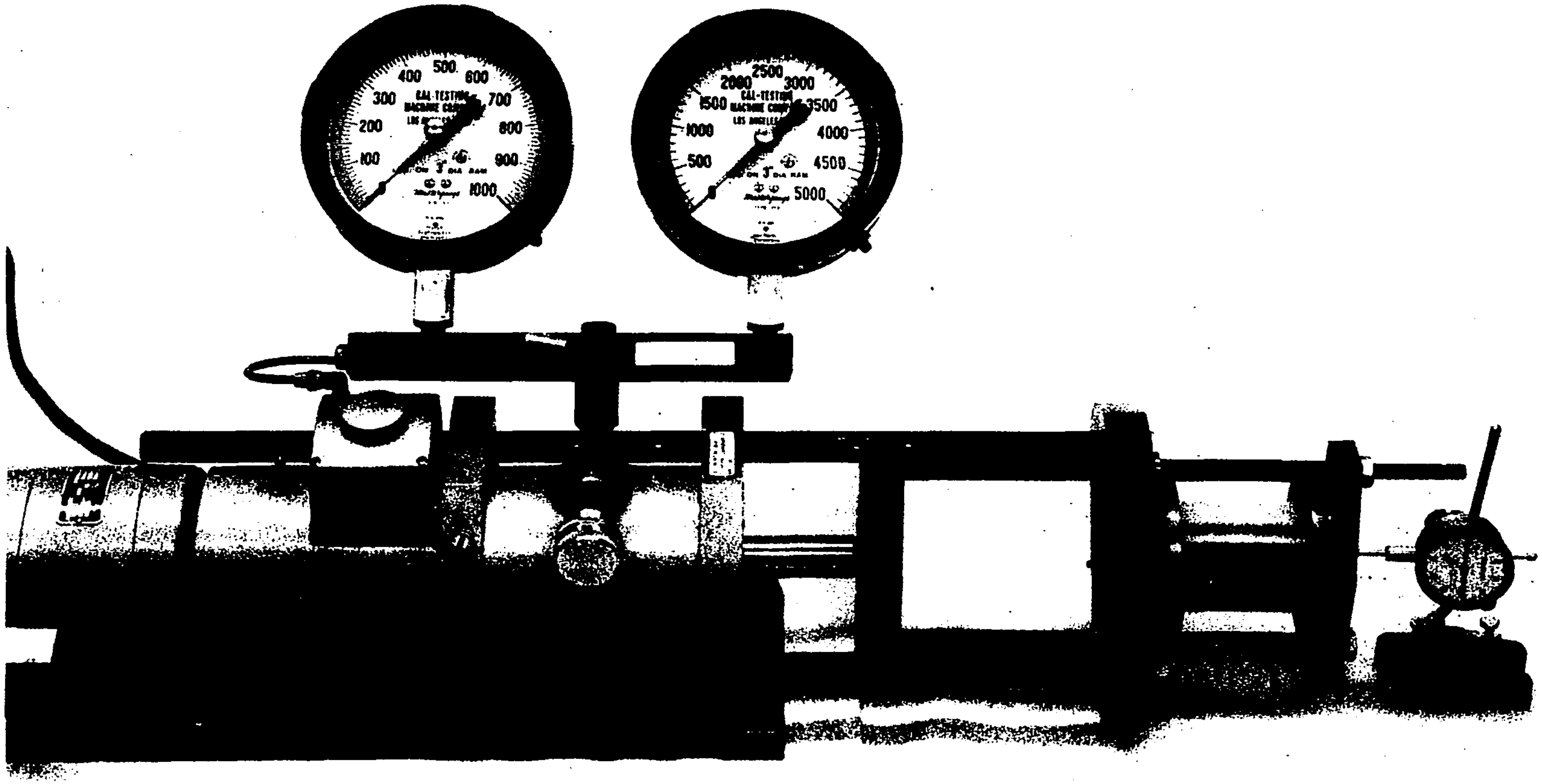

Figure 4-1. 5000 Pound Test Machine Equipped with Compressive Attachment.

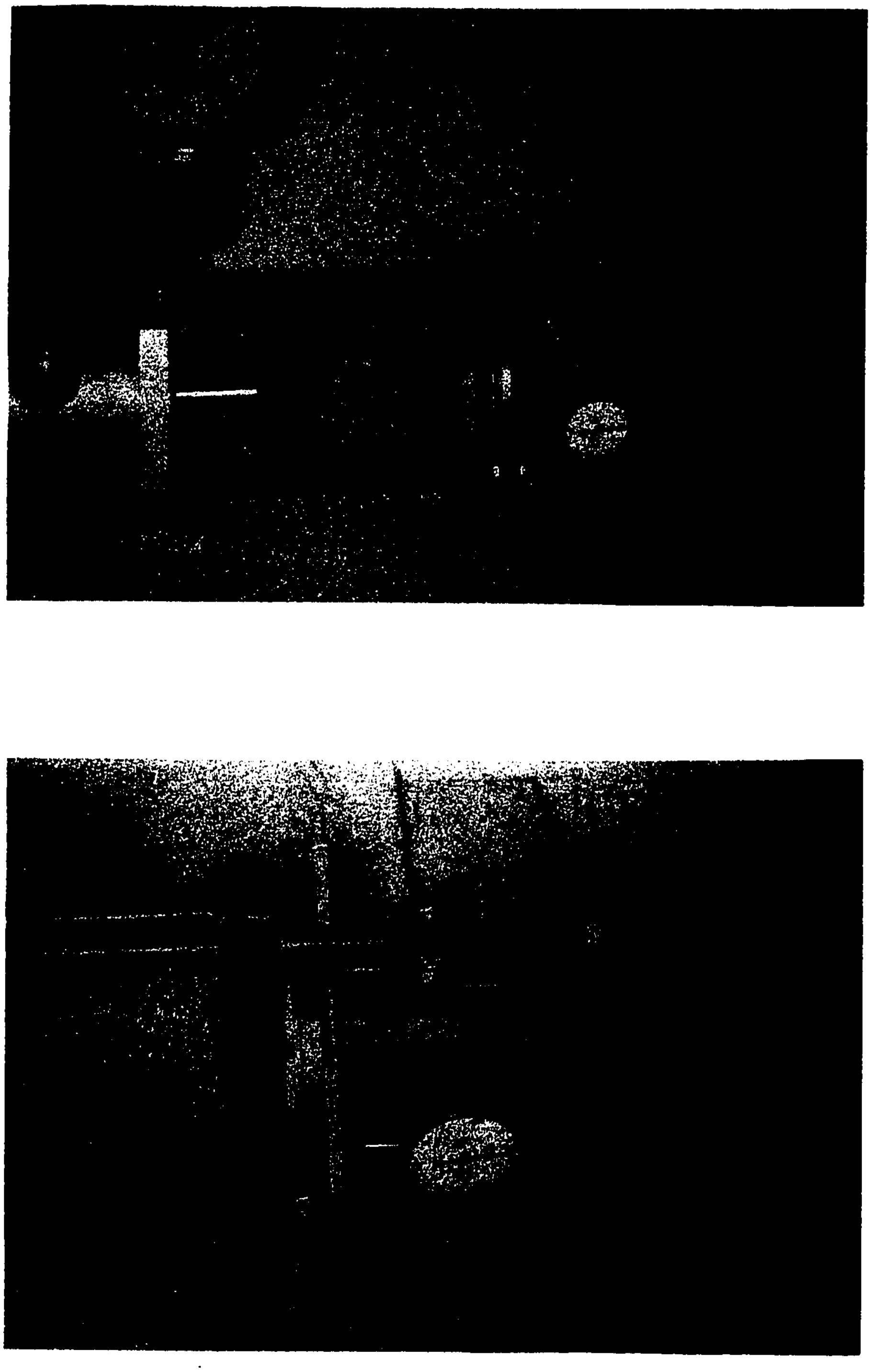

Figure 4-2. Dial Indicator Arrangement in Compressive Tests of Pressedwood.

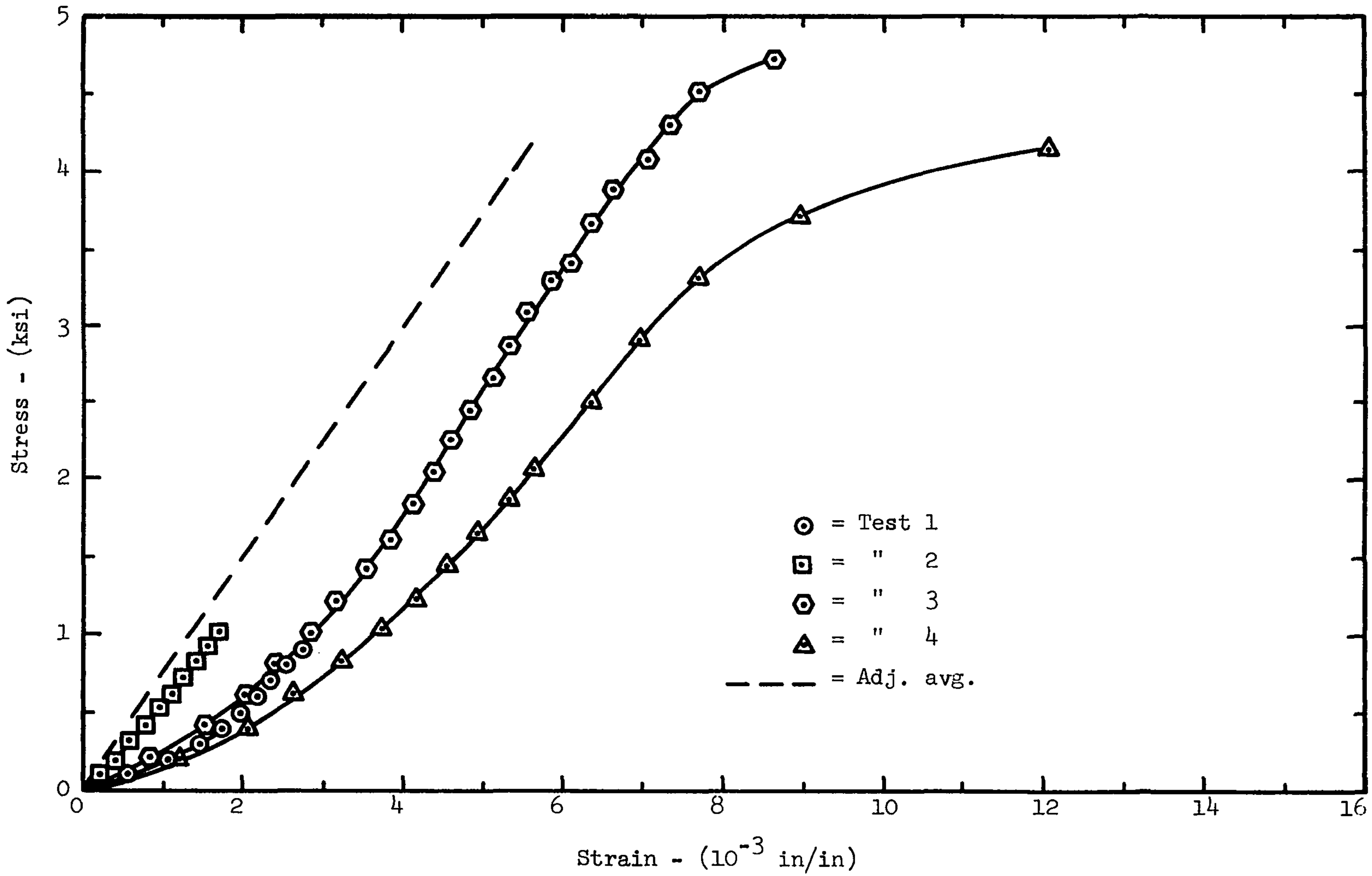

Figure 4-3. Douglas Fir (1/4 in.) Compression Stress-Strain Curves.

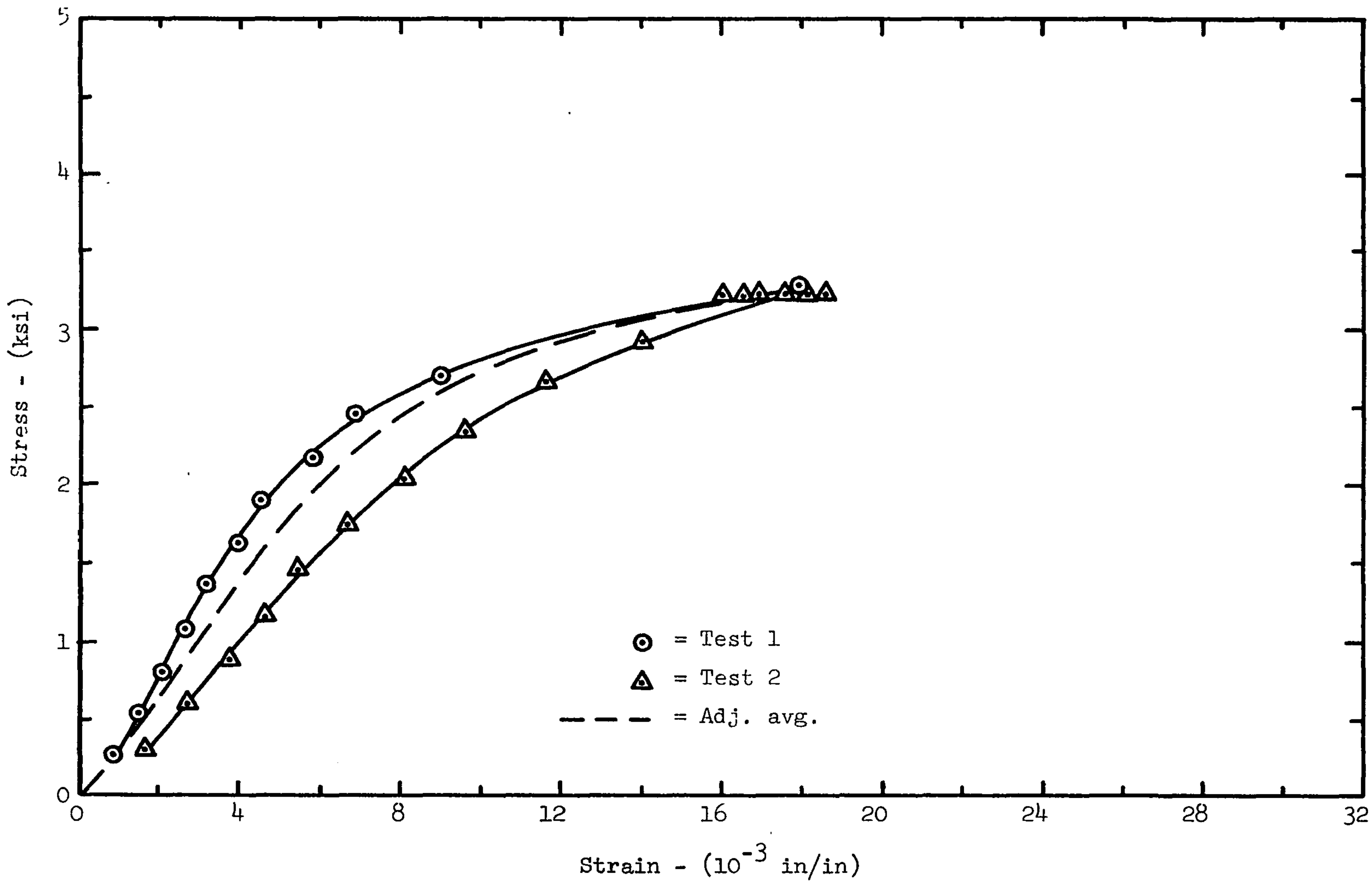

Figure 4-4. Ash Plywood (1/8 in.) Compression Stress-Strain Curves; Load Parallel to Face Grains (3 ply).

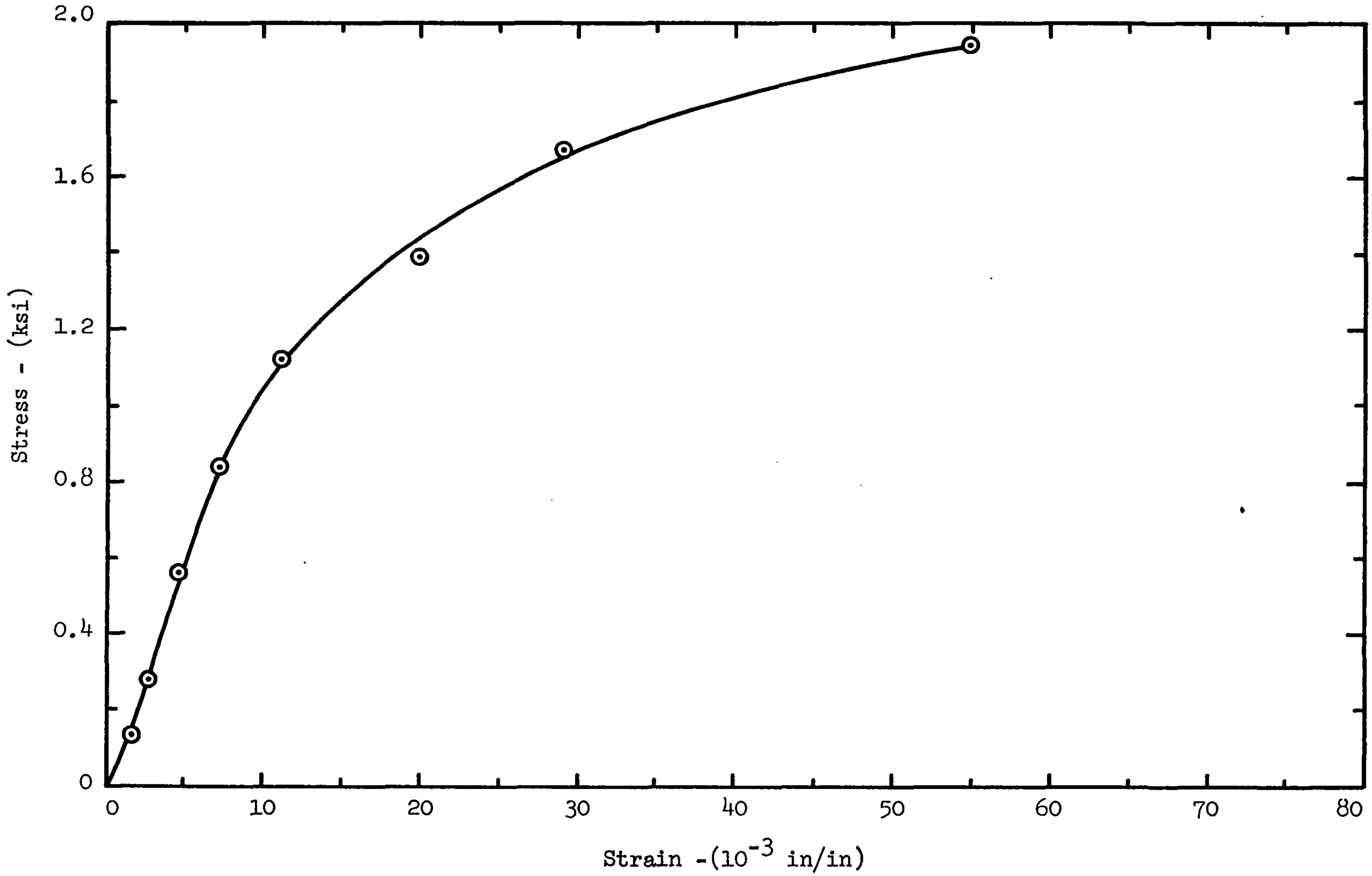

Figure 4-5. Ash Plywood (1/4 in.) Compression Stress-Strain Curve; Load Parallel to Face Grains (3 ply).

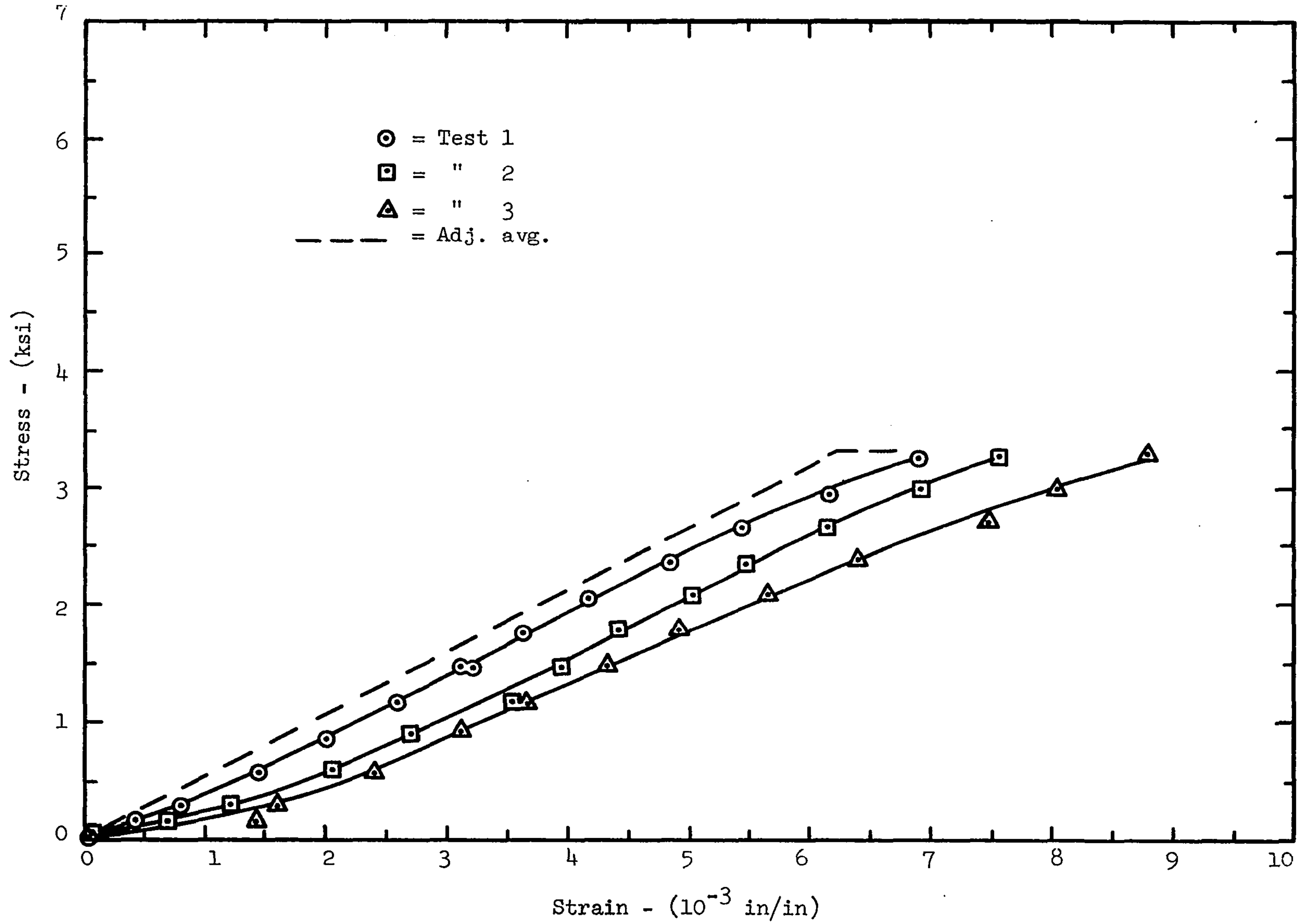

Figure 4-6. Standard Pressedwood (3/16 in.) Compression Stress-Strain Curves.

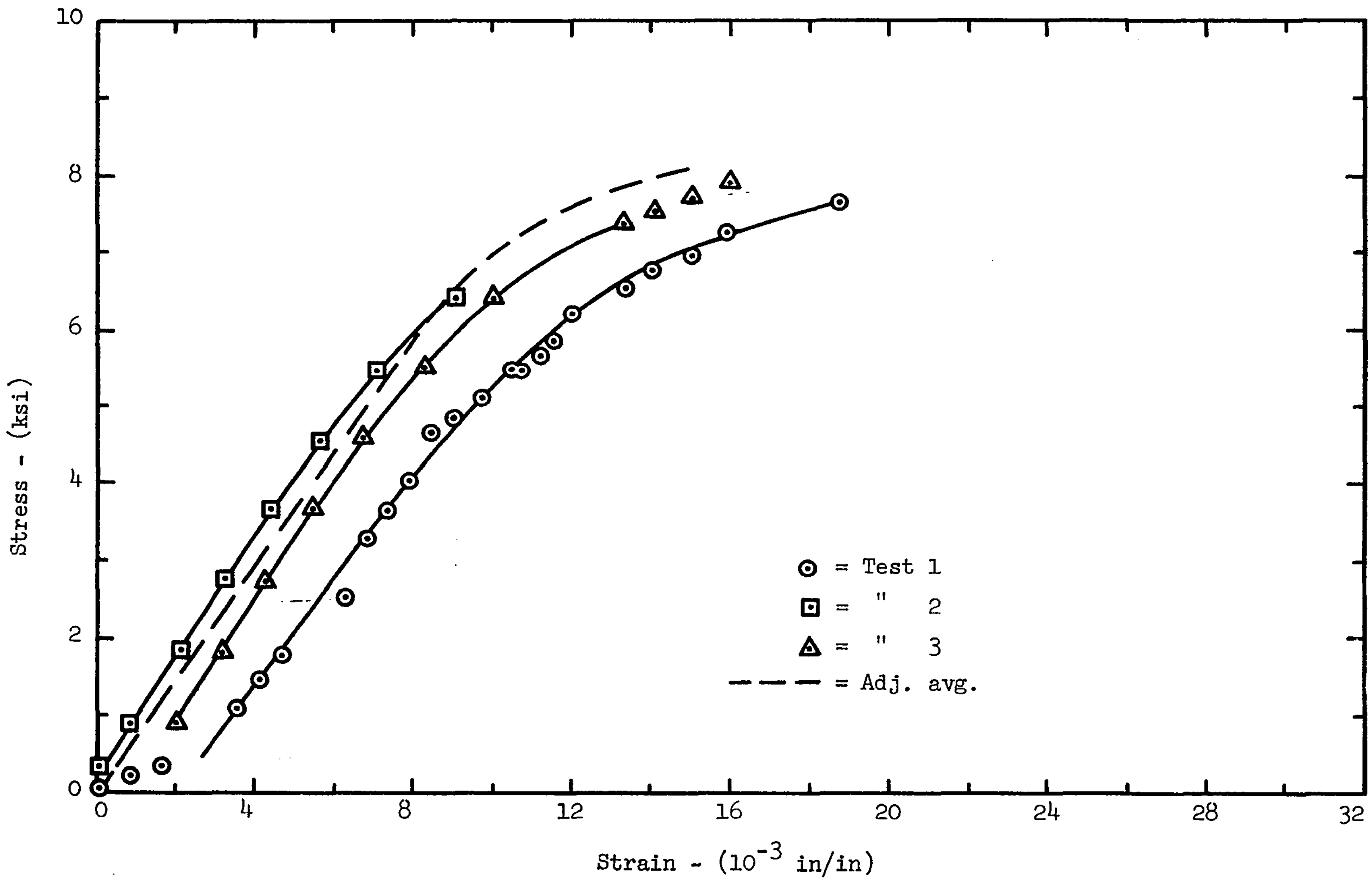

Figure 4-7. Tempered Pressedwood (3/16 in.) Compression Stress-Strain Curves.

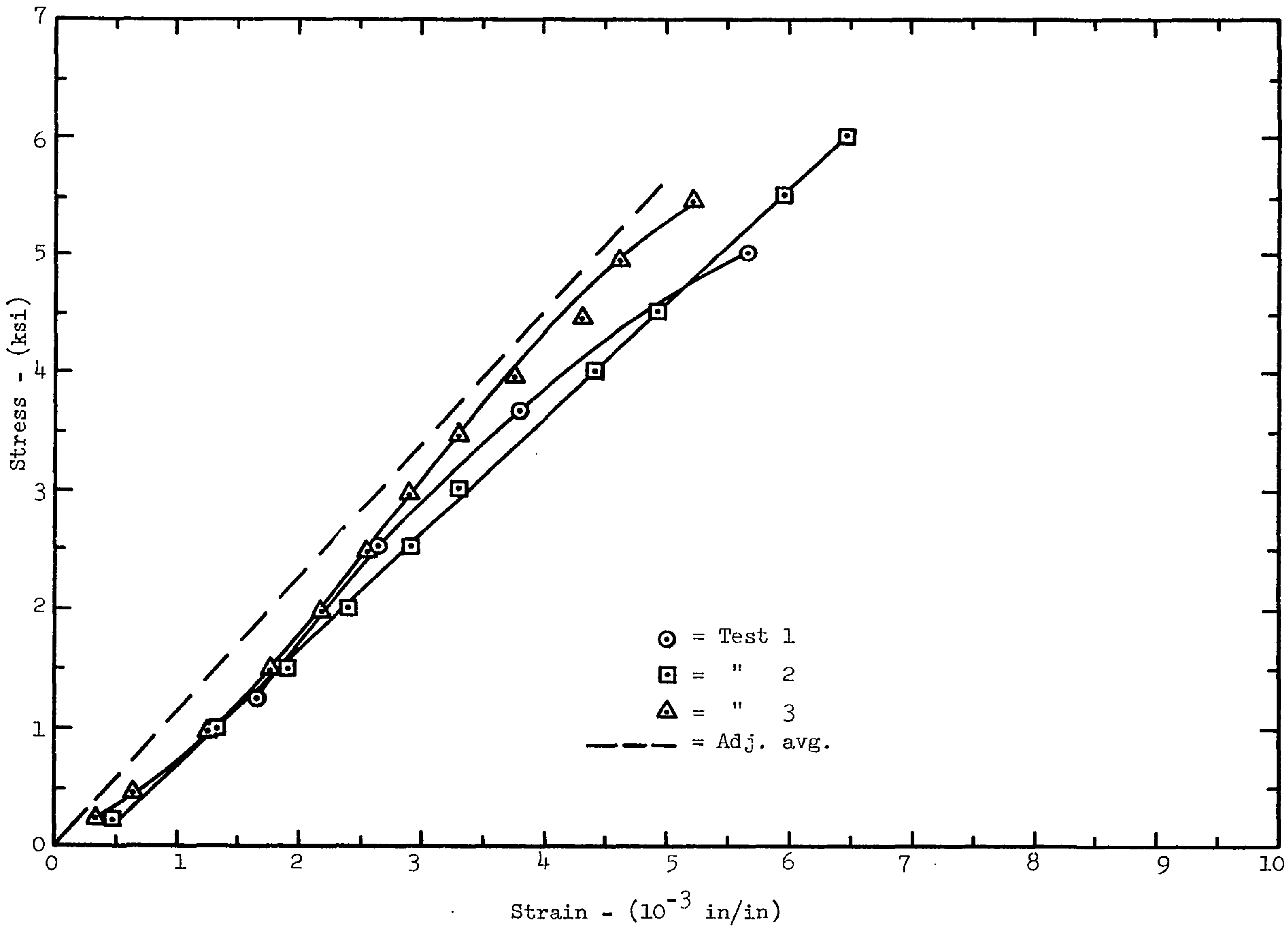

Figure 4-8. Cement Asbestos (1/8 in.) Compression Stress-Strain Curves.

Shear plane failures were noted in all of the tests except the 1/8 inch ash plywood which failed in bending. An excellent example of shear failure in a 1/4 inch ash plywood specimen is shown in Figure 4-9.

Compression elastic modulus values for the facing tests are listed in Table 4-1. Also shown are elastic modulus values from manufacturer's data. The Douglas fir specimens tested did not come up to the expected level of rigidity as determined in FPL tests.[27]

TABLE 4-1

FACING COMPRESSION MODULUS FROM TEST AND MANUFACTURER'S DATA

Face Material	Compression Modulus Test (10^6 psi)	Compression Modulus Mfg. Data (10^6 psi)
1/4" D. F. Plywood	0.75	0.96*
1/8" Ash Plywood	0.35	--
1/4" Ash Plywood	0.134	--
3/16" Std. Pressedwood	0.53	0.50-0.53**
3/16" Temp. Pressedwood	0.73	0.73**
1/8" Cem. Asbestos	1.12	--

*FPL data.

**Masonite data.

Plywood used in glued sandwiches was purchased later. It was of excellent quality and graded "A-C Exterior." Strain gaged, glued sandwiches made with the better plywood exhibited a 46 percent increase in rigidity over the poorer plywood used in the foamed-in-place sandwiches from Kopper's Company. This implies that individual facing tests on the

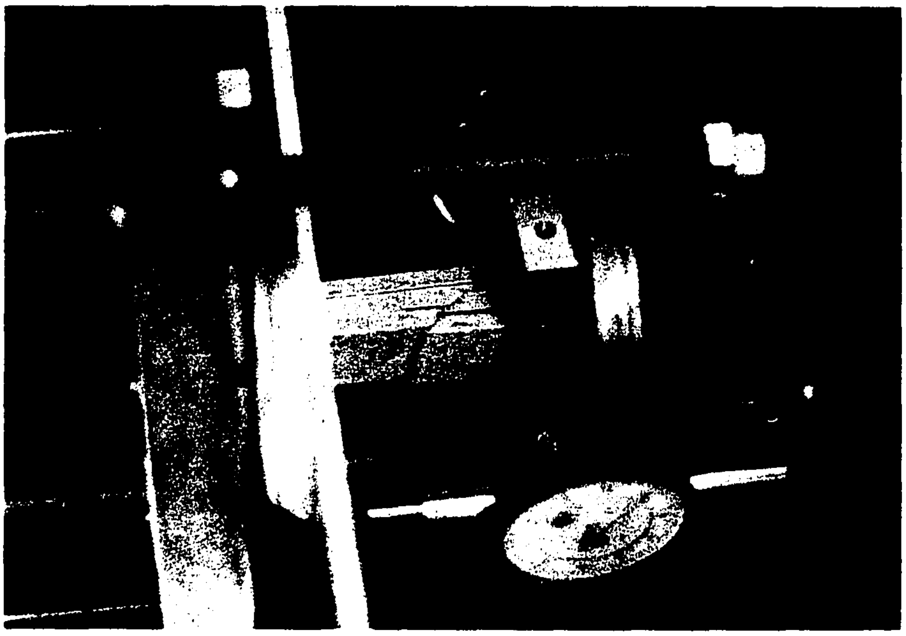

Figure 4-9. Example of Shear Failure in 1/4 in. Ash Plywood.

better plywood should have produced a compression modulus of approximately 1.0×10^6 psi, very near the typical value of 0.96×10^6 psi given by Forests Products Laboratory.

Masonite Corporation provided compression modulus test data for standard pressedwood and tempered pressedwood.[28] As shown in Table 4-1, test values were in perfect agreement with Masonite data for both materials.

C. Core Material Tests

Materials--Tension, compression, and shear tests were conducted on the following expanded polystyrene foam core materials with indicated nominal densities:

Dylite (Koppers), foamed-in-place 1.0 pcf

Dorvon (Dow), 1.0 pcf

Styrofoam FR (Dow), 1.9 pcf

Styrofoam RM (Dow), 2.5 pcf

Styrofoam HD-300 (Dow), 3.3 pcf

Specimen sizes, compression and tension tests:

Nominal length = 3.0 in.

Nominal cross section = 1.5 in x 1.5 in.

Specimen sizes, shear tests:

Nominal depth = 2.0 in.

Nominal width = 1.0 in.

Nominal length = 1.0 in.

Test Equipment--The equipment used in this study consisted of a specially designed and fabricated testing machine, strain-gage load cell and readout indicator, and deflection measuring equipment.

The testing machine consisted of a platform having mounting posts to hold the specimen, a loading system made up of a cable extending over a pulley to a weight container below, and built-in mounts for deflection gages. Photos are shown in Figure 4-10 which visibly illustrate the machine set up for tension tests. Compression tests were conducted similarly as shown in Figure 4-11(a). Shear tests required a change in the platform arrangement to facilitate the cantilever type test, as shown in Figure 4-11(b).

Measuring Equipment--The load cell consisted of an aluminum bar with a 2.0 inch long, constant-area center section having dimensions of 0.500 x 0.100 inches. Budd "Metalfilm" electric-resistance strain gages, Type C6-141, were mounted on each side. Temperature compensating gages were mounted on a separate aluminum plate. The four strain gages were connected in a full-bridge arrangement which would cancel out bending strains but would act additively for axial strains. The load cell was then calibrated by dead weights in increments of 5.0 pounds up to 150 pounds. The dead weights had been checked on a Fairbanks-Morse scale of recent calibration. The load cell calibrated exactly linear with repeatability within 1.0 percent. The calibration equation for applied load as a function of strain indicator reading (set at a gage factor of 2.09) was

$$\text{Load} = (0.264)\ (\text{Reading in } 10^{-6} \text{ in./in.})$$

The load cell was checked for accuracy before each group of tests and was always within 2.0 percent. Another check on the load cell was made using the "Cal-Tester" testing machine with perfect agreement. Figure 4-12 shows photos of these two accuracy checks on the load cell.

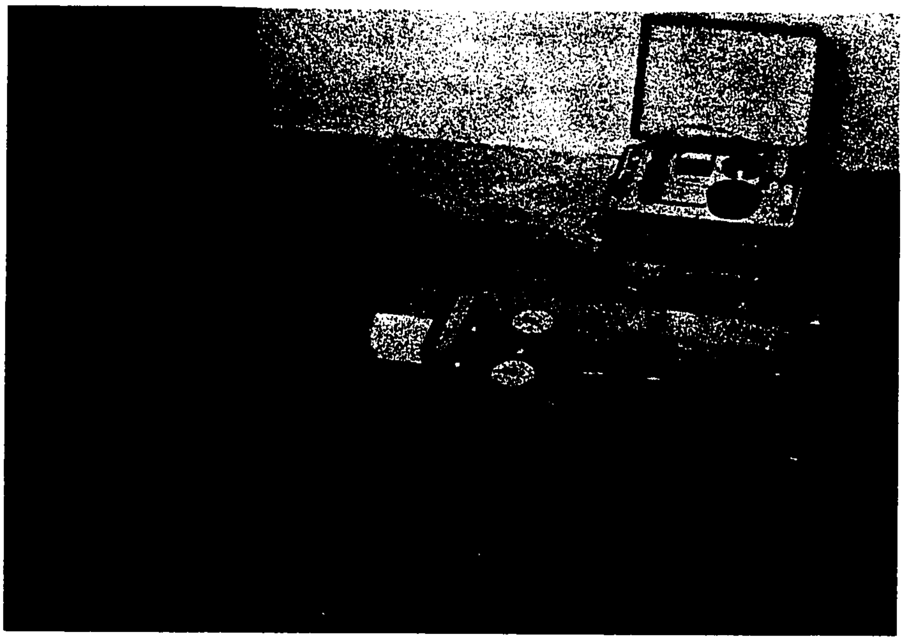

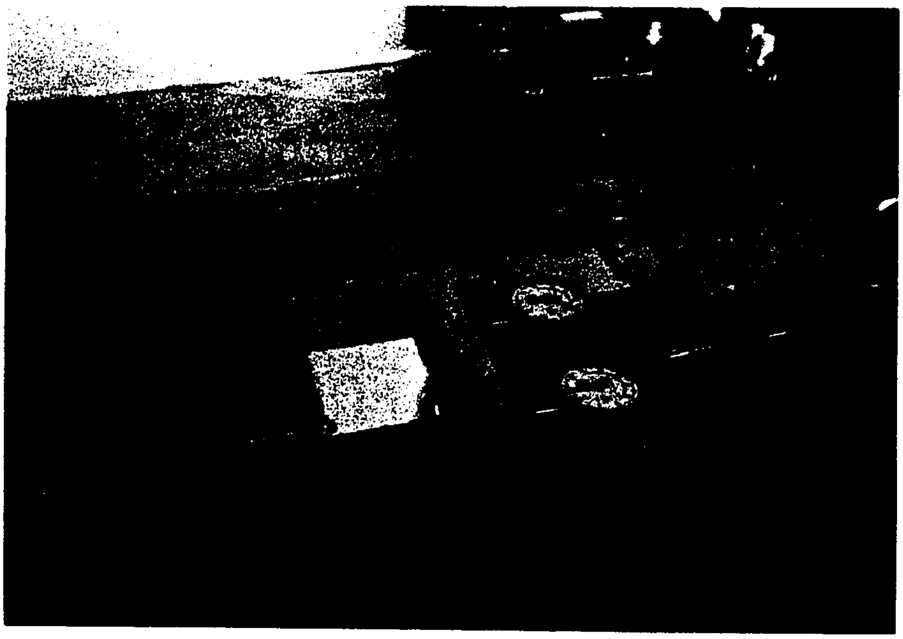

Figure 4-10. Photos of Special Testing Set-up for Plastic Foam in Tension

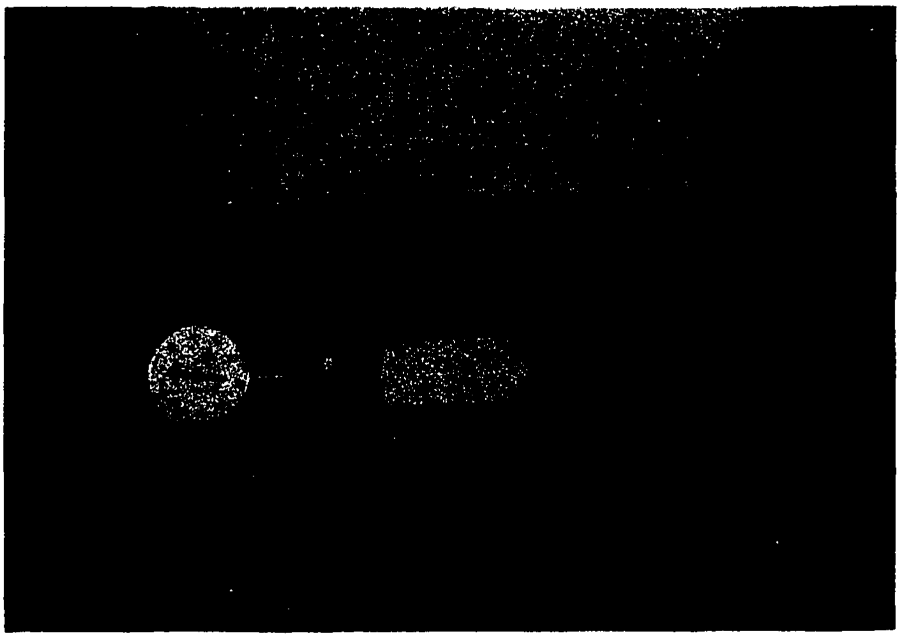

A

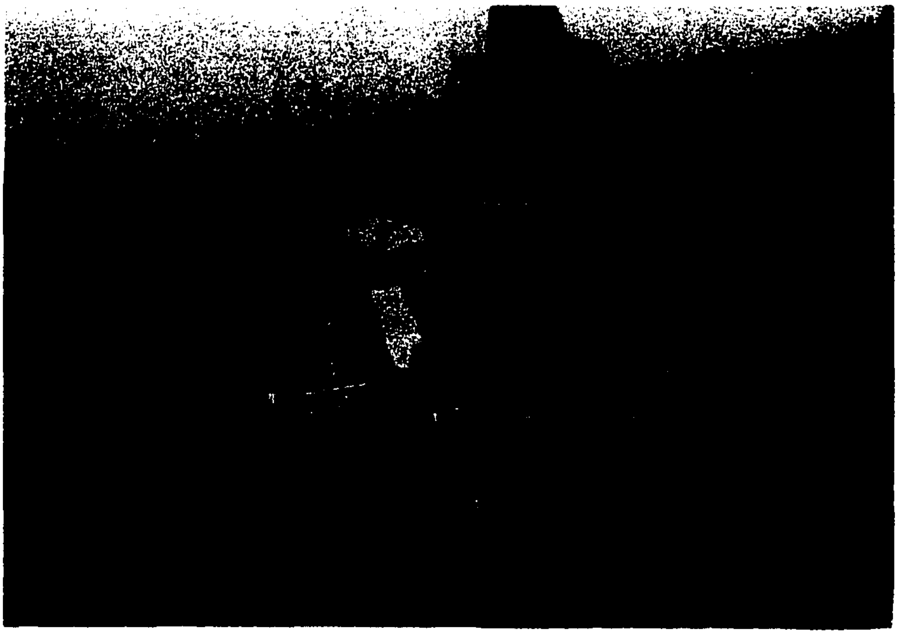

B

Figure 4-11. Typical Plastic Foam Tests in (A) Compression and (B) Cantilever Shear.

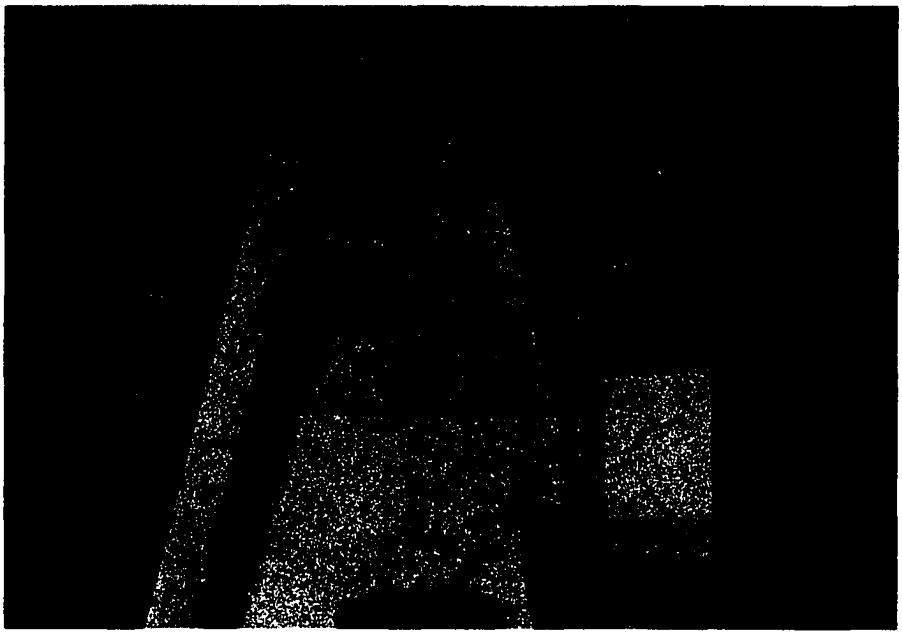

A

B

Figure 4-12. (A) Calibration Check on Tension Load Cell Using Dead Weights and (B) Calibration Check Using the "Cal-Tester."

Since sizeable deflections were expected in the foam tests, Soiltest, Inc., deflection gages of 0.001 inch accuracy were used.

Compression and Tension Tests--The compression tests were performed by simply inserting the specimen between a yoke plate and the restraining post as shown in Figure 4-11(a). The deflection was measured at the center of the plate. The most critical phase was aligning the specimen such that the load vector was coincident with the longitudinal axis of the specimen.

Results of the compression tests are shown in Figures 4-13 through 4-17. Good agreement is shown for the elastic region. The tests which went non-linear and failed earlier were always the result of bowing (or bending) collapse. For comparison purposes, three of the series, Styrofoam FR and RM, and Dorvon,[29,30] show Dow Chemical Company data. Note that the Dow curve shows much less strength, probably intentionally overly conservative.

Tension tests required the additional application of end plates to the foam specimens. These end plates were glued in place and used to attach the specimen on one end to the fixed post and the other end to the tension load plate. The mechanics of this loading arrangement are shown in detail in Figure 4-10. Note that deflection gages are mounted on each side of the load plate, thereby measuring rotation effects. The axial deflection would be the average of the two deflection readings.

Results of the tension tests are shown in Figures 4-18 through 4-22. Excellent data were obtained. Dow Chemical Company did not provide tension stress-strain curves for comparison.

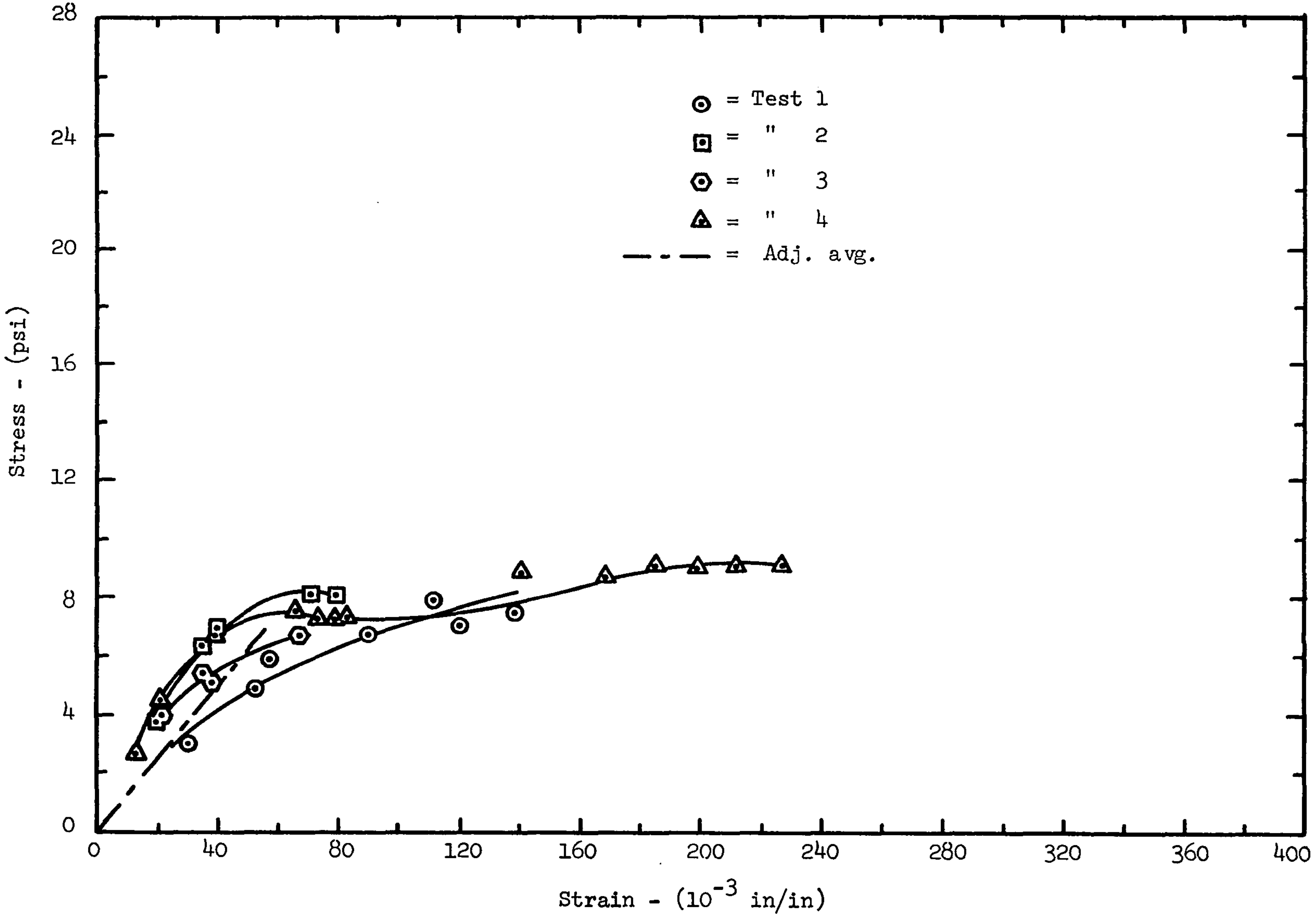

Figure 4-13. Dylite Compression Stress-Strain Curves.

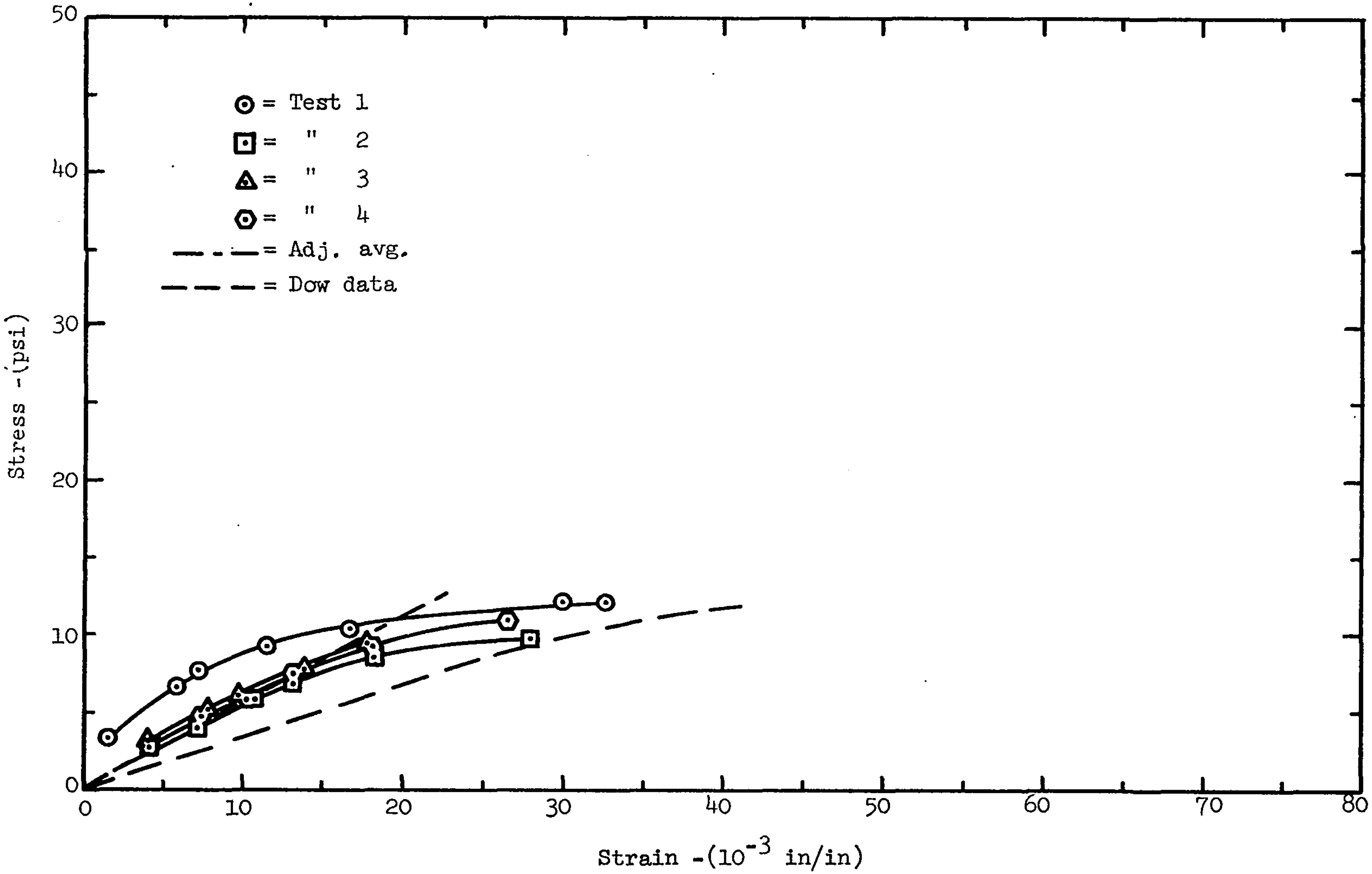

Figure 4-14. Dorvon Compression Stress-Strain Curves.

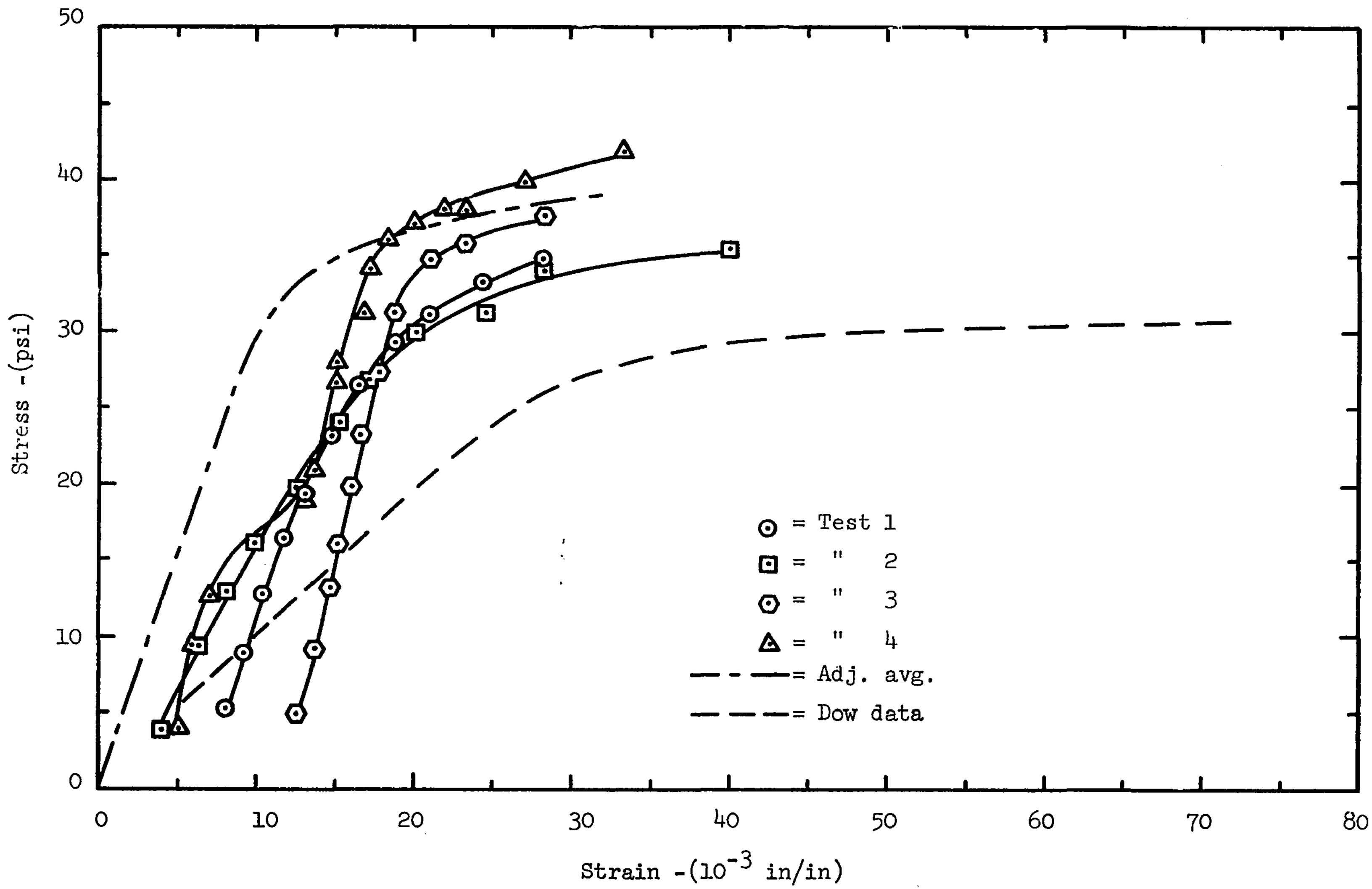

Figure 4-15. Styrofoam FR Compression Stress-Strain Curves.

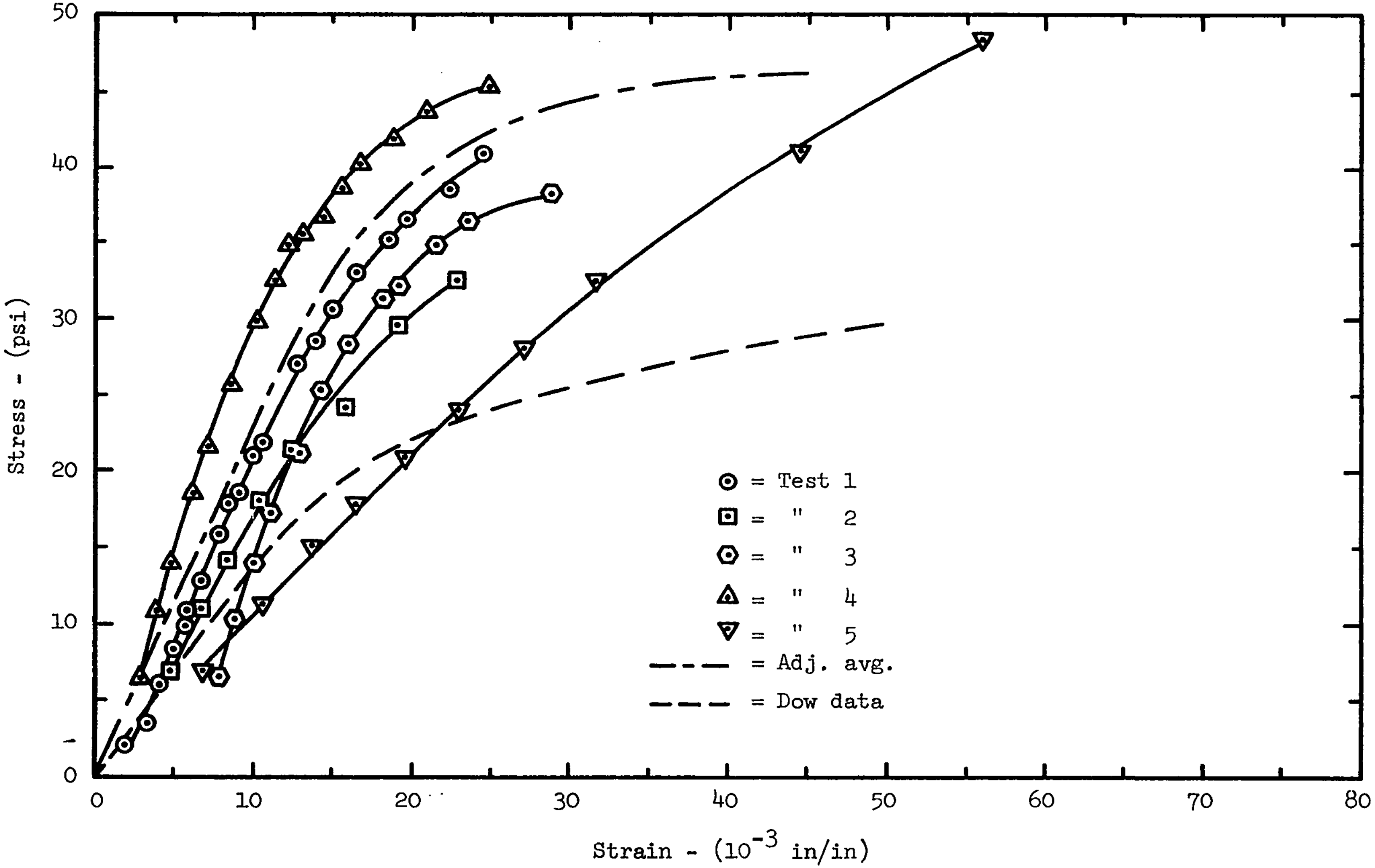

Figure 4-16. Styrofoam RM Compression Stress-Strain Curves.

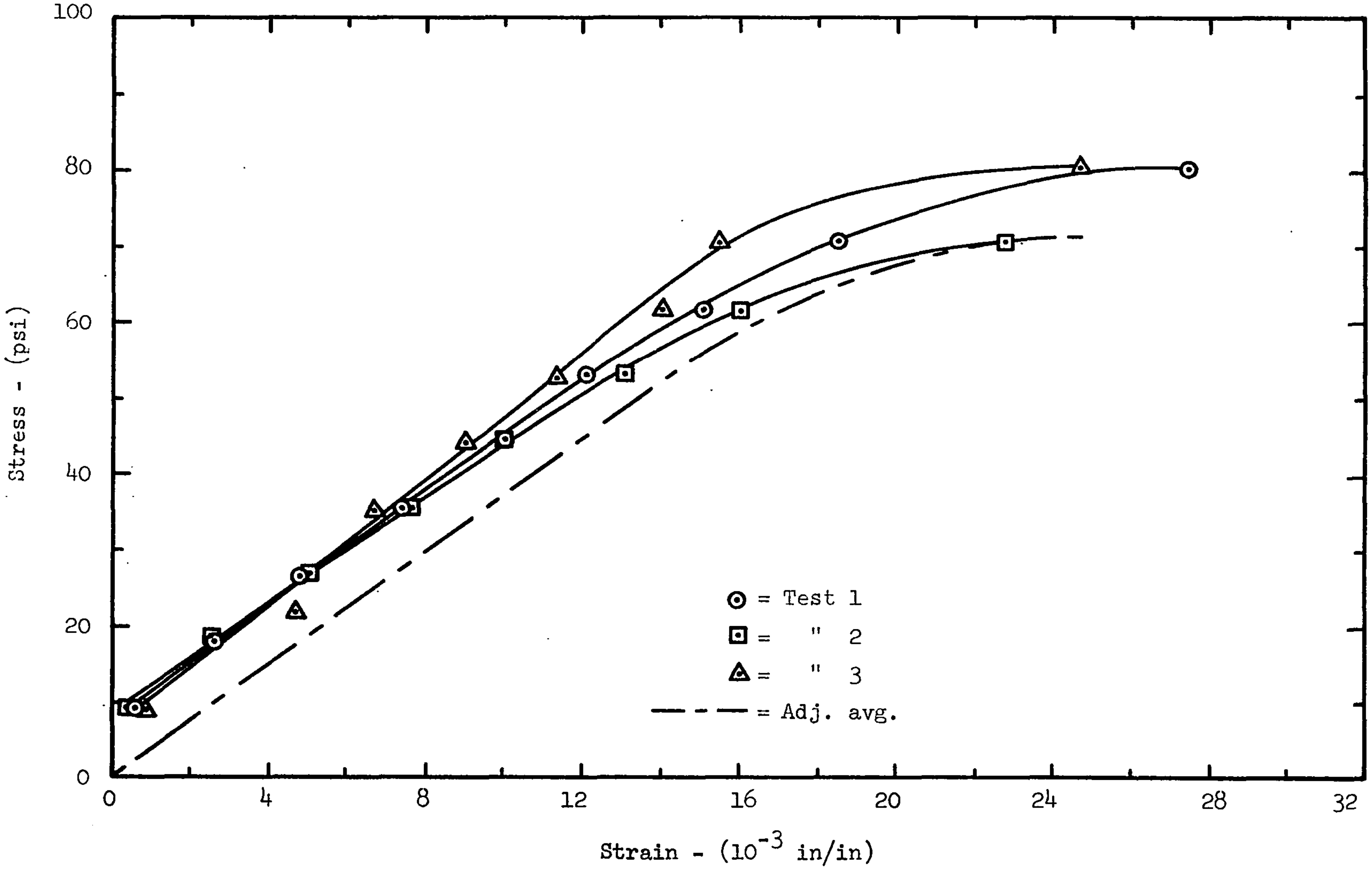

Figure 4-17. Styrofoam HD-300 Compression Stress-Strain Curves.

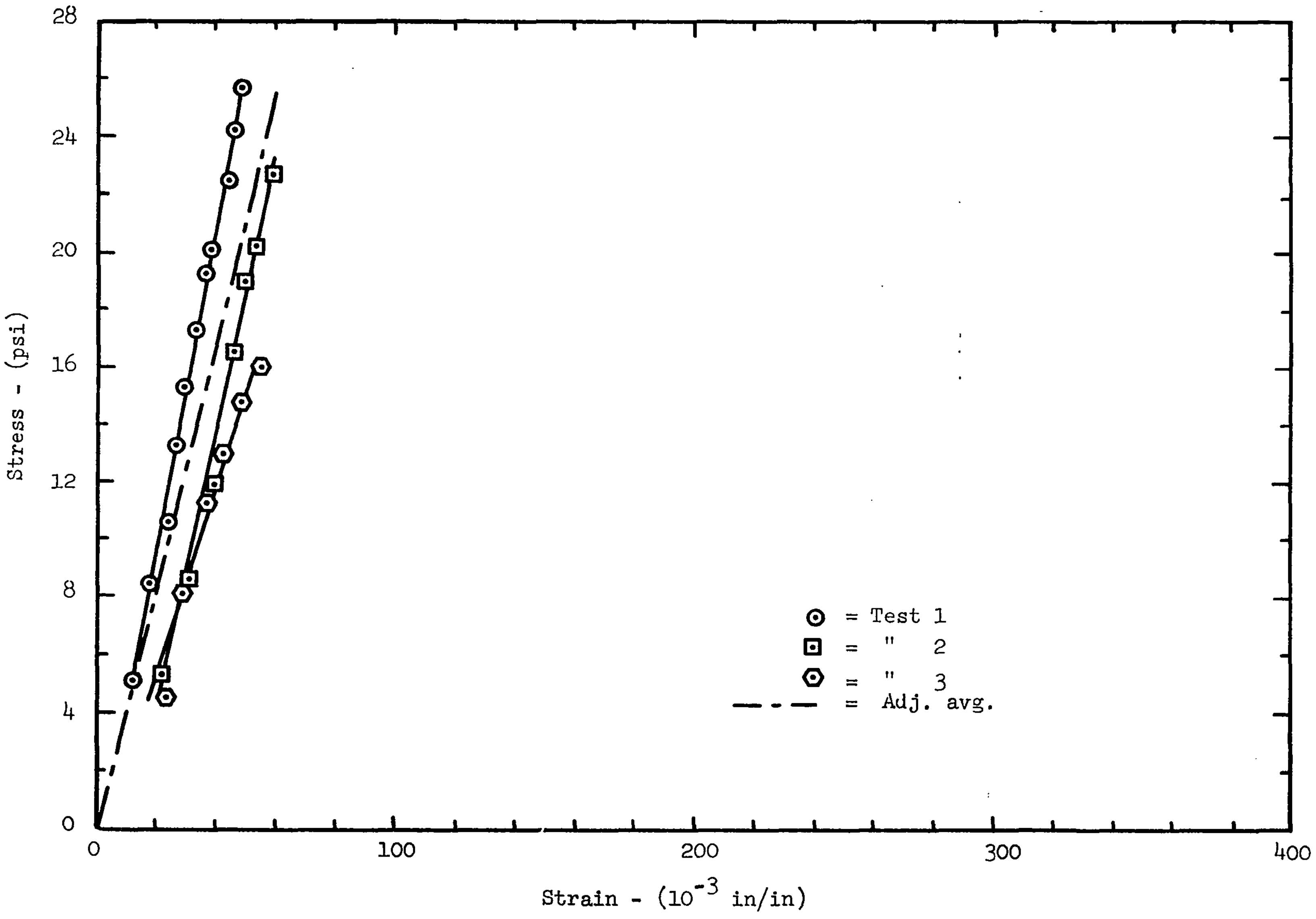

Figure 4-18. Dylite Tension Stress-Strain Curves.

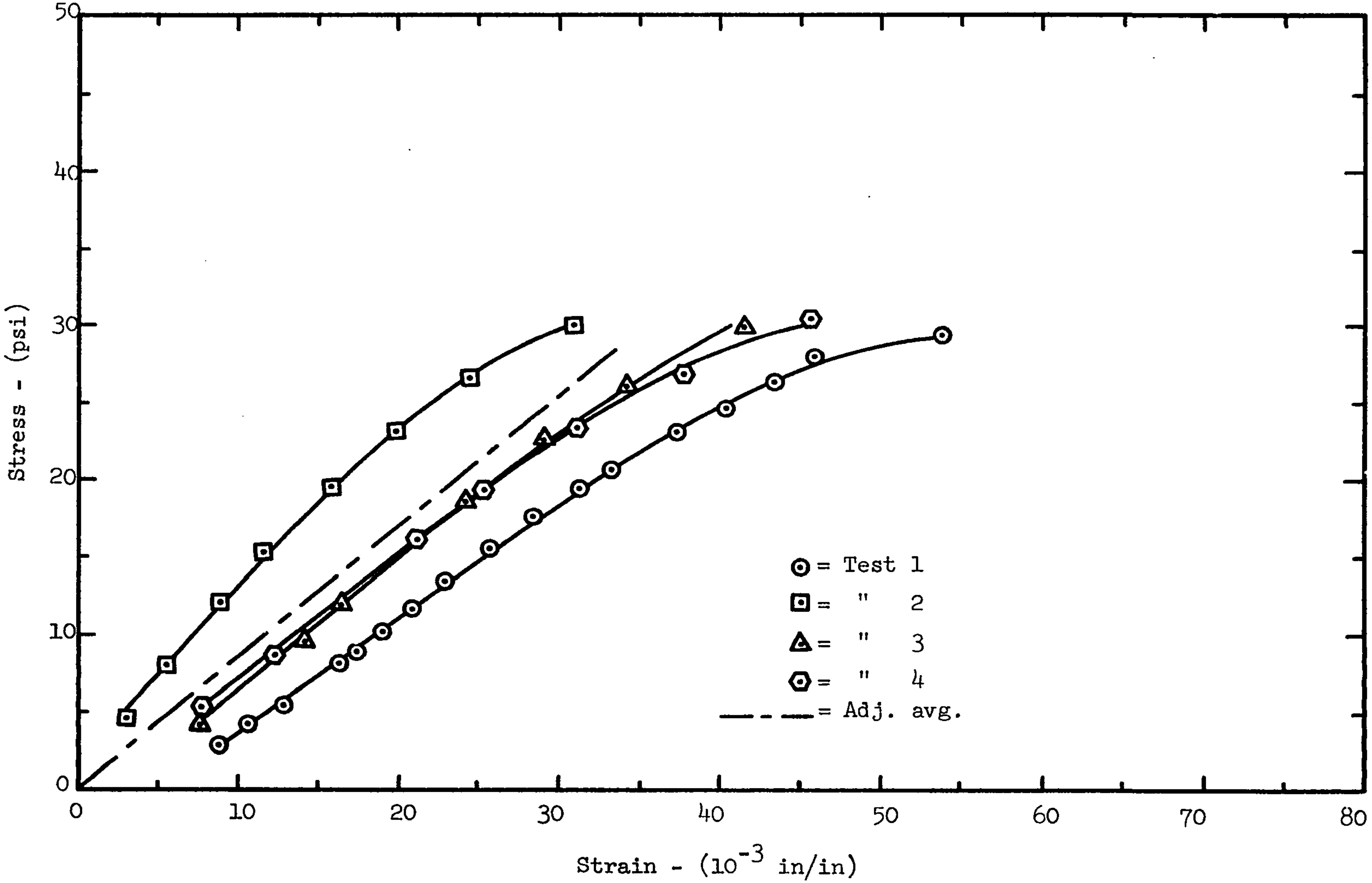

Figure 4-19. Dorvon Tension Stress-Strain Curves

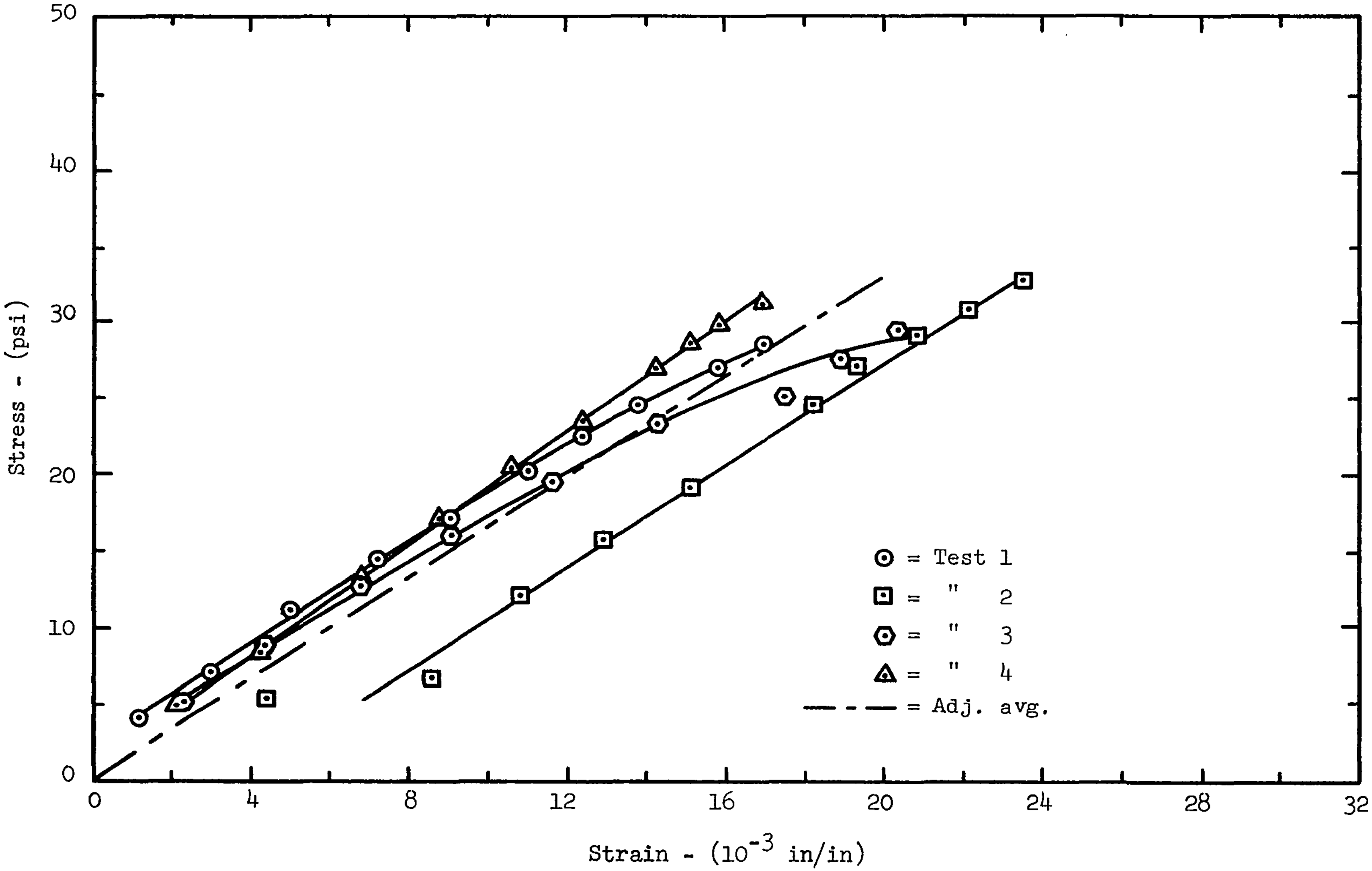

Figure 4-20. Styrofoam FR Tension Stress-strain Curves.

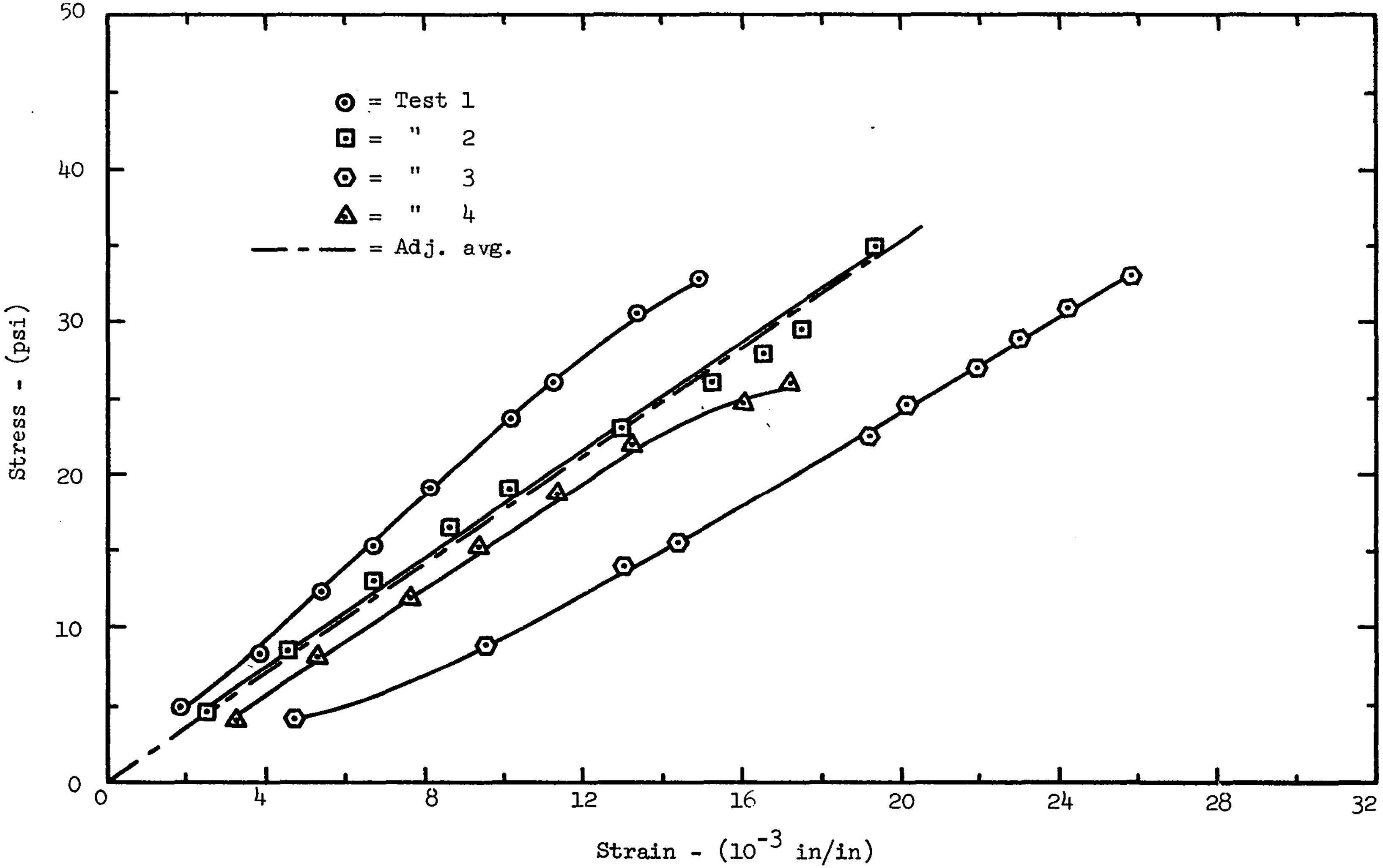

Figure 4-21. Styrofoam RM Tension Stress-Strain Curves.

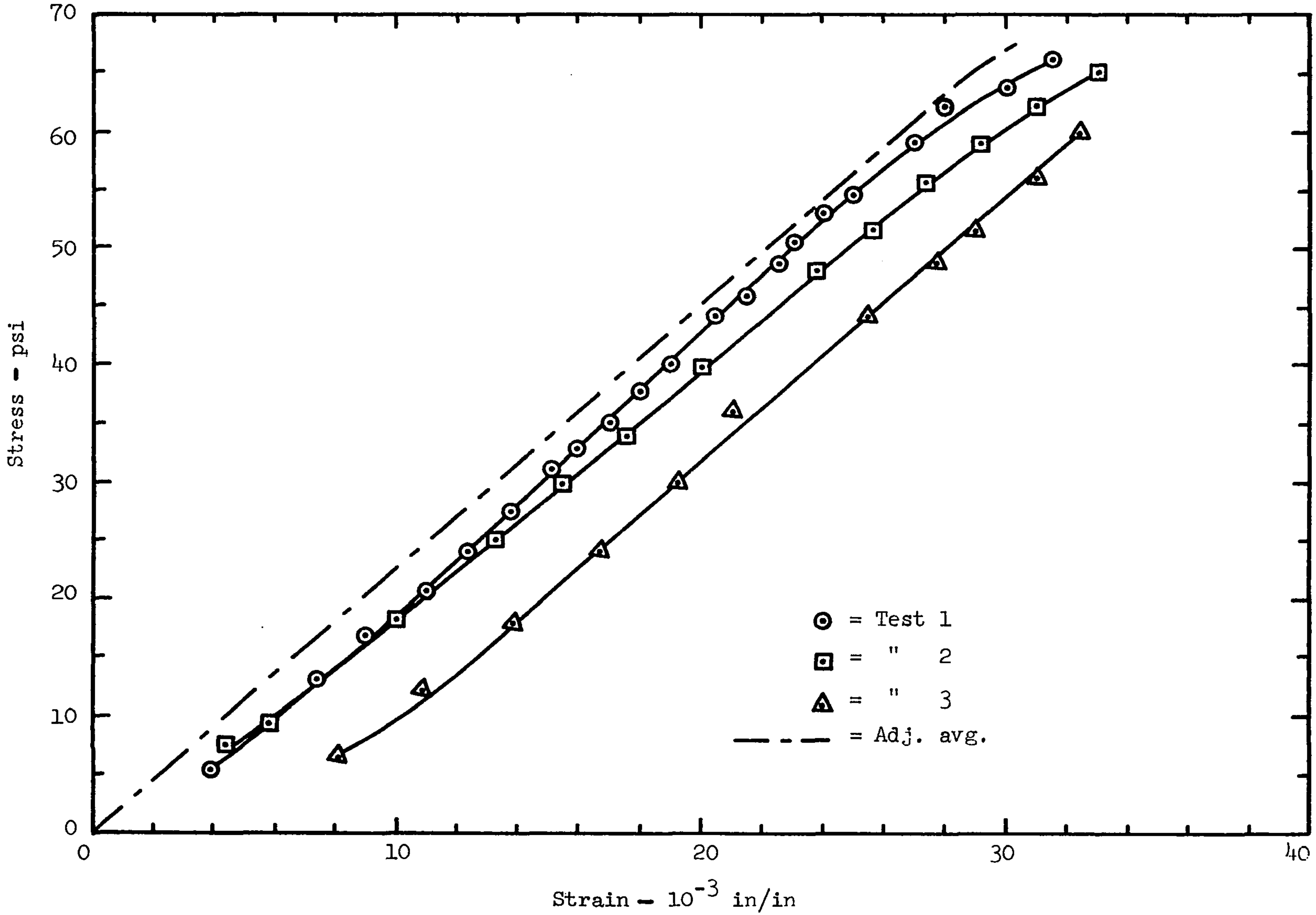

Figure 4-22. Styrofoam HD-300 Tension Stress-Strain Curves.

Shear Tests--As will be noted in Chapter V, linear elastic shear modulus will be needed. The usual procedure in determining shear modulus for aircraft sandwich panels is to use the long-plate shear method outlined in Reference 31. The plate shear method is also described in ASTM C273-61. O'Dell and Graham[32] do not believe that the plate shear method is accurate for weak plastic foams. They feel that torsion methods will soon be feasible since work is currently being done to determine the effect and extent of anisotropy in extruded polystyrene foam. Also shear modulus has been determined by beam flexure methods. One method is to load single-span beams with two different load arrangements and determine midspan deflections for each. The deflections would be expressed in terms of shear and bending modulus which could be obtained from the two simultaneous equations. This method is also useful for determining shear modulus of a composite sandwich as explained in detail by Engel, Hemming, and Merriman.[33]

A short cantilever method was used in this study to determine shear modulus of plastic foams. A method was desired which would be compatible with the special testing machine built for the compression and tension tests. The short cantilever method is actually very similar to the plate shear method but allows some bending action which is then subtracted out. A short cantilever appears quite desirable for this purpose since it allows much larger shear to bending deflection ratios than in simply supported beams. The equations for determining shear modulus for a homogeneous solid are developed in detail.

Total strain energy for an end loaded (load P) cantilever beam of length $\underline{L}$ and cross-sectional area $\underline{A_c}$ is expressed in terms of shear and bending strain energies, U_γ and U_b, as[34]

$$U = U_\gamma + U_b .$$

$$= \int_0^L \frac{C_F V^2(X)}{2A_c G_c} dx + \int_0^L \frac{M^2(X)}{2EI} dx \qquad (4\text{-}1)$$

where $V(X)$ and $M(X)$ are local transverse shear and bending moment, $\underline{G_c}$ is shear modulus, $\underline{E}$ is bending modulus, $\underline{I}$ is bending moment of inertia, and $\underline{C_F}$ is a factor often referred to as "form factor." Factor $\underline{C_F}$ is often erroneously defined as the ratio of the maximum to the average shear stress in a beam. The writer has developed in Appendix A a more rigorous theoretical expression for $\underline{C_F}$. Using the equation from Appendix A, $C_F = 1.2$ for a rectangular cross section. This is quite different from the 1.5 ratio of maximum to average shear stress. The integration of (4-1) gives

$$U = \frac{C_F P^2 L}{2A_c G_c} + \frac{P^2 L^3}{6EI} \qquad (4\text{-}2)$$

Using Castigliano's Theorem,[34] the end deflection may be determined as

$$\delta = \frac{\partial U}{\partial P} \qquad (4\text{-}3)$$

$$= \frac{C_F P L}{A_c G_c} + \frac{P L^3}{3EI} \qquad (4\text{-}4)$$

In equation (4-4) the first term on the right side corresponds to the shear deformation while the second term corresponds to the bending deflection.

When deflection δ and applied load P are measured quantities, geometric properties are known, and bending modulus, E, is assumed, the shear modulus, G_c, remains the only unknown quantity in equation (4-4). The bending modulus used in this study was the average of compression and tension elastic moduli.

Figure 4-11(b) shows the arrangement used to perform the shear tests. Rigid plates were glued to each end of the specimen to allow relatively uniform shear transmission. Deflection was measured by a dial indicator, as shown in Figure 4-11(b), where it was found that rotation of the end plate had negligible effect on transverse deflection measurement.

In each test, a load-deflection point would yield a shear modulus value after applying equation (4-4). This usually consisted of from three to eight points. These individual values of shear modulus were then averaged, excluding the last point in all cases due to large deflections. All of the individual test values of shear modulus for a particular specimen group were then averaged to obtain a final elastic shear modulus value.

Shear test data are given in Appendix B. Shear modulus results are listed in Table 4-2. Large variations in shear modulus are noted between individual tests. This reflects significant end effects, and also indicates that specimen size was probably too small. In the following section, core physical properties will be examined in light of such large variations in foam test results, both by the writer and by Dow Chemical Company.

TABLE 4-2

CORE SHEAR MODULUS RESULTS

Foam	Test No.	Calculated Shear Modulus	Group Average Shear Modulus
Dylite	1	330	
	2	750	
	3	480	519
Dorvon	1	500	
	2	453	
	3	303	
	4	419	419
Styro FR	1	861	
	2	455	
	3	640	651
Styro RM	1	1442	
	2	1424	
	3	2093	1651
Styro HD	1	852	
	2	1351	
	3	1824	1341

D. Correlation of Core Properties

Large variations in test determined physical properties appear inherent in plastic foams. Large variation in stress-strain slopes were noted along with similar large variations in shear modulus calculations. Such scatter in test data of cellular materials is not unusual. Ferrigno[5] illustrated polyurethane foam data which have larger variations than reported herein.

Ferrigno[5] and others showed that foamed plastic strength properties are density dependent. Although nominal densities were given for each of the tested foams, density measurements were conducted and sizable variations were noted. The density measurements are reported in Table 4-3.

A tabulation of compression and tension elastic moduli is given in the Table 4-4, for tests conducted and Dow Chemical Company nominal values. Average measured foam densities are also listed.

Tension and compression elastic modulus values are plotted versus foam density in Figure 4-23. It is noted that the compression value for Styrofoam FR (1.9 pcf nominal density) appears out of line but all other values are very consistent. A sketched average of the compression and tension modulus values was selected to be used in the wrinkling analysis as the isotropic extensional modulus, $\underline{E_c}$. This average modulus is shown as the dashed line in Figure 4-23.

Shear modulus values from Table 4-2 and Dow Chemical Company data[29,32] are plotted versus foam density in Figure 4-24. Very good correlation was obtained with Dow data. An average of the shear modulus values was selected to be used in the wrinkling analysis. This average modulus is shown as the dashed line in Figure 4-24.

TABLE 4-3

FOAM DENSITY MEASUREMENTS

Foam	Board Thickness (in)	Nominal Density (pcf)	Measured Density (pcf)	Avg. Group Density (pcf)
Dylite		1.0		
Dorvon	1	1.0	1.22	
	2	1.0	1.24	
	3	1.0	1.18	
	3	1.0	1.13	
	4	1.0	1.11	1.18
Styro FR	1	1.9	2.13	
	2	1.9	1.95	
	3	1.9	1.78	
	4	1.9	2.02	1.97
Styro RM	2	2.5	2.25	2.25
Styro HD	2	3.3	3.50	3.50

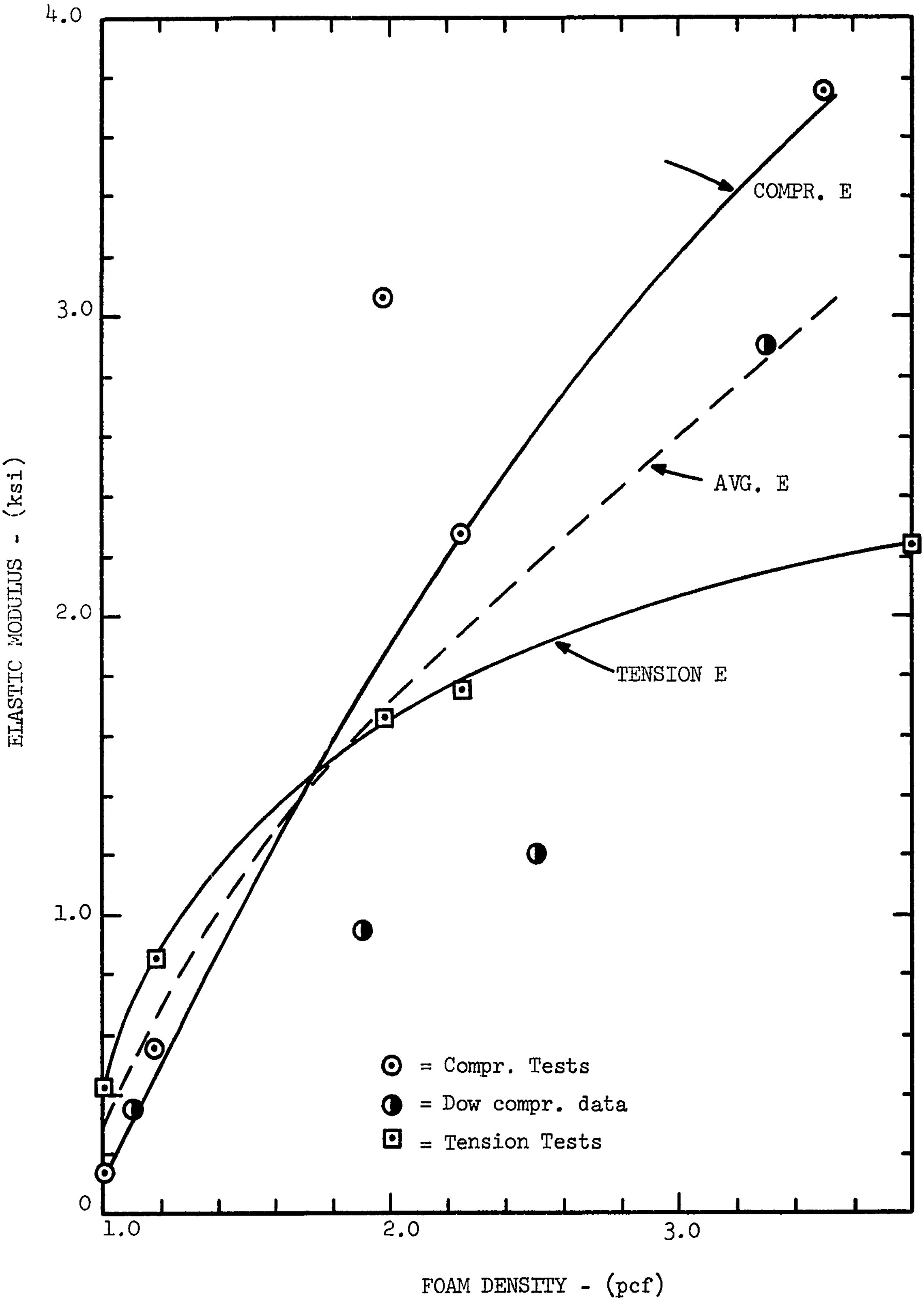

Figure 4-23. Compression and Tension Elastic Moduli as Functions of Foam Density.

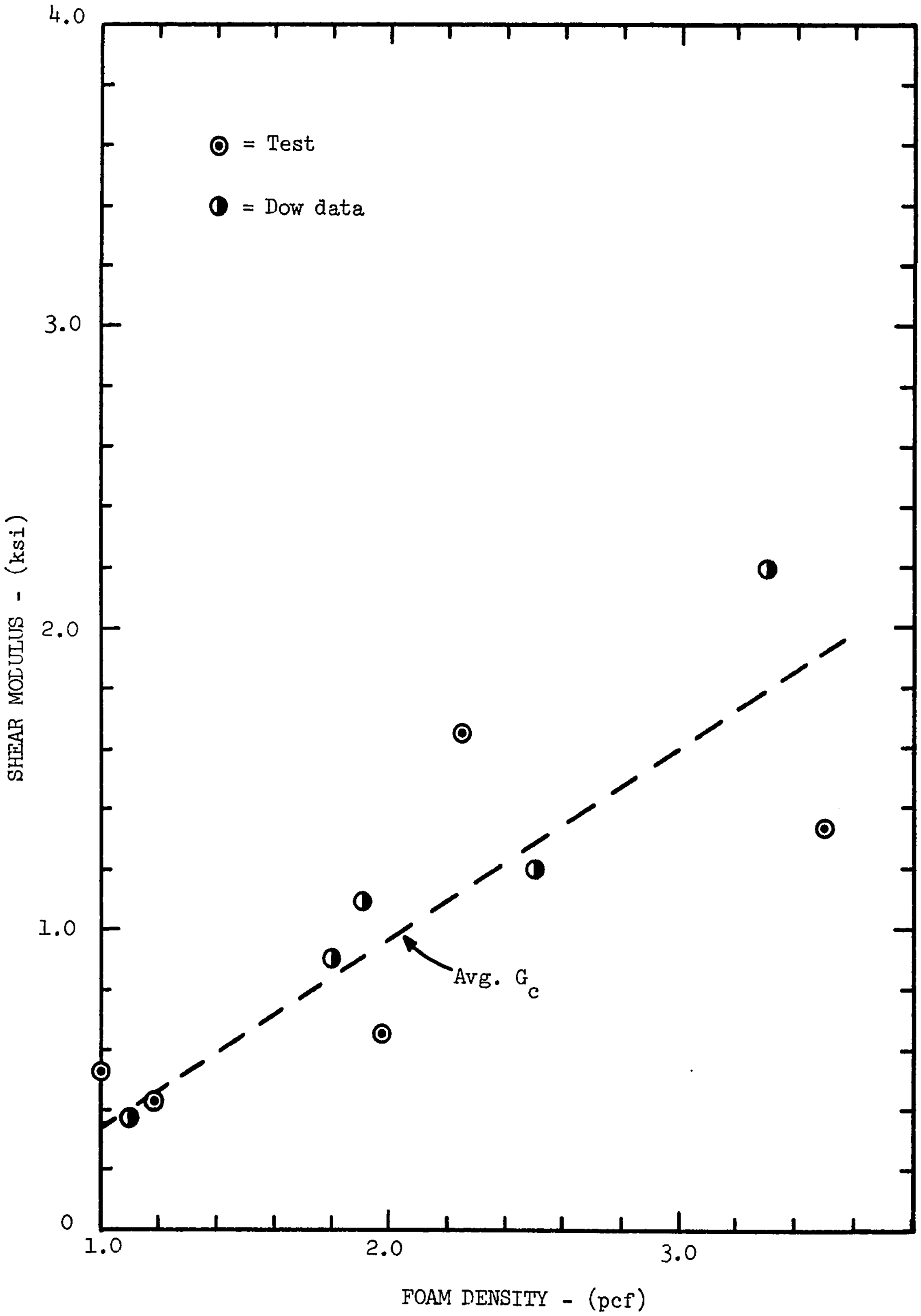

Figure 4-24. Shear Modulus as Function of Foam Density.

TABLE 4-4

SUMMARY OF TENSION AND COMPRESSION ELASTIC MODULUS VALUES FROM TEST AND MANUFACTURER

Foam	Density (pcf)	Compression Modulus Test (psi)	Compression Modulus Dow* (psi)	Tension Modulus Test (psi)
Dylite	1.0	126		416
Dorvon	1.18	556	350	850
Sytro FR	1.97	3060	950	1656
Styro RM	2.25	2278	1200	1752
Styro HD	3.50	3758	2900	2230

*See references 29, 30.

Ultimate Strength of Core--The primary purpose of the core testing program was to determine elastic moduli, however, it was possible to also determine ultimate strengths in all cases. These ultimate strengths are listed in Table 4-5. Also listed are Dow Chemical Company nominal values. Generally, the agreement with Dow data was good except for the shear tests, where test values are much lower than Dow values.

E. Summary of Facing and Core Elastic Constants

Suggested facing elastic compression modulus for use in the sandwich study are listed in Table 4-6.

The previous correlation section on core properties provided consistent elastic moduli values which were suggested for use in the wrinkling study. These values are summarized in Table 4-7.

TABLE 4-5

RESULTS OF TESTS FOR FOAM STRENGTH

Type	Dylite	Dorvon	Styro FR	Styro RM	Styro HD
Tension:					
Bond, Test	23	30	31	35	65
Ult., Test	29	--	65	87	140
Ult., Dow	31	35	70	60(?)	200
Compression:					
Ult., Test	10	12	37	43	89
Ult., Dow	14	14	30	30	120
Shear:					
Ult., Test	9	11	11	13	20
Ult., Dow	-	30	35	35	100

TABLE 4-6

FACING ELASTIC COMPRESSION MODULI

Facing Material	Compression Moduli (10^6 psi)
Douglas fir plywood, 1/4" (A-C Exterior)	1.00
Ash plywood, 1/8"	0.35
Ash plywood, 1/4"	0.14
Standard pressedwood	0.53
Tempered pressedwood	0.73
Cement asbestos	1.12

TABLE 4-7

CORE ELASTIC EXTENSIONAL AND SHEAR MODULI

Material	Ext. Mod., E_c (psi)	Shear Mod., G_c (psi)
Dylite	620	450
Dorvon	620	450
Styro FR	1680	950
Styro RM	1950	1130
Styro HD	3030	1920

F. Composite Sandwich Tests

This section deals with the heart of the experimental program. The purposes of these tests were (1) to record the structural behavior of short architectural type, foamed-filled sandwiches under uniaxial compressive loading, and (2) to provide a statistical base for developing semi-empirical failure prediction techniques.

Tests were planned in a parametric manner to systematically vary facing and core combinations of physical and geometric properties. Of the 25 combinations, at least three sandwiches were tested in each group, except for four groups near the end of the program which had only two tests each. There were 83 tests conducted on glued sandwiches plus nine additional tests on controlled unbonded specimens. Koppers Company provided plywood faced, Dylite foamed-in-place panels in three nominal thicknesses of 2, 4, and 7 inches. There were 18 short column tests conducted on the Dylite panels.

Test Specimen Sizes--The guide lines set down for sizing aircraft sandwich test specimens[31] were followed as closely as possible. This included specifications that edgewise compression specimens shall be at least 2 inches wide, but not less than twice the sandwich thickness, and shall have an unsupported length not greater than eight times the sandwich thickness. After several experiments the nominal width and length of 6 and 12 inches, respectively, were chosen. The 12 inch length was considered sufficient since the maximum wrinkling half-wave length was estimated to be 5 inches. The 6 inch width was convenient although it violated the aircraft standard for sandwiches over 3 inches thick. This did not affect results.

Fabrication of Sandwiches--It was decided early in the program that more accurate control on sandwich fabrication could be achieved in laboratory lay-up rather than contracting with an outside fabricator.

Fabrication procedures suggested by Dow Chemical Company[23,26,35] were closely followed. Glueing information was provided by United States Plywood Corporation.[36]

Resorcinol adhesive was applied with a 3 inch wide roller spreader at the spreading rate of 0.2 grams per square inch. The adhesive was applied to the core and then laminated with the facing. After adhesive application the sandwiches were cured overnight under room temperature at approximately 6 psi. After a one-day cure the specimens were cut to proper size. The panels were then allowed to cure a week before testing.

The curing press had to be designed and fabricated since existing hydraulic presses were not considered reliable to hold such close tolerance on pressure. The press was a simple beam arrangement having four screw down bars applying mechanical pressure through plywood plattens. Two views of this press are shown in Figure 4-25. Curing pressure was determined by the compressive deflection, using Hooke's Law and neglecting facing deformations. That is,

$$\text{pressure} = \frac{E_c \text{ x deflection}}{\text{Total foam thickness}}$$

Test Equipment--The test equipment consisted of a 60,000 pound compression testing machine and auxiliary deflection and strain measuring equipment.

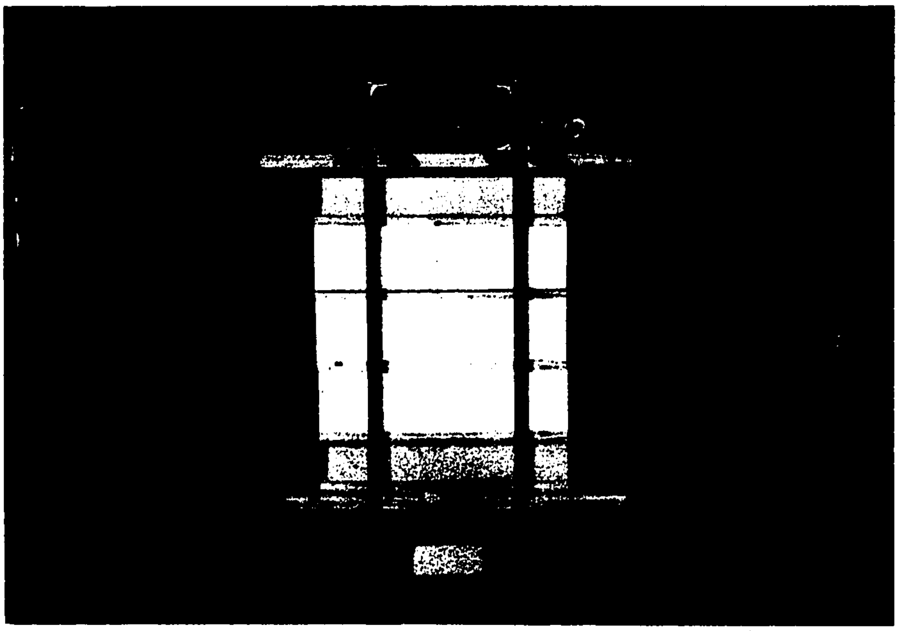

Figure 4-25. Curing Press for Sandwich Fabrication.

The testing machine was a Riehle Model FH-60 equipped with electric type load cell. Load was applied through a spherical head.

Sandwich lateral deflections were measured by a tree arrangement of six deflection gages mounted at the quarter points on each face.

Photographs of a typical sandwich test set-up are shown in Figure 4-26. The testing machine and instrumentation arrangement are also shown.

There was strain gage instrumentation on at least one test for each type of facing material. As suggested by FPL,[37] one-inch gage length SR-4 wire strain gages were used and were applied with nitrocellulose cement. The gages were type A-12 manufactured by Baldwin-Lima-Hamilton Corporation. The strain indicator was a Budd Model P-350 having AC or battery supply. Battery power was used to eliminate fluctuations of the balance needle. The switch and balance unit was a ten channel, individual balancing, Budd Model SB-1.

<u>Test Schedule</u>--The following table shows the testing schedule of sandwich facing and core combinations. The numbers in parenthesis following the core material abbreviations are the core nominal thicknesses in inches.

Facing	Core
1/4" Douglas fir plywood	FR(1,2,3,4), Dorvon(1,2,3,4), RM(2), HD(2), Dylite(2,4,7)
3/16" Temp. pressedwood	FR(3), Dorvon(3)
1/8" Temp. pressedwood	FR(3), Dorvon(3)
1/4" Std. pressedwood	FR(3), Dorvon(3)
3/16" Std. pressedwood	FR(3), Dorvon(3)
1/8" Std. pressedwood	FR(3)
1/4" Ash plywood	FR(3), Dorvon(3)
1/8" Ash plywood	FR(3), Dorvon(3)
1/8" Cement asbestos	FR(3), Dorvon(3)

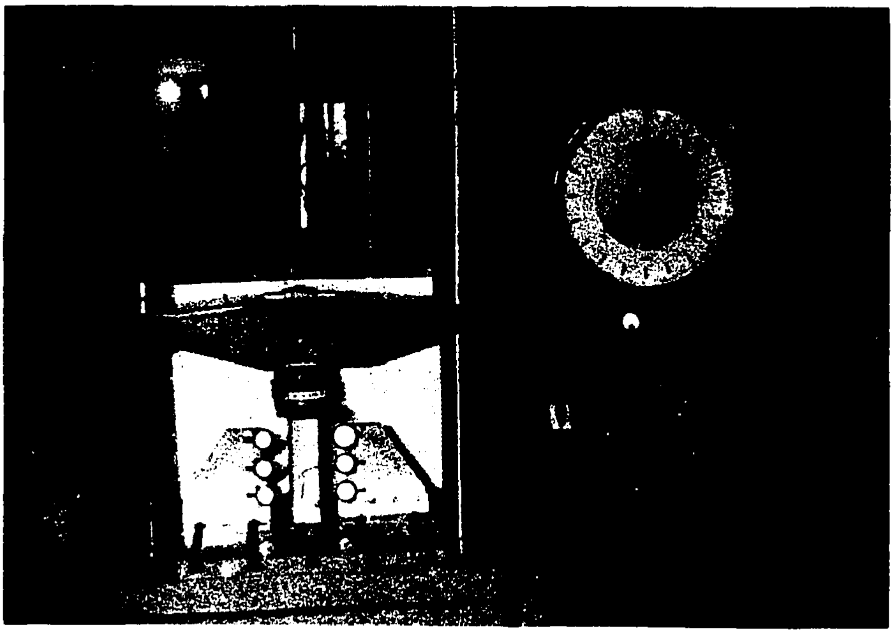

Figure 4-26. Sandwich Test Set-up Showing Testing Machine and Instrumentation.

Introduction to Test Results--The sandwich tests were performed with little difficulty. Generally, the mode of failure was identified as face wrinkling. There were indistinguishable cases where the failure appeared as possible facing compression failure. However, all of these cases indicated slight lateral deflections before failure as in wrinkling. All of the indistinguishable cases failed at stress levels very close to other cases which were definitely identified as wrinkling failures. The compression failure limit was difficult to define due to the large strength increases discovered in composite sandwich stress-strain relationships when compared with individual facing test data.

Strain Gage Results--The first specimen tested with strain gages was also intended to survey the axial strain distribution to see if it was uniform laterally across the faces. Three longitudinal gages were mounted at midlength on each side. One was mounted along the center and the other two were mounted one inch in from each side of the 6 inch wide specimen. The results were excellent as shown by the stress-strain curves in Figure 4-27 for the North face and in Figure 4-28 for the South face. Five of the six gages produced almost identical strains. This indicates that the applied load was very uniform over each end of each face and that the load was transmitted very uniformly throughout the facings.

Strain gage test results are reported in graphical form in Figures 4-27 through 4-39. The following tabulation lists the sandwich combination and the corresponding figure number.

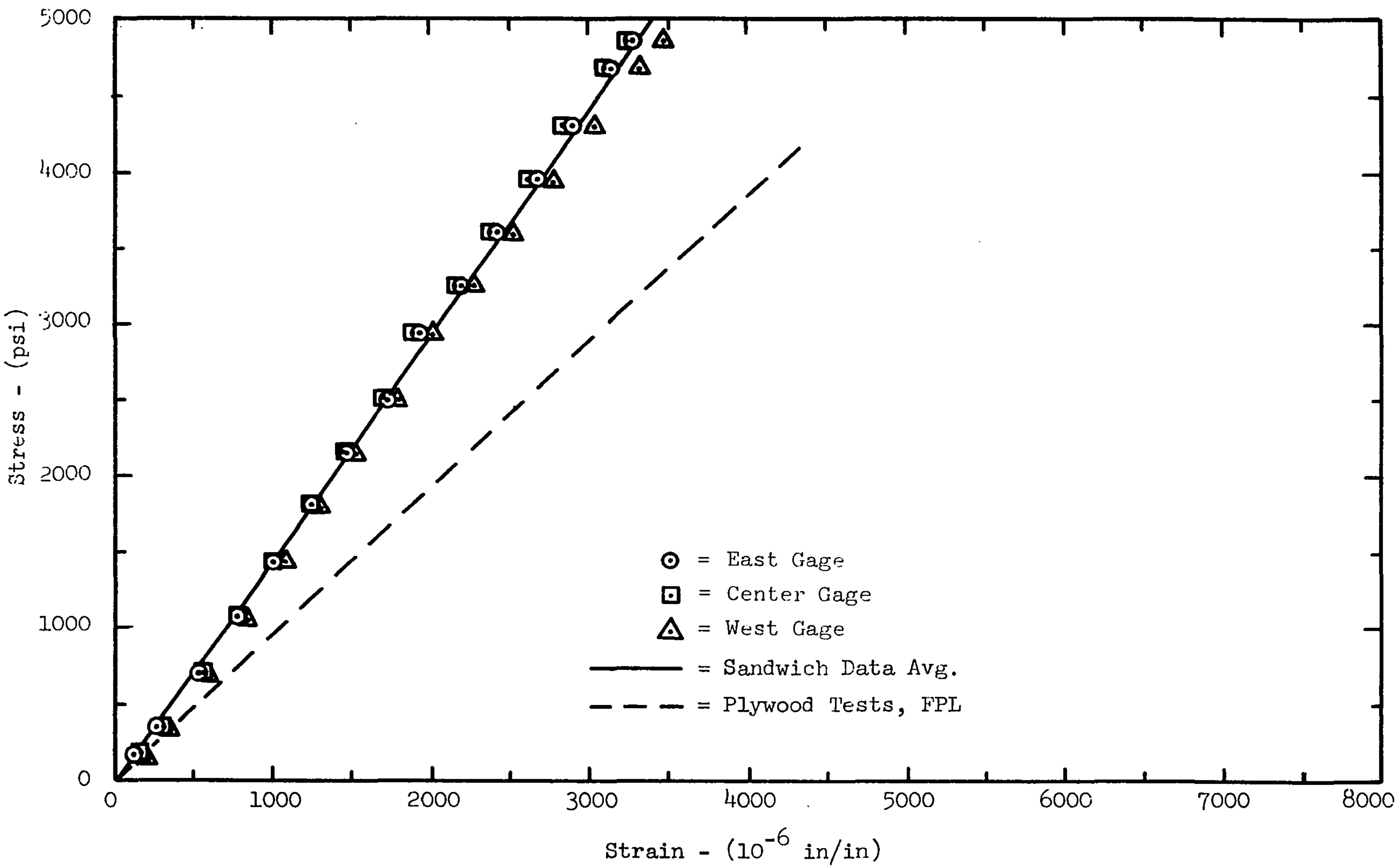

Figure 4-27. Strain Gage Test Data for North Face of Sandwich with 1/4 in. Douglas Fir Faces, 3 in. Styro FR Core.

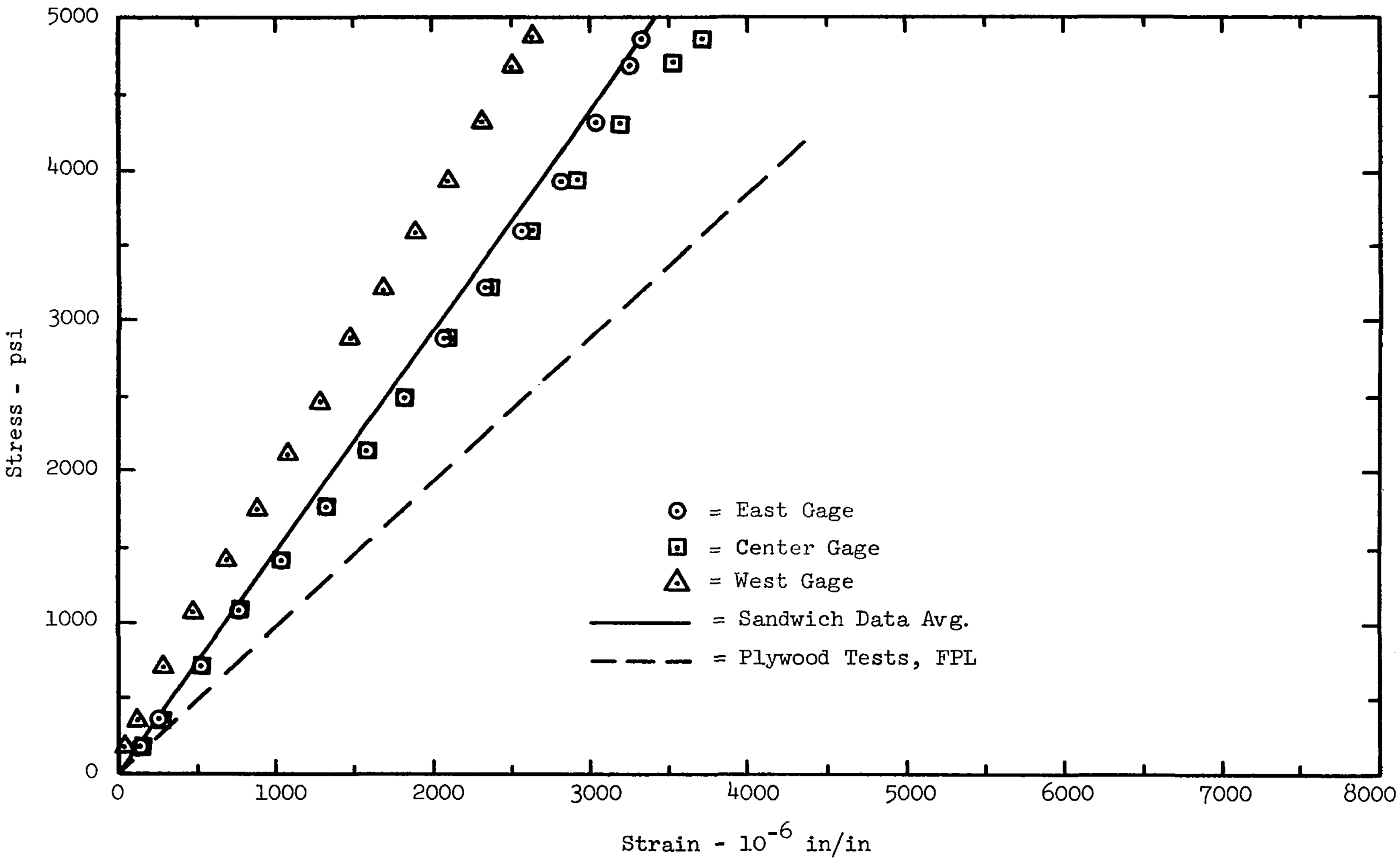

Figure 4-28. Strain Gage Test Data for South Face of Sandwich with 1/4 in. Douglas Fir Faces, 3 in. Styro FR Core.

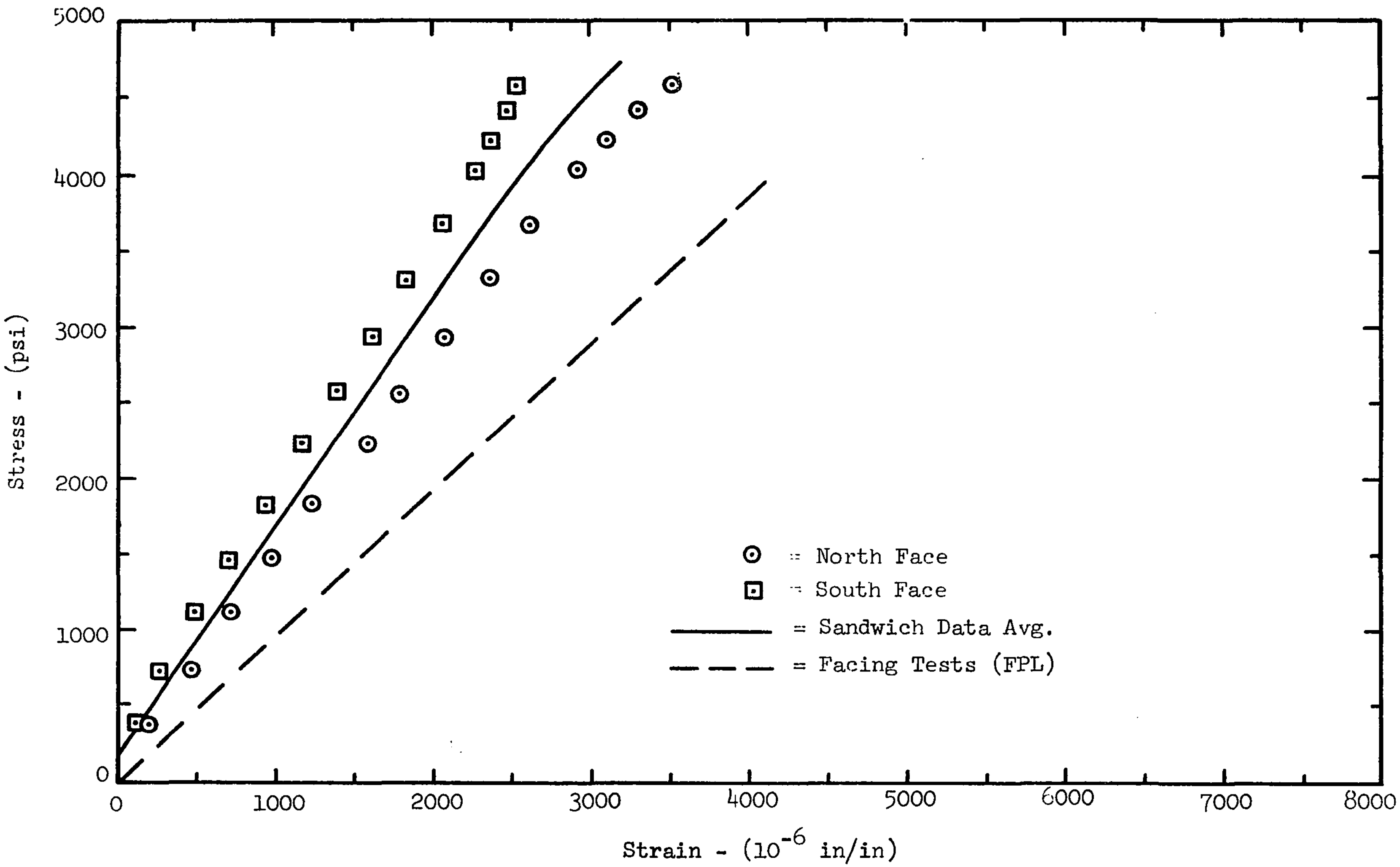

Figure 4-29. Strain Gage Test Data for Sandwich with 1/4 in. Douglas Fir Faces, 3 in. Dorvon Core.

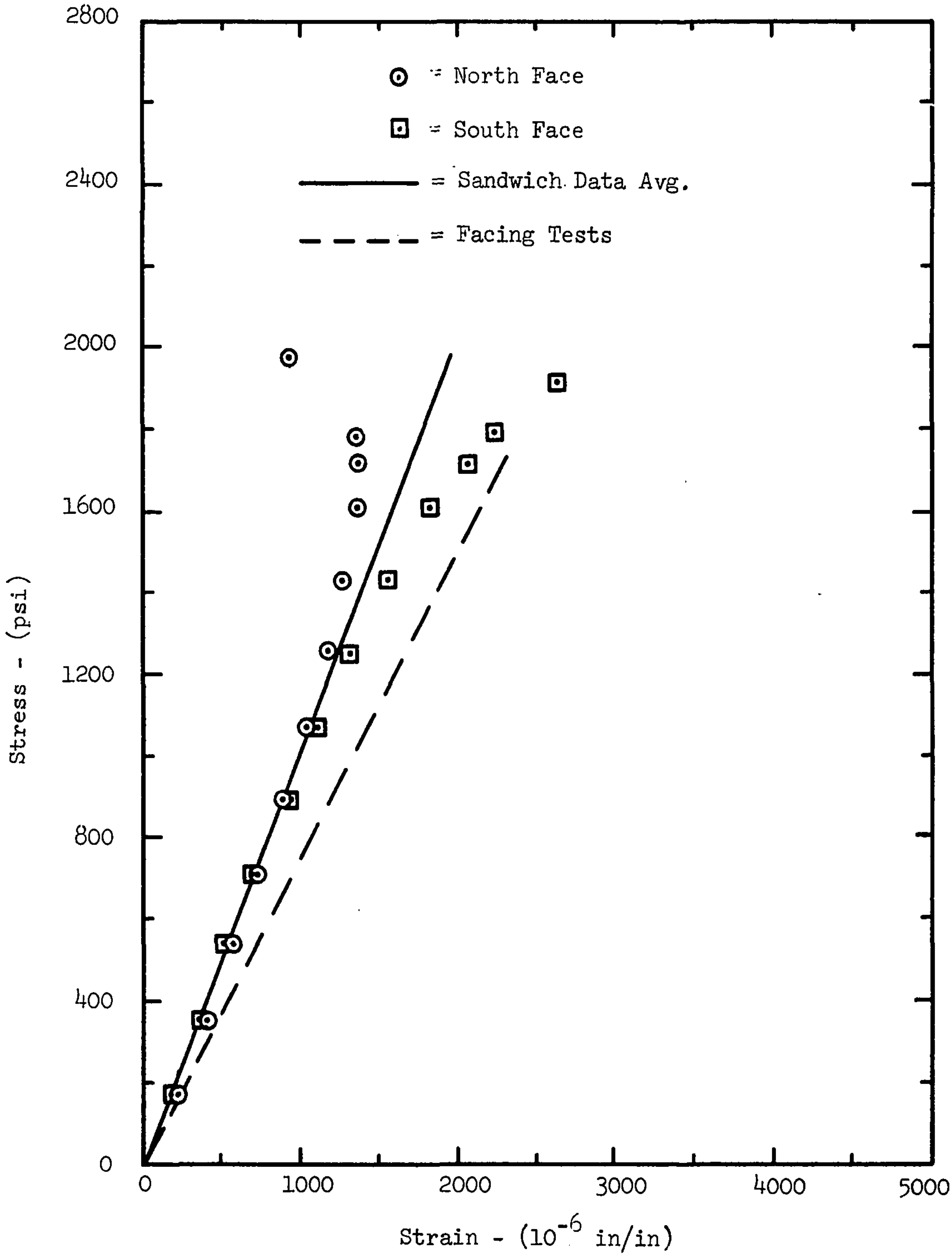

Figure 4-30. Strain Gage Test Data for Sandwich with 1/4 in. Douglas Fir Faces, 2 in. Dylite Foam Core.

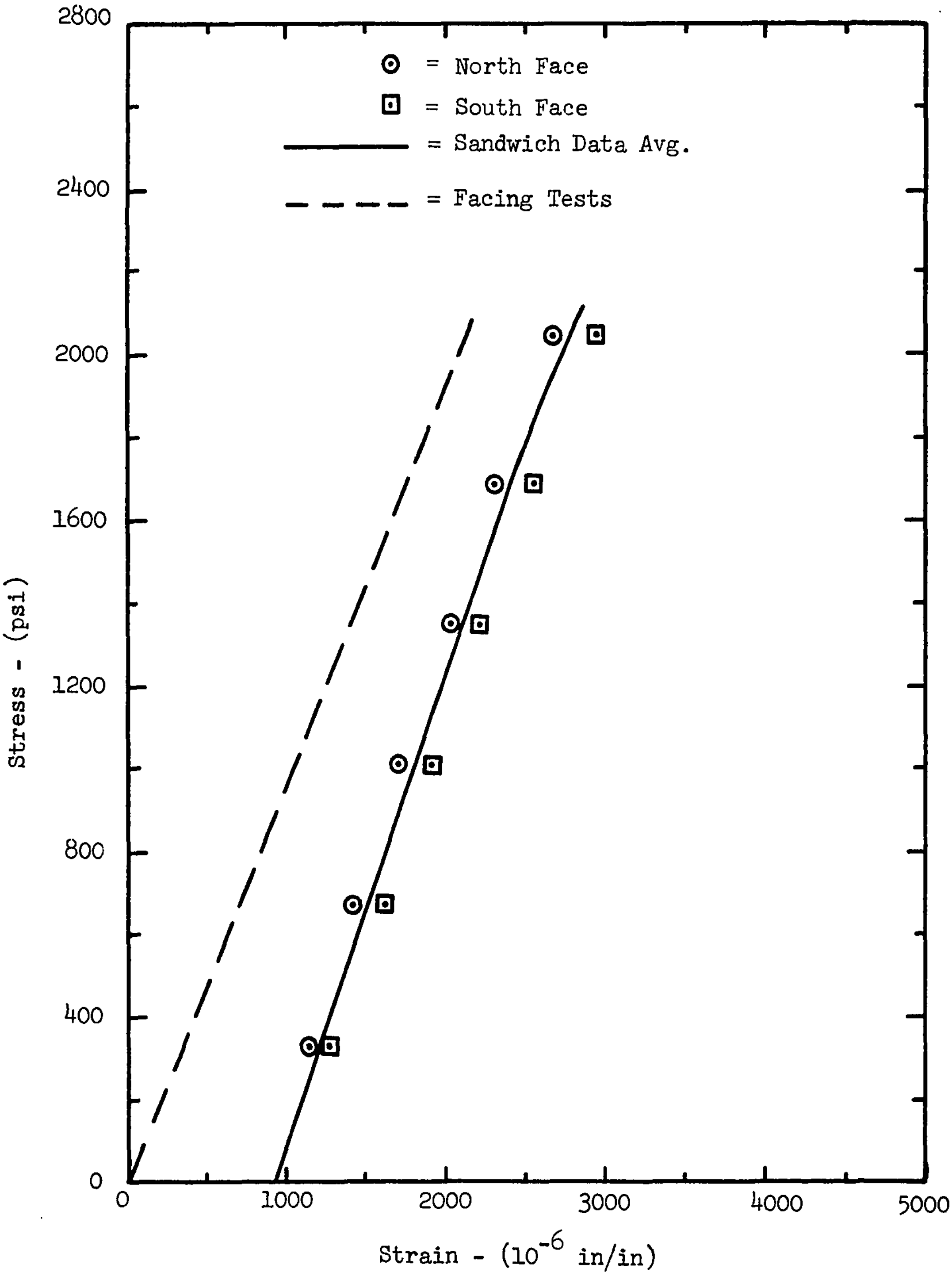

Figure 4-31. Strain Gage Test Data for Sandwich with 1/4 in. Douglas Fir Faces, 4 in. Dylite Foam Core.

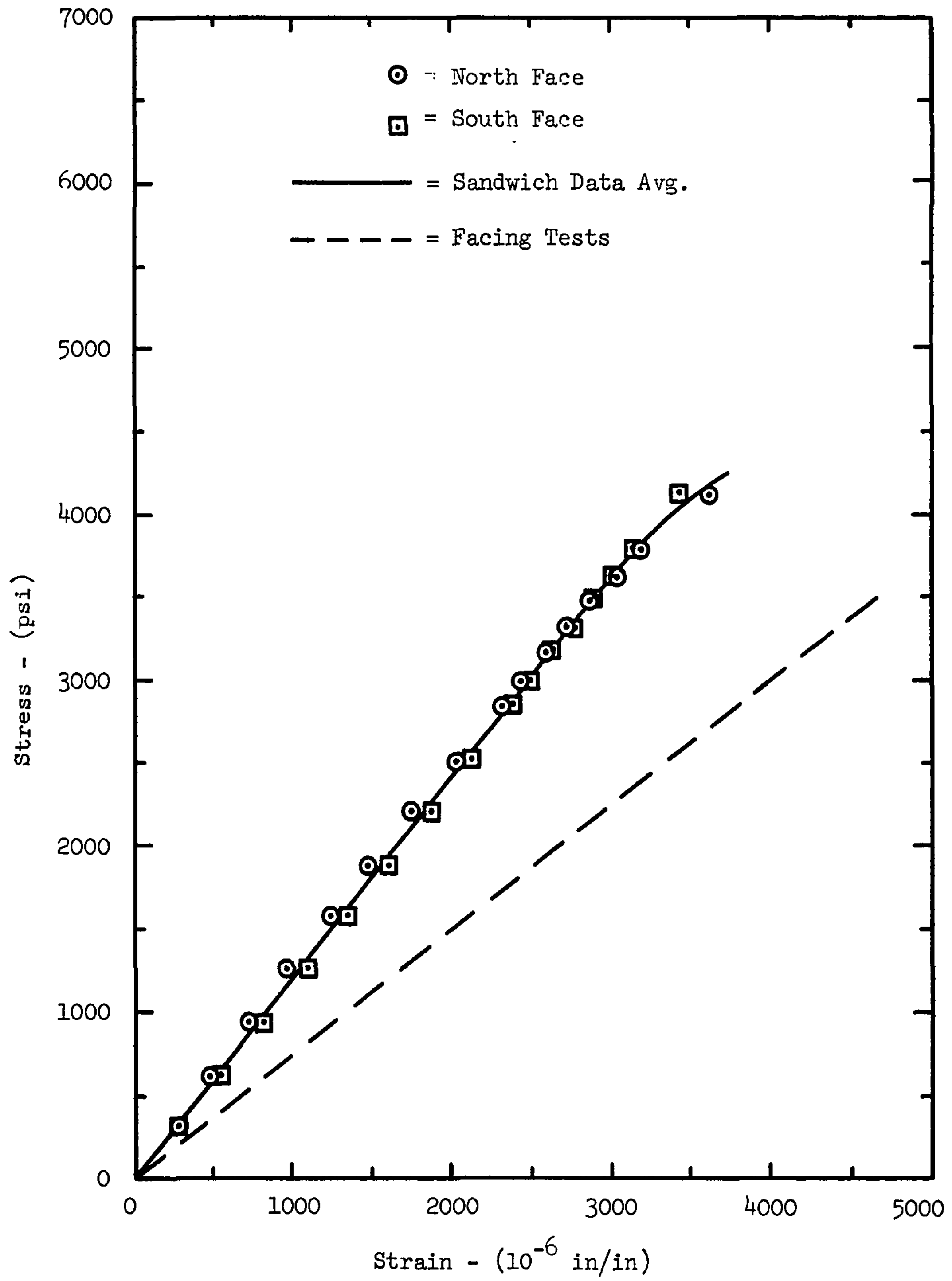

Figure 4-32. Strain Gage Test Data for Sandwich with 1/4 in. Douglas Fir Faces, 7 in. Dylite Foam Core.

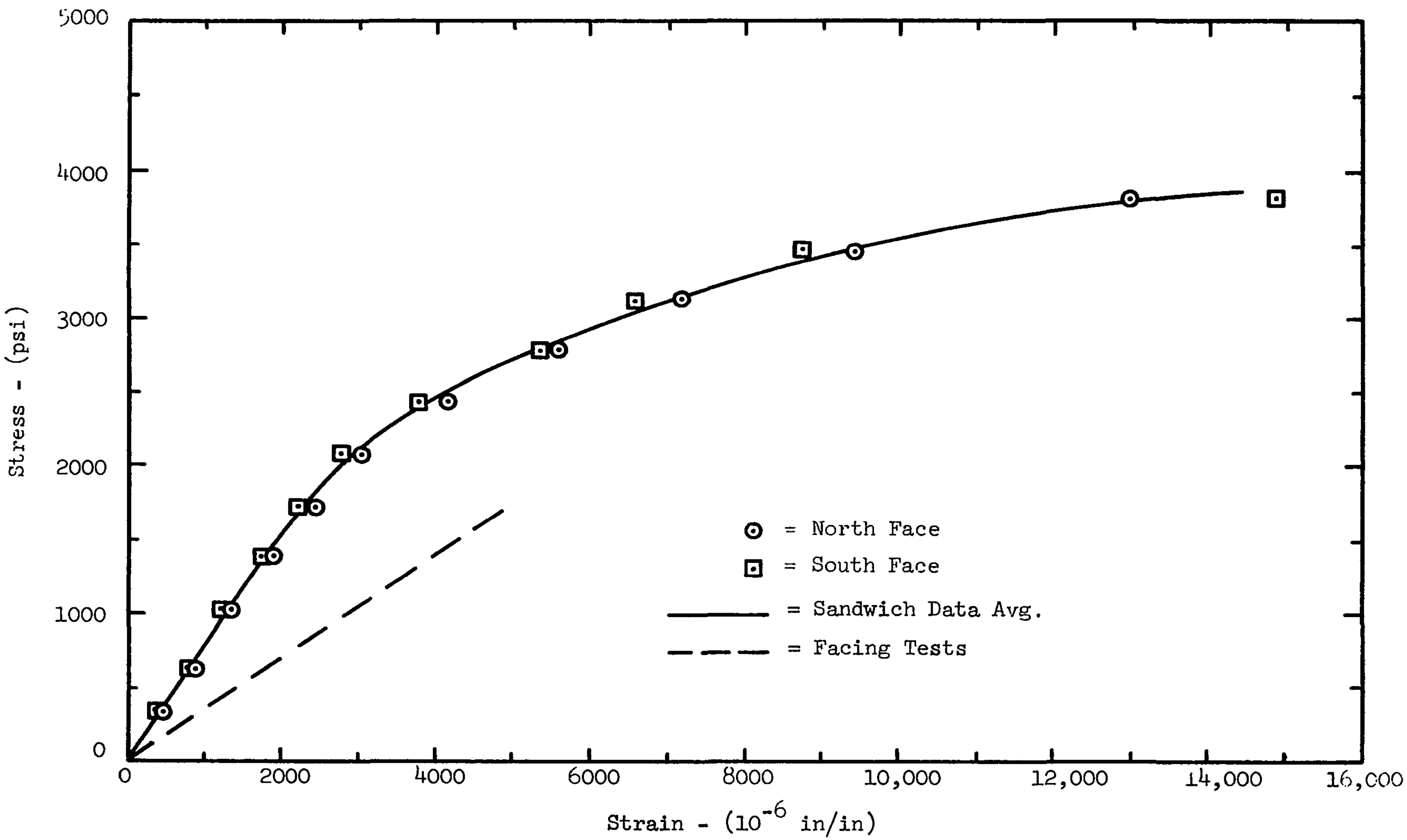

Figure 4-33. Strain Gage Test Data for Sandwich with 1/8 in. Ash Plywood Faces, 3 in. Styro FR Core.

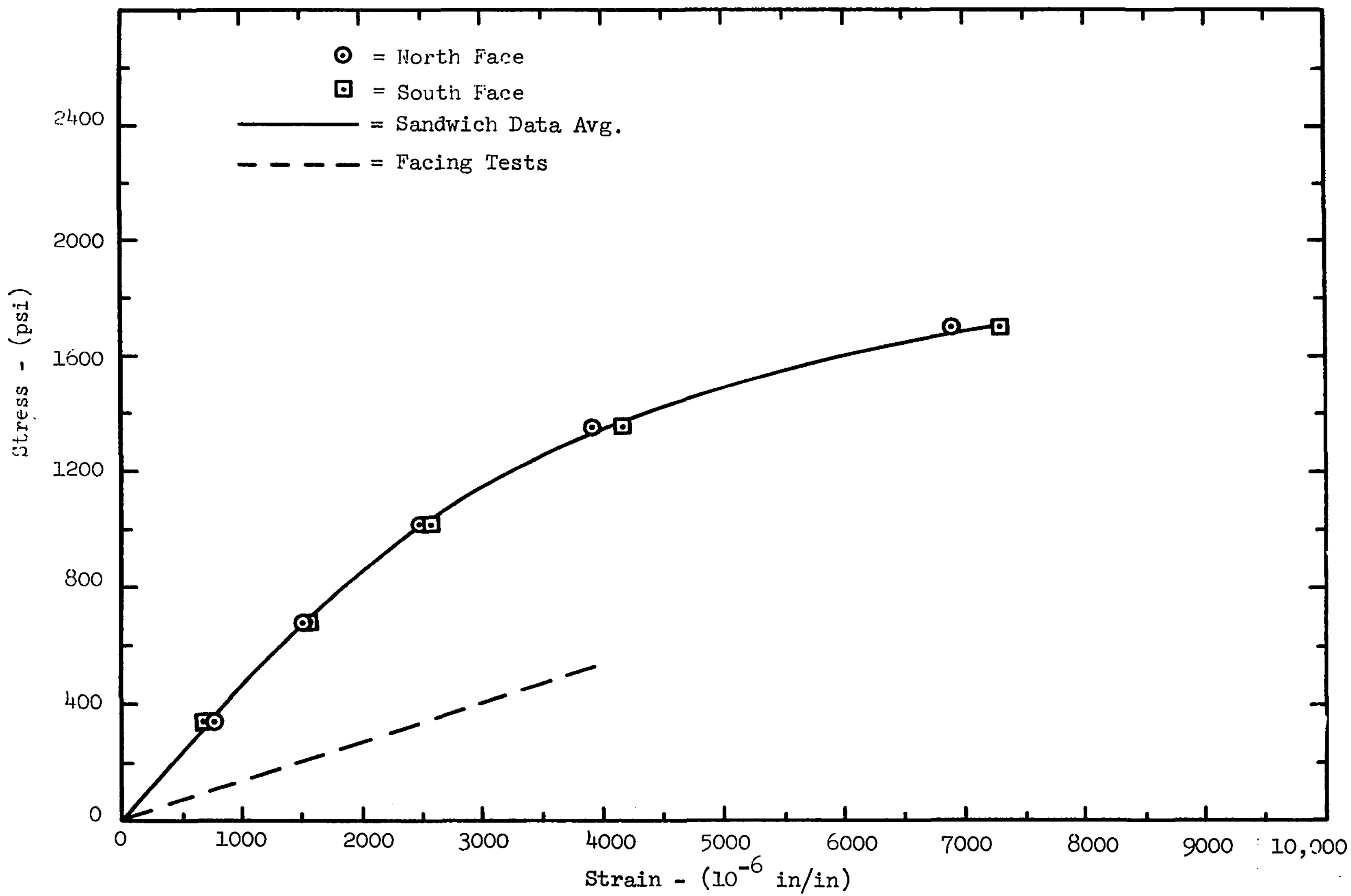

Figure 4-34. Strain Gage Test Data for Sandwich with 1/4 in. Ash Plywood Faces, 3 in. Dorvon Core.

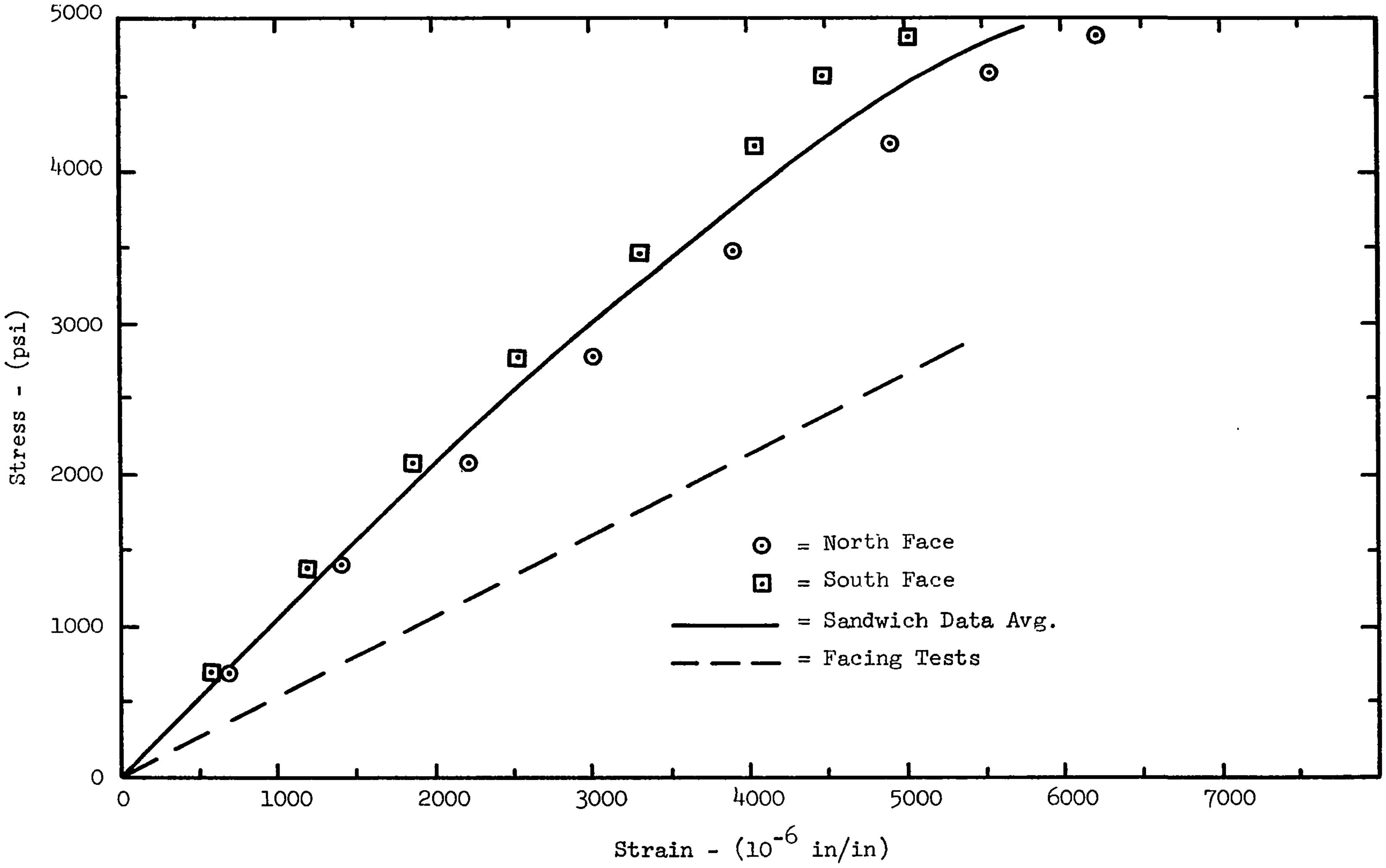

Figure 4-35. Strain Gage Test Data for Sandwich with 1/8 in. Standard Pressedwood Faces, 3 in. Styro FR Core.

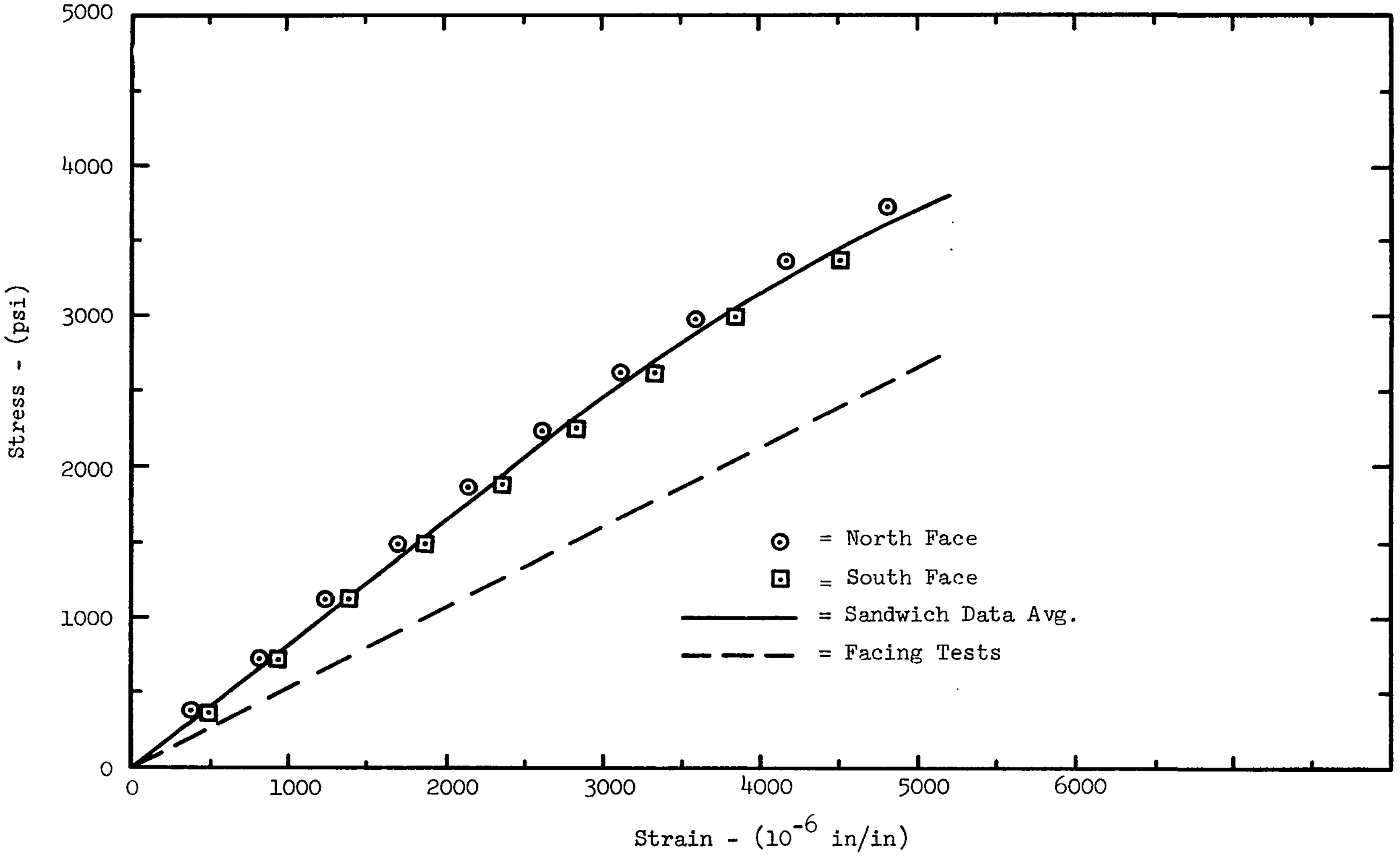

Figure 4-36. Strain Gage Test Data for Sandwich with 1/4 in. Standard Pressedwood Faces, 3 in. Styro FR Core.

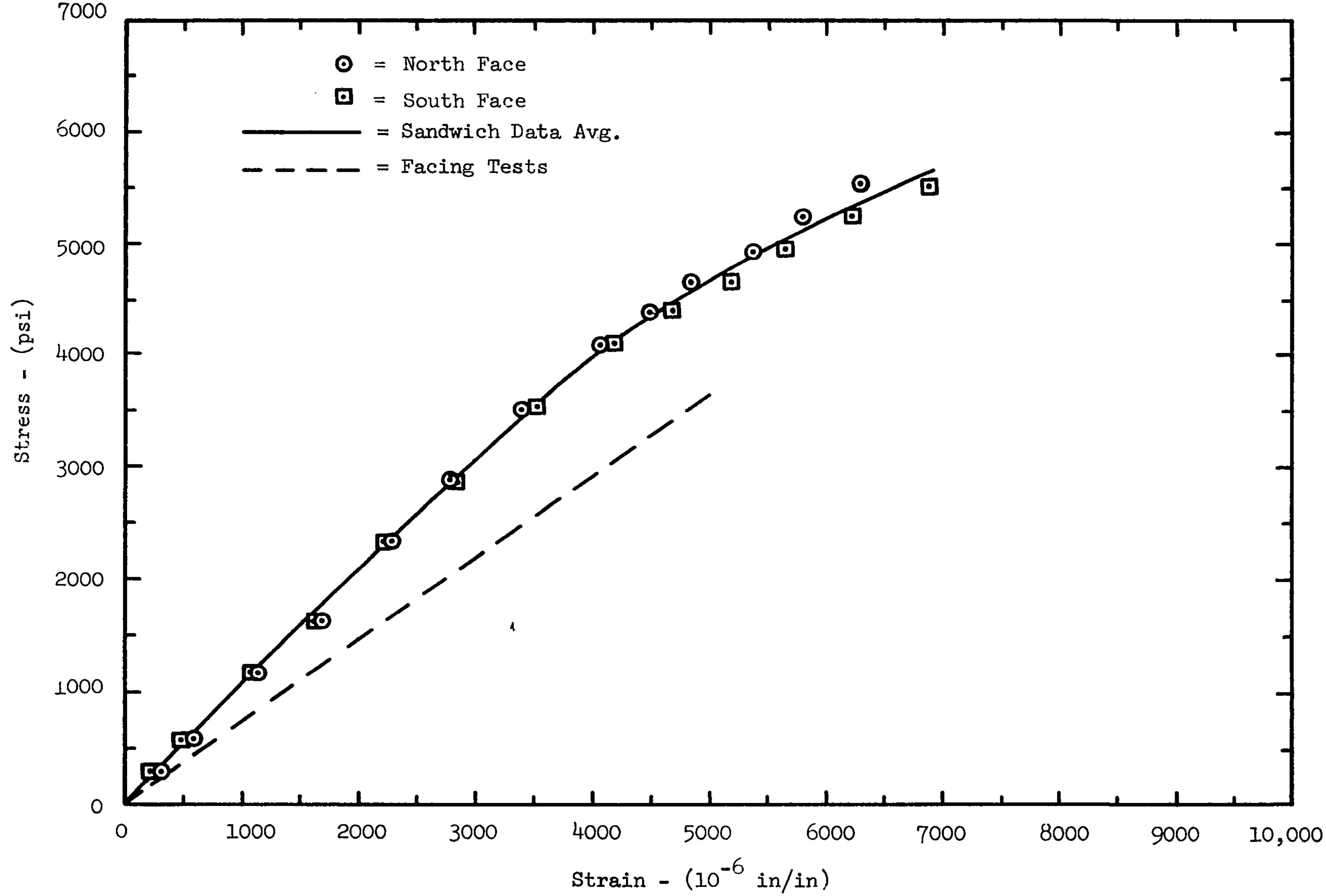

Figure 4-37. Strain Gage Test Data for Sandwich with 1/8 in. Tempered Pressedwood Faces, 3 in. Styro FR Core.

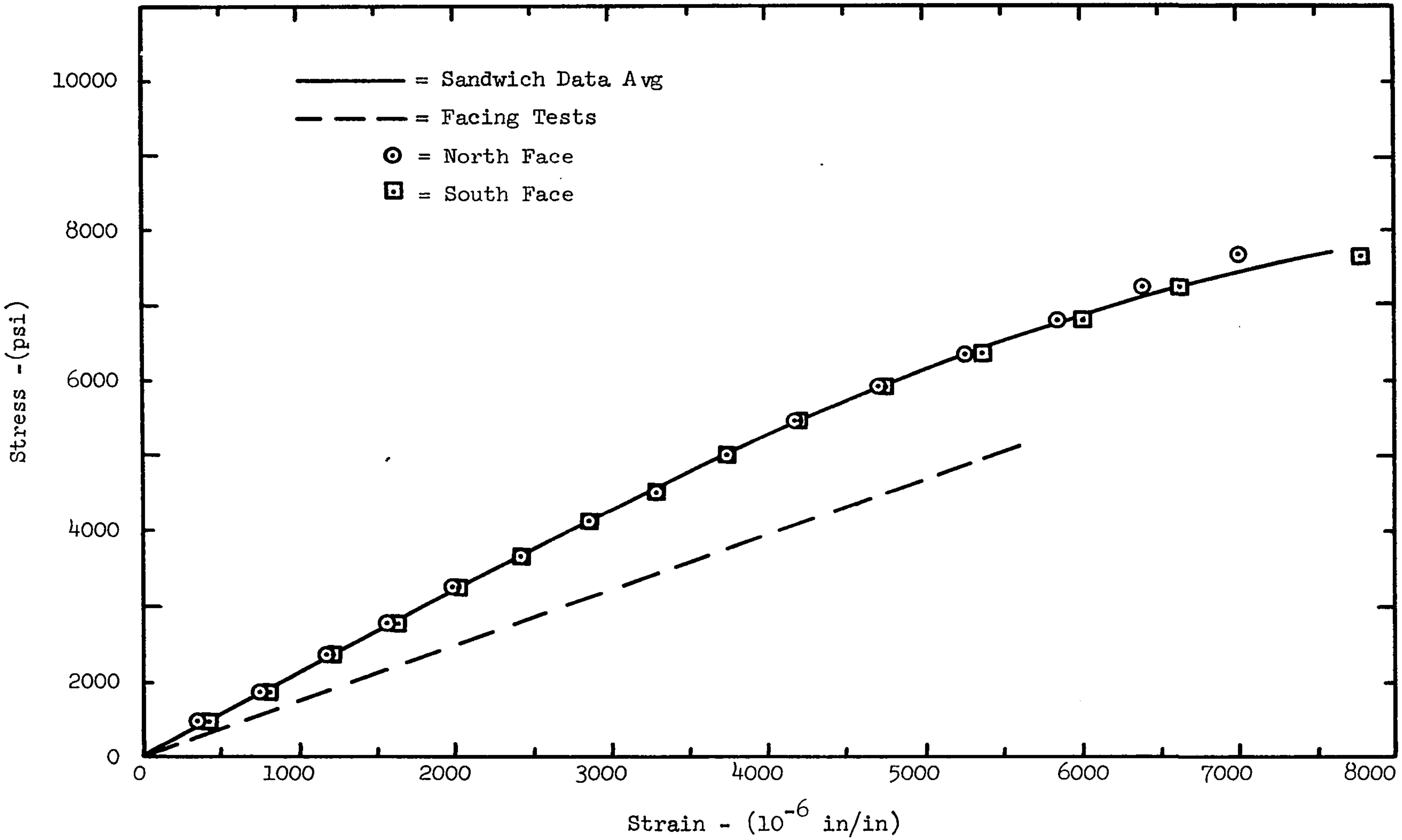

Figure 4-38. Strain Gage Test Data for Sandwich with 3/16 in. Tempered Pressedwood Faces, 3 in. Styro FR Core.

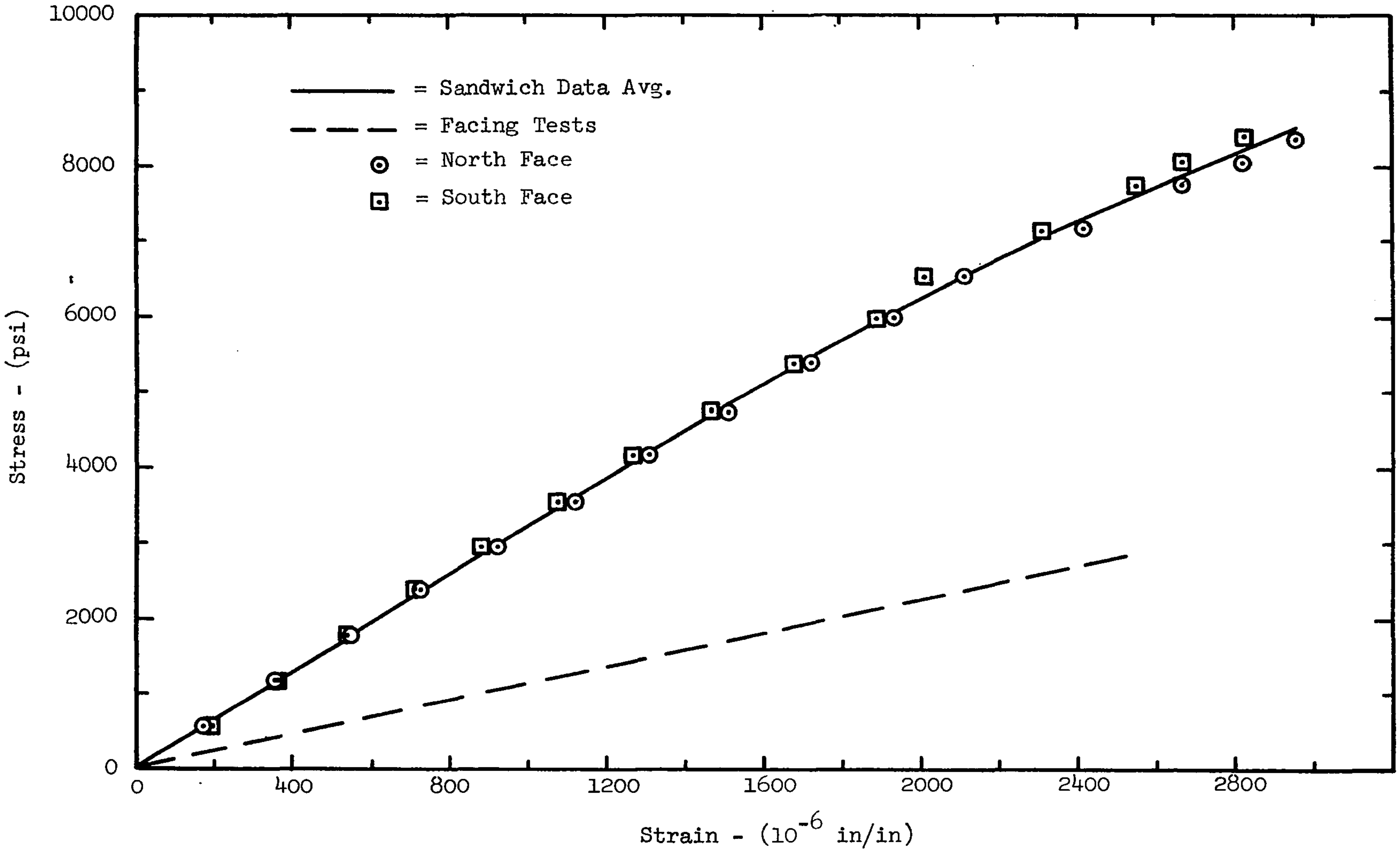

Figure 4-39. Strain Gage Test Data for Sandwich with 1/8 in. Cement Asbestos Faces, 3 in. Styro FR Core.

Sandwich		Figure Number
Facing	Core	
1/4" Douglas fir	3" Styro FR	4-27, 28
1/4" Douglas fir	3" Dorvon	4-29
1/4" Douglas fir	2" Dylite	4-30
1/4" Douglas fir	4" Dylite	4-31
1/4" Douglas fir	7" Dylite	4-32
1/8" Ash	3" Styro FR	4-33
1/4" Ash	3" Dorvon	4-34
1/8" Std. Pressedwood	3" Styro FR	4-35
1/4" Std. Pressedwood	3" Styro FR	4-36
1/8" Temp. Pressedwood	3" Styro FR	4-37
3/16" Temp. Pressedwood	3" Styro FR	4-38
1/8" Cem. asbestos	3" Styro FR	4-39

As noted in the stress-strain curves, only very small bending effects were encountered until the specimen approached failure. The most significant fact noted was the difference in slopes between the sandwich test data and the individual facing test data. The facing test results are shown as dashed lines in the above mentioned figures. The differences in the composite sandwich tests and the individual facing tests are summarized in Table 4-8. A discussion of the apparent increase in compressive strength of the composite sandwich over the individual facing material is presented in Chapter V, "Development of Face Wrinkling Theory."

Buckling Data--Of the 87 glued sandwiches which were tested, 45 definitely failed in a wrinkling type buckle and 38 tests were indistinguishable but believed to be possible wrinkle type buckle failures. There were four invalid tests. All of the 19 foamed-in-place Dylite panels tested as short columns definitely failed in face wrinkling.

Excellent examples of symmetric type wrinkles are shown in Figure 4-40. These panels were of 1/4 inch ash plywood faces and

TABLE 4-8

FACING COMPRESSION MODULI, COMPOSITE SANDWICH TESTS AND FACING TESTS

Material (Face/core)	Compression Modulus, E_f Sand. Tests (10^6 psi)	Compression Modulus, E_f Facing Tests (10^6 psi)	Ratio of Test Results (Sand./Fac.)
DF/3" FR	1.48	1.00	1.48
DF/3" Dorvon	1.49	1.00	1.49
DF/2" Dylite	1.02	0.75	1.36
DF/4" Dylite	1.16	0.75	1.55
DF/7" Dylite	1.21	0.75	1.61
1/8 Ash/3" FR	0.76	0.35	2.17
1/4 Ash/3" Dorvon	0.47	0.14	3.36
1/8 Std.P.W./3" FR	1.04	0.53	1.96
1/4 Std.P.W./3" FR	0.83	0.53	1.57
1/8 Tem.P.W./3" FR	1.03	0.73	1.41
3/16 Tem.P.W./3" FR	1.10	0.73	1.51
1/8 Cem.Asb./3" FR	3.20	1.12	2.86

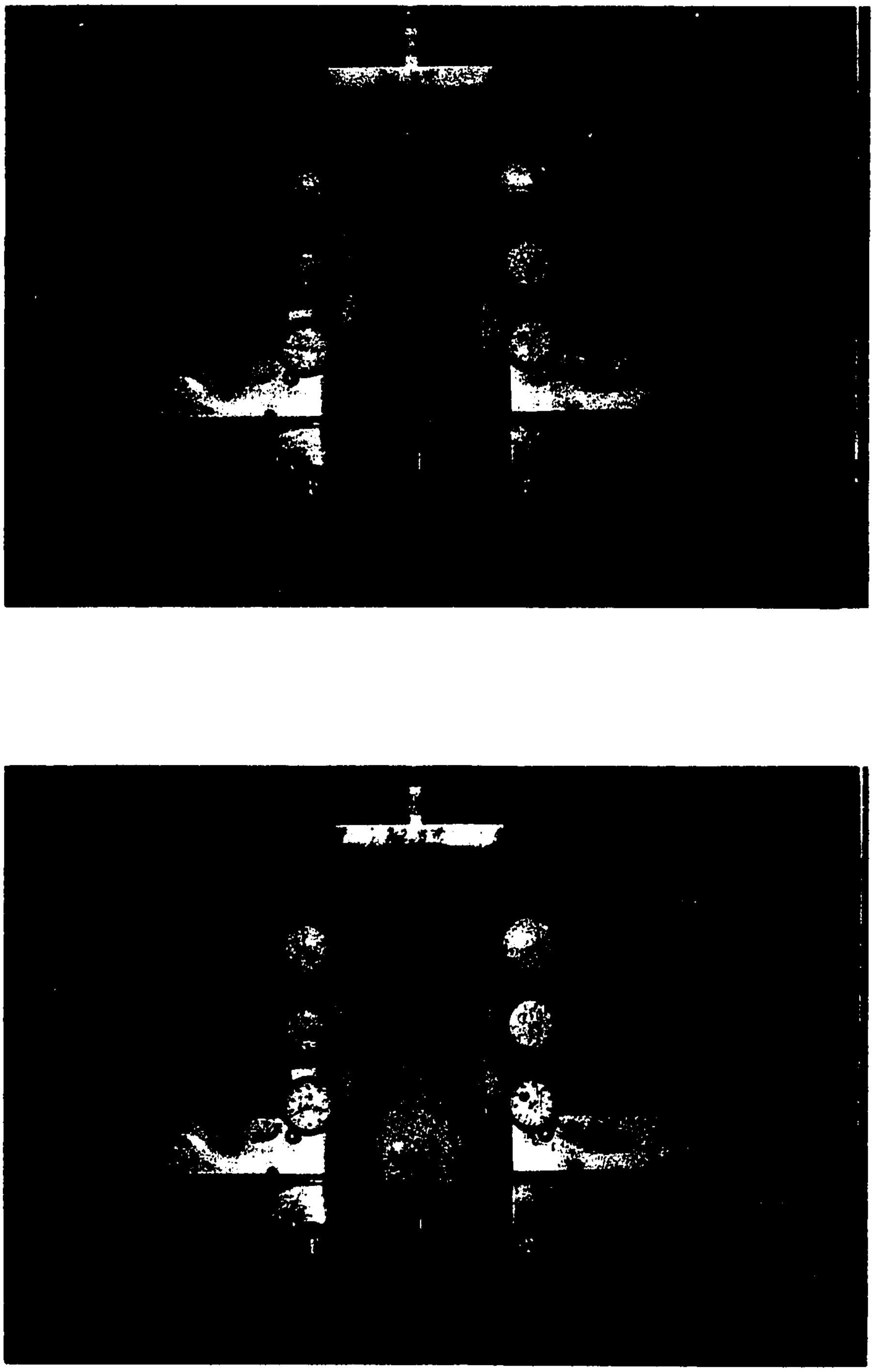

Figure 4-40. Typical Sandwich Column Test Exhibiting Symmetrical Face Wrinkling Failure.

3 inch Styrofoam FR cores. In these two tests the theoretical critical buckling half wave length was 0.91 inches which agrees well with the observed results.

A typical example of anti-symmetrical wrinkling is shown in Figure 4-41. Also shown in this figure is a photograph of postbuckling damage to a sandwich in which wrinkling was not distinguishable.

A listing of results from all sandwich tests is presented in Table 4-9. This table presents measured facing and core thicknesses, midspan deflections, failure facing stresses, and observed failure modes. The facing material abbreviations used were:

D.F. Ply. = Douglas fir plywood

Temp. Pw. = Tempered pressedwood

Std. Pw. = Standard pressedwood

Ash Ply. = Ash plywood

Cem. Asb. = Cement asbestos

The available midspan deflections are listed for the North and South faces. These deflection values correspond to the last measured values just before failure. The observed failure modes are listed as W or I. The W indicates definite face wrinkling failure. The I indicates indistinguishable failure mode, often appearing as a compression failure.

As will be discussed in Chapter V, "Development of Face Wrinkling Theory," the type of wrinkling which should precipitate failure, symmetrical or anti-symmetrical, is theoretically predictable. However, it was observed that the final failure configuration was not always the one which precipitated the failure. As was observed in additional tests on sandwiches with very poor bond, using a polyvinyl

A

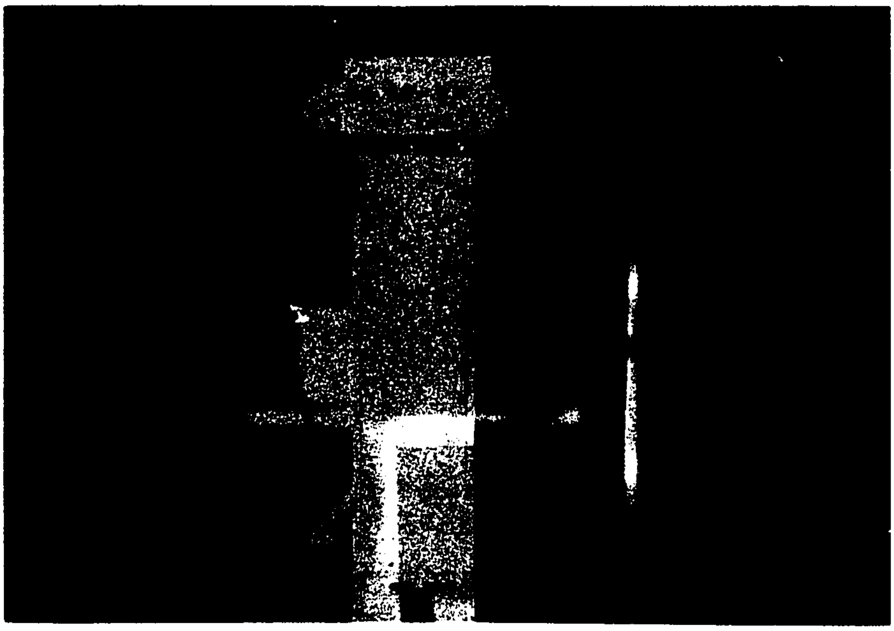

B

Figure 4-41. (A) Example of Anti-symmetrical Wrinkling. (B) Post Buckling Damage to a Sandwich in Which Failure Mode Was Indistinguishable.

TABLE 4-9

SANDWICH TEST RESULTS

Test No.	Facing Mat'l	Facing Thick. (in)	Core Mat'l	Core Thick. (in)	Midspan Defl. N.Face (10^{-3} in)	Midspan Defl. S.Face (10^{-3} in)	Failure Stress (psi)	Observed Failure Mode
1	D.F.Ply.	0.23	Styro FR	1.0	-35	40	5700	W
2				1.0	45	-43	5160	W
3				1.0	30	-26	5440	W
4				1.0	-31	33	5140	W
5	D.F.Ply.	0.23	Styro FR	2.0	26	-22	5720	I
6				2.0	0	8	5640	I
7				2.0	-12	20	6048	I
8				2.0	- 9	16	6000	I
9	D.F.Ply.	0.23	Styro FR	3.0	2	1	5040	W
10				3.0	26	-22	5045	I
11				3.0			5060	I
12				3.0			5190	I
13*				3.0			5460	W
14*				3.0			5950	W
15**				3.0			5080	W
16**				3.0			5160	I
17	D.F.Ply.	0.23	Styro FR	4.0	9	- 5	6090	I
18				4.0	- 4	9	6300	I
19				4.0	8	- 4	6220	I
20				4.0	12	- 7	4530[a]	W
21	D.F.Ply.	0.23	Dorvon	1.0	-39	43	3060	W
22				1.0	-56	58	2635	W
23				1.0	-18	20	2970	W
24	D.F.Ply.	0.23	Dorvon	2.0	21	-15	4861	W
25				2.0	49	-45	4660	W
26				2.0	-23	24	3958	W

*Length = 6 inches.

**Length = 18 inches.

[a]Invalid results, large knotty region.

W = Face wrinkling mode of failure

I = Indistinguishable mode of failure

TABLE 4-9--(Continued)

Test No.	Facing Mat'l	Facing Thick. (in)	Core Mat'l	Core Thick. (in)	Midspan Defl. N.Face (10^{-3} in)	Midspan Defl. S.Face (10^{-3}in)	Failure Stress (psi)	Observed Failure Mode
27	D.F.Ply.	0.23	Dorvon	3.0	76	-78	4450	W
28				3.0	-42	45	4160	W
29				3.0	8	7	4770	W
30	D.F.Ply.	0.23	Dorvon	4.0	-14	17	4386	W
31				4.0	-37	39	4386	W
32				4.0	29	-28	4480	W
33	D.F.Ply.	0.23	Styro RM	2.0	- 4	12	4633	I
34				2.0	5	- 1	4993	I
35				2.0	-13	15	5336	I
36	D.F.Ply.	0.23	Styro HD	2.0	2	3	5519	I
37				2.0	2	3	5436	I
38				2.0	- 2	6	5667	I
39	Temp.Pw.	0.195	Styro FR	3.0	15	-11	6933	I
40				3.0			7140	W
41				3.0			7200	W
42				3.0	28	-19	7360	W
43	Temp.Pw.	0.195	Dorvon	3.0	6	- 5	4790	W
44				3.0	-22	29	4460	W
45				3.0	-24	36	4070	W
46	TempPw.	0.144	Styro FR	3.0	9	- 3	5015[b]	I
47				3.0	0	6	5810	I
48				3.0			5820	I
49				3.0			6450	I
50	Temp.Pw.	0.144	Dorvon	3.0	13	- 9	5050	W
51				3.0	- 8	14	4625	W
52				3.0	8	- 2	4625	W

[b]Delamination at end.

W = Face wrinkling mode of failure.

I = Indistinguishable mode of failure.

TABLE 4-9--(Continued)

Test No.	Facing Mat'l	Facing Thick. (in)	Core Mat'l	Core Thick. (in)	Midspan Defl. N.Face (10^{-3}in)	Midspan Defl. S.Face (10^{-3}in)	Failure Stress (psi)	Observed Failure Mode
53	Std.Pw.	0.223	Styro FR	3.0	3	2	3984	I
54				3.0	3	2	4073	I
55				3.0	10	- 5	4671	I
56				3.0	2	3	3737	I
57	Std.Pw.	0.223	Dorvon	3.0	27	-21	4030	W
58				3.0	-14	22	4010	W
59	Std.Pw.	0.174	Styro FR	3.0	1	6	5177	I
60				3.0	1	5	4795	I
61				3.0	1	4	4737	I
62				3.0	0	5	4603	I
63	Std.Pw.	0.174	Dorvon	3.0	35	-29	3920	W
64				3.0	- 6	12	4090	W
65	Std.Pw.	0.120	Styro FR	3.0	- 1	3	2290[b]	I
66				3.0			2360[b]	I
67				3.0			4670	I
68				3.0	0	5	4860	I
69	Ash Ply.	0.245	Styro FR	3.0	- 9	18	2109	I
70				3.0	9	- 1	2041	W
71				3.0	2	10	2109	W
72				3.0	- 3	11	2245	W
73	Ash Ply.	0.245	Dorvon	3.0	0	9	2035	W
74				3.0	- 2	11	2170	W
75	Ash Ply.	0.127	Styro FR	3.0	4	4	3652	W
76				3.0	4	2	3850	W
77				3.0	- 1	15	3910	I
78				3.0			3710	W

[b]Delamination at end.

W = Face wrinkling mode of failure.

I = Indistinguishable mode of failure.

TABLE 4-9--Continued

Test No.	Facing Mat'l	Facing Thick. (in)	Core Mat'l	Core Thick. (in)	Midspan Defl. N.Face (10^{-3}in)	Midspan Defl. S.Face (10^{-3}in)	Failure Stress (psi)	Observed Failure Mode
79	Ash Ply.	0.127	Dorvon	3.0	- 3	7	2960	W
80				3.0	- 5	12	3125	W
81				3.0	5	2	2900	I
82	Cem.Asb.	0.136	Styro FR	3.0	0	3	7075	I
83				3.0	3	- 1	8350	I
84				3.0			8060	I
85				3.0			6920	I
86	Cem.Asb.	0.136	Dorvon	3.0	28	-23	5820	W
87				3.0	58	-53	5840	W
88	D.F.Ply.	0.237	Dylite	2.26	-27	27	1814	W
89				2.26	31	-29	2048	W
90				2.26			2513	W
91				2.26			2539	W
92				2.26			2243	W
93				2.26			2441	W
94				2.26			2567	W
95				2.26			2191	W
96				2.26			2539	W
97				2.26			1970	W
98	D.F.Ply.	0.247	Dylite	3.56			2541	W
99				3.56			2632	W
100				3.56			3182	W
101				3.56			2854	W
102				3.56			3428	W
103				3.56			2989	W
104	D.F.Ply.	0.249	Dylite	7.33			4713	W
105				7.33			4343	W
106				7.33			4428	W

W = Face wrinkling mode of failure.

I = Indistinguishable mode of failure.

resin adhesive, some panels began to fail in perfect symmetric wrinkles with separation of bond actually visible, but as the compression load continued to increase, one face would experience a change in wave form which then resulted in an overall anti-symmetrical failure configuration. This same behavior, though not as pronounced, was observed in many of the regular sandwich tests.

G. Debonding Tests

A special set of tests was conducted to observe experimentally the behavior of short sandwich columns which have large unbonded areas between the core and facing materials. This problem of bonding voids is called "debonding." The specimens were of the same size as those used in the regular sandwich tests (12 inches long and 6 inches wide). The facings were 1/4 inch Douglas fir plywood and the cores were 3 inch Dorvon foam. The unbonded areas were simulated by placing desired widths of wax paper between the adhesive coated core and the facing on one side. The unbonded strips were 2, 4, and 6 inches wide, extending transversely across the 6 inch panel and located at midspan.

The results of these tests are reported in Figure 4-42. Also shown in this figure are data points for the sandwich tests without debonding strips. Surprisingly the 2 inch strips did not affect the buckling behavior at all and the 4 inch strips only slightly reduced the failure stress. However, the 6 inch strips reduced the failure stress appreciably.

Figure 4-43 shows photographs of buckling of two sandwiches having 2 inch and 6 inch debonded strips, respectively, in photographs

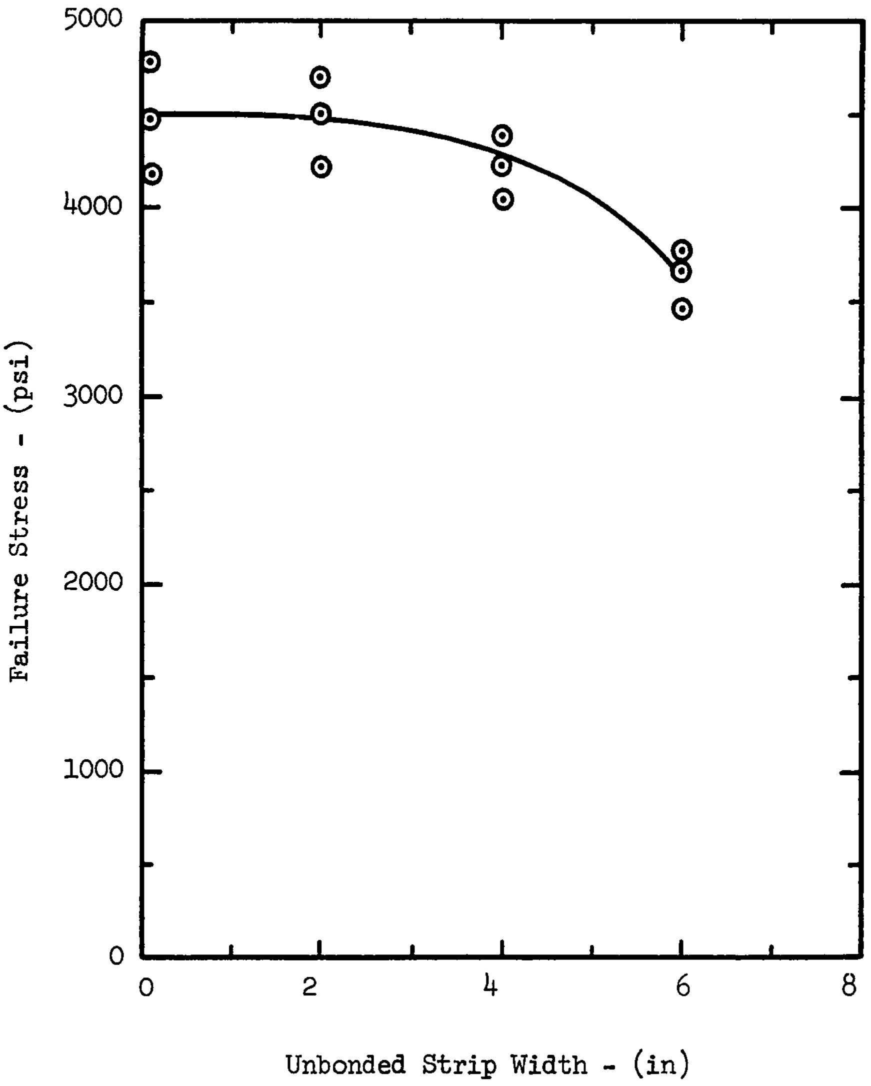

Figure 4-42. Effect of Debonding On Failure Stress.

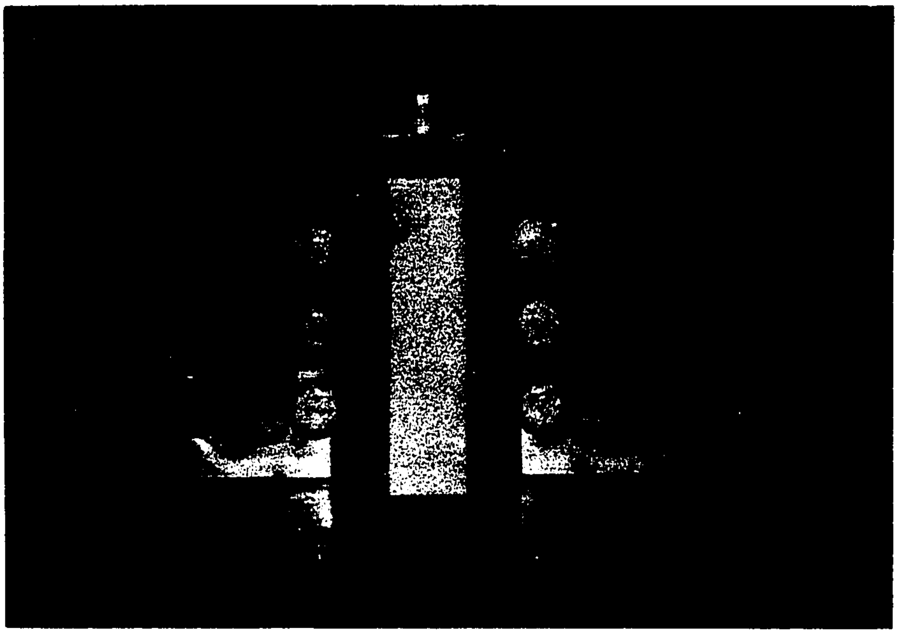

A

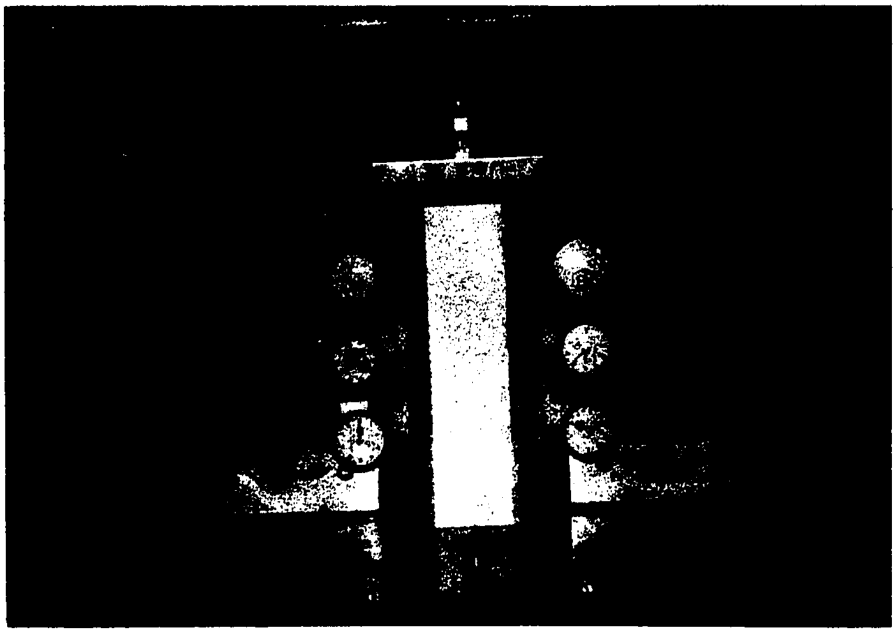

B

Figure 4-43. Photographs of Buckling of Sandwiches Having Debonded Strips: (A) 2 inches; (B) 6 inches.

(a) and (b). An anti-symmetrical wrinkle is noted in both faces of the 2 inch debonded case.

Although the number of tests was small, it appears quite conclusive that for the sandwich combination tested, the effects of small unbonded areas of less than 2 inches across would be relatively unnoticed. The effect of areas less than 4 inches across would result in a reduction in buckling strength of approximately 10 percent. These effects appear surprisingly low, hence, this should be an essential topic for further study.

CHAPTER V

DEVELOPMENT OF FACE WRINKLING THEORY

A. Introduction

The works of Hoff and Mautner,[38] and the British team of Gough, Elam, and de Bruyne[39] form the primary references to most papers on sandwiches. Other early works include those of Williams,[40] Wan,[41] and Troxell and Engel.[42] The face wrinkling phenomenon is generally investigated by considering it as a beam supported by an elastic foundation. Strain energies are determined from the core and facing strains based on assumed displacement models. External work done by applied axial force is equated to strain energies, and critical facing stresses are found through minimization techniques. Some of the papers also treat the problem more mathematically by using complicated stress functions. This is true of a more recent paper by Norris, et al.,[43] which serves as the basis for the U. S. government design manual on sandwich construction for aircraft.[44]

Some of the early papers (including some that are not listed above) are quite complex in form and yield only classical upper stress limits of wrinkling failure. Much lower failure stresses are usually encountered in experimentation; apparently the result of surface irregularities often referred to as initial waviness. Initial waviness would seem to be a manufacturing defect occurring randomly; hence, it is often believed that prediction of initial waviness is an impossible task.[10] In the writer's opinion, a rational specification or definition of initial waviness has prevented the accurate failure prediction of face wrinkling since the 1940's. E. W. Kuenzi[9] recently stated: "Theories for wrinkling are dependent upon unknown facing waviness, as you know, which is an elusive thing to determine experimentally." The writer has discovered in past studies,[10] that initial waviness, as calculated from test data from five independent laboratories, appears to have a definite correlation with sandwich physical constants, rather than being a random manufacturing problem. The physical explanation for this apparent dependence of the term referred to as initial waviness upon sandwich physical constants remains a mystery at this time. However, as will be reported later in this dissertation, tests on foam-filled sandwiches revealed a similar dependence. This indicates that the initial waviness parameter does not really reflect random physical irregularities but must represent some unknown phenomena associated with present wrinkling theory. Even if this hypothesis is true, it does not detract from the usefulness of the developed theory. But it does suggest that definition of the waviness parameter in its present form is fictitious.

The British engineer Yusuff[45,46] developed a theory of local instability by eventually considering the effect of initial imperfections assumed at critical wavelength. Yusuff assumed that a distorted core zone existed which extends inward from the faces a calculated distance. The width of the distorted zone is then taken as the criterion for discriminating between two symmetrical wrinkling models. As noted, he treats only symmetrical wrinkling. The work of Yusuff is considered quite significant and is referenced in the 1966 Applied Mechanics Surveys.[47] It must be noted, however, that discrepancies exist between the equations of Yusuff and those of Hoff and Mautner.[38] These discrepancies have been traced to errors in the minimization procedures used by Yusuff. The importance of the work of Yusuff lies in his adapting core strain energies to an equivalent spring constant which is then used in the classic beam-on-elastic foundation equation. Initial imperfections may be included in the solution of the differential equation in a manner that is physically perceptible. The solutions of the differential equation instabilities are convenient and practical for use, compared with the mathematical elasticity solutions of Forest Products Laboratory.[43] This is not intended to detract from the importance of the FPL procedure. In fact, the FPL analysis is probably as rigorous and complete as any method available today. The practical viewpoint, however, must be weighed heavily when considering architectural applications. Designers simply will not use an overly complex analysis, particularly, when they do not understand the theory behind it.

Waviness was actually considered before Yusuff focused attention on it. Wan[41] contended that wrinkling stress of the facings is closely related to the initial waviness present in the facings. Wan was convinced that it is possible to derive a rational expression to represent the general characteristics of the initial waviness. He proposed the use of the Donnell assumption that the amplitude of the initial waviness is proportional to the square of the wave length and inversely proportional to the facing thickness. The wrinkling reports of Forest Products Laboratory (FPL)[43,48,49] also include waviness. The equations of FPL Report 1810[43] are based on amplitude being proportional to core thickness, while FPL Report 1810A[48] presents equations for honeycomb cores based on the Williams assumption that original wrinkles are proportional to their wave lengths.

As stated earlier, the studies of Forest Products Laboratory[43] are reported in quite complex mathematical form. The writer has studied the FPL report extensively and reported a summary review in reference.[50] Initial waviness is assumed proportional to core thickness. Hyperbolic functions were developed which included the initial waviness term. These functions require minimization to produce a prediction of the lowest buckling stress. FPL investigators worked out a single special case which is stated to be representative of a typical aircraft sandwich panel. A set of curves were presented for this special case for a representative range of initial waviness proportionality constants. The use of the FPL curves requires two prerequisites: first, that the physical properties of the materials of the user's sandwich are in close agreement with the special case assumed by FPL, and secondly, that the user produce test data for a sandwich similar to his design, and manufactured in exactly the same procedure, so that a design waviness constant may be read from the FPL curves. This waviness parameter would then be available for use in predicting the critical stress for the exact configuration desired by the designer. Obviously, this method must be ruled out for application to architectural foam-filled sandwich panels where physical properties may vary by three orders of magnitude from the stronger aircraft panels.

It appears to the writer that a combination of the best qualities of the Hoff and Mautner[38] and Yusuff[46] approaches afford the most realistic face wrinkling analysis for foam-filled sandwiches. Hoff and Mautner pursued a pure energy approach using the Raleigh method of an assumed deflected shape. They recognized from experiments that wrinkling can occur either as a symmetrical sinusoidal deflection of faces, where each face deflects out of phase, or an in-phase deflection of faces referred to as anti-symmetrical. Sketches of these two types of deflections are shown in Figure 5-1. Hoff and Mautner developed complete shear strain expressions for both the symmetrical and anti-symmetrical cases. Their strain energy expressions for the anti-symmetrical case were significant contributions. The writer will not present the development of the anti-symmetrical shear strain expressions but encourages the reader's reference to this important work of Hoff and Mautner. Hoff and Mautner introduced the concept of a marginal zone of core displacement in their analysis.

Yusuff attacked the problem slightly differently. He made use of the differential equation of a beam-on-elastic foundation by determining equivalent spring constants from core strain energy. He did not consider shear deformations in thin cores and only treated symmetrical wrinkling. Furthermore, he incorrectly minimized critical stress equations. These errors will be pointed out in a following section. Although the equations of Yusuff are incorrect due to mathematical errors and the omission of shear in one case, plus the restriction to symmetrical wrinkling, he did present a simple and rational way to include initial waviness.

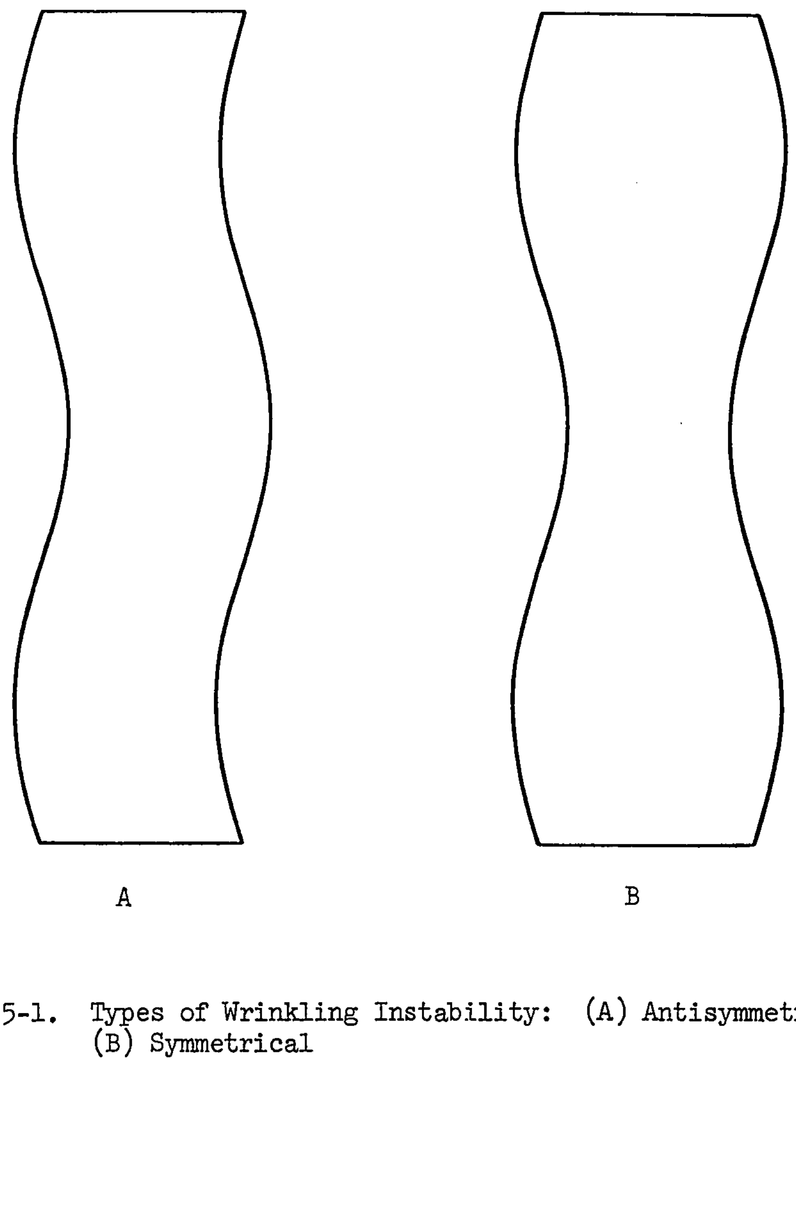

Figure 5-1. Types of Wrinkling Instability: (A) Antisymmetrical; (B) Symmetrical

The wrinkling analysis developed herein for foam-filled sandwiches incorporates the differential equation approach with initial waviness but does so with the unified use of Hoff and Mautner's core strain equations for both symmetrical and anti-symmetrical deflections.

Correlation of developed theory with results from 83 tests has led to a definite relationship between the initial waviness parameter and critical wave length. In contrast to the FPL method, the designer may calculate the initial waviness parameter and directly calculate predicted face wrinkling stress. A simple test is presented whereby the designer can establish whether face deflections are symmetrical or anti-symmetrical thereby precluding unnecessary calculations in the determination of wrinkling stress.

In the development which follows, the core is assumed isotropic. This assumption is not exactly correct for plastic foams since cell wall orientation during the forming cycle definitely influences foam strength in an anisotropic manner. At this period in the development of sandwich theory for plastic foams, the anisotropic nature of the foam is not well understood, nor predictable. Matonis[51] has constructed cellular models from which he has developed a theory of strength accounting for orientation of cell elongation. His theory might be practical for some extruded boards but would be meaningless for most foamed-in-place applications.

Sandwich facing materials are assumed orthotropic with one principal direction aligned with the load plane. It is further assumed that both facings in a sandwich are of equal, constant thickness.

B. Beam-On-Elastic Foundation Concept

Yusuff[45,46] presented a governing differential equation for beams-on-elastic foundations. He did not explain the development of the equation or list the assumptions involved. The writer has developed the basic equations and agrees with the particular form in which Yusuff has presented his equations. However, it appears important that all of the steps and assumptions be well understood, hence, a complete development of the governing differential equation and its solution are presented herein. The solution of the differential equation is somewhat parallel to that given by Yusuff, but is more rigorous and avoids his mathematical errors.

Assume that facings are sufficiently strong that shear deformations of the facing may be neglected in comparison with bending deflections. Further assume that facings are sufficiently thick and that lateral displacements are small such that small deflection theory holds. Unit column width is assumed in this development.

Lateral displacement of a facing neutral axis, as measured from a flat reference plane coinciding with the undisplaced facing neutral plane, is designated as

$$w = w_o + w_b \tag{5-1}$$

where w_o = initial displacement of facing

w_b = additional displacement of facing due to bending.

The bending displacement, for small deflections, may be related to bending moment through the curvature equation

$$\frac{d^2 w_b}{dx^2} = -\frac{M}{E_f I_f} \qquad (5\text{-}2)$$

where x = longitudinal coordinate

M = local bending moment

E_f = bending modulus of the facing

I_f = moment of inertia of facing about its own center

Taking the basic static equations for beam-columns as given by Timoshenko and Gere,[52]

$$\frac{dM}{dx} = V + P\frac{dw}{dx} \qquad (5\text{-}3)$$

where V = shearing force

P = axial compressive force

Introducing the shorthand prime superscript notation for differentiation with respect to the independent variable $\underline{x}$, (5-3) becomes

$$\begin{aligned} M' &= V + P\,w' \\ &= V + P(w_o' + w_b') \qquad (5\text{-}3a) \end{aligned}$$

Differentiating (5-2) and rearranging,

$$M' = -E_f I_f w_b''' \qquad (5\text{-}4)$$

Equating (5-3a) and (5-4) we obtain

$$\begin{aligned} V &= -E_f I_f\, w_b''' - P(w_o' + w_b') \\ V' &= -E_f I_f\, w_b^{iv} - P(w_o'' + w_b'') \qquad (5\text{-}5) \end{aligned}$$

But

$$V' = -q(x) \tag{5-6}$$

where $q(x)$ is the local beam lateral load corresponding to the response of the elastic foundation. If the elastic foundation is approximated to respond as a linear spring having a spring constant $\underline{k}$, then $q(x)$ may be written as

$$q(x) = -k\, w_b \tag{5-7}$$

Substituting (5-6) and (5-7) into (5-5),

$$E_f I_f\, w_b^{iv} + P(w_o'' + w_b'') = -k\, w_b \tag{5-8}$$

or

$$w_b^{iv} + \frac{P}{E_f I_f} w_b'' + \frac{k\, w_b}{E_f I_f} = -\frac{P\, w_o''}{E_f I_f} \tag{5-9}$$

The deflected shape is observed in practice to be sinusoidal. The initial waviness would probably be a complicated Fourier series; however, as load increases, the Fourier components having wave lengths near the critical buckling wave length would be the only significant terms causing magnification of the beam deflection amplitude. This fact has been proved elsewhere.[43] In consideration of this fact, only the component of initial waviness having the same wave length and in phase with the critical buckling deflected shape will be considered. Under these assumptions we may express deflections as

$$w_b = A_b \sin\frac{\pi x}{L} \tag{5-10}$$

$$w_o = A_o \sin\frac{\pi x}{L} \tag{5-11}$$

where A_b = maximum amplitude of additional bending displacements

A_o = maximum amplitude of initial displacements

L = wave length of assumed deflection pattern

Substituting (5-10) and (5-11) into (5-9), we obtain

$$A_b\left(\frac{\pi}{L}\right)^4 \sin\frac{\pi x}{L} - \frac{A_b\, P}{E_f I_f}\left(\frac{\pi}{L}\right)^2 \sin\frac{\pi x}{L} + \frac{k\, A_b}{E_f I_f}\sin\frac{\pi x}{L}$$

$$= + \frac{P\, A_o}{E_f I_f}\left(\frac{\pi}{L}\right)^2 \sin\frac{\pi x}{L}$$

Equating coefficients gives

$$A_b\left[\left(\frac{\pi}{L}\right)^4 - \frac{P}{E_f I_f}\left(\frac{\pi}{L}\right)^2 + \frac{k}{E_f I_f}\right] = \frac{P\, A_o}{E_f I_f}\left(\frac{\pi}{L}\right)^2$$

or,

$$A_b = \frac{A_o}{\frac{1}{P}\left[\left(\frac{\pi}{L}\right)^2 E_f I_f + k\left(\frac{L}{\pi}\right)^2\right] - 1} \qquad (5\text{-}12)$$

Instability occurs when $A_b \rightarrow \infty$, or when

$$\frac{1}{P}\left[\left(\frac{\pi}{L}\right)^2 E_f I_f + k\left(\frac{L}{\pi}\right)^2\right] \rightarrow 1.0 \qquad (5\text{-}13)$$

The buckling load, $\underline{P_b}$, may then be determined from (5-13). $\underline{P_b}$ may be written as

$$P_b = \left(\frac{\pi}{L}\right)^2 E_f I_f + k\left(\frac{L}{\pi}\right)^2 \qquad (5\text{-}14)$$

Equation (5-14) does not give the critical buckling load in face wrinkling. It must be minimized with respect to wave length, $\underline{L}$, and equivalent spring constant, $\underline{k}$. This ties in specifically with the following sections dealing with the determination of equivalent spring constant from core strain energy. First, however, note that the instability equation, (5-14), is independent of the initial displacement amplitude, $\underline{A_o}$. Note also that the first term on the right side of (5-14) is the Euler buckling load for a pinned end column without lateral load. The second term is the contribution to stability afforded by the lateral support of the core.

When the core material is relatively weak in comparison with the facing material, finite deflections of the facing (precipitated by initial waviness, $\underline{A_o}$), will produce extensional and shear strains which may cause core failure at a load, $\underline{P}$, much lower than critical buckling load, $\underline{P_{cr}}$. At critical buckling, $P_b = P_{cr}$ and (5-12) becomes

$$A_b = \frac{A_o}{\frac{P_{cr}}{P} - 1}$$

Converting forces to stresses,

$$A_b = \frac{A_o}{\frac{p_{cr}}{p} - 1}$$

or,

$$p = \frac{p_{cr}}{1 + \frac{A_o}{A_b}} \qquad (5\text{-}15)$$

Critical buckling stress, $\underline{p_{cr}}$, represents the classical wrinkling theory. The actual failure wrinkling stress, $\underline{p}$, is shown to be a function of the amplitude ratio, A_o/A_b. Amplitude $\underline{A_b}$ will be shown later to be limited by the physical strength of the core. Amplitude $\underline{A_o}$ will be shown to be an experimental function of critical wave length.

C. Development of Symmetrical Wrinkling

Symmetrical wrinkling is defined by the symmetrical deflection pattern illustrated in Figure 5-1. A more detailed illustration is given in Figure 5-2. Since a short wave on the surface of a thick sandwich can hardly have any effect upon the material in the middle of the core, it is assumed that displacements occur only in marginal zones of depth B. The displacement u in the x direction is assumed to be negligibly small when buckling is reached. The horizontal displacement w of the point originally at x,y in the marginal zone is assumed linear as given by the equation

$$w = \frac{y}{B} A \sin\frac{\pi x}{L} \tag{5-16}$$

where $A = A_b + A_o$

Due to symmetry it is only necessary to work with one-half of the sandwich.

The normal strain in the core is

$$\epsilon_y = \frac{\partial w}{\partial y} = \frac{A}{B} \sin\frac{\pi x}{L} \tag{5-17}$$

The extensional strain energy within one-half wave length, L, becomes

$$U_\epsilon = \frac{1}{2} E_c \int_0^L \int_0^B \epsilon_y^2 \, dy \, dx$$

$$= \frac{A^2 E_c L}{4 B} \tag{5-18}$$

where E_c is Young's modulus for the core. The shear strain in the core

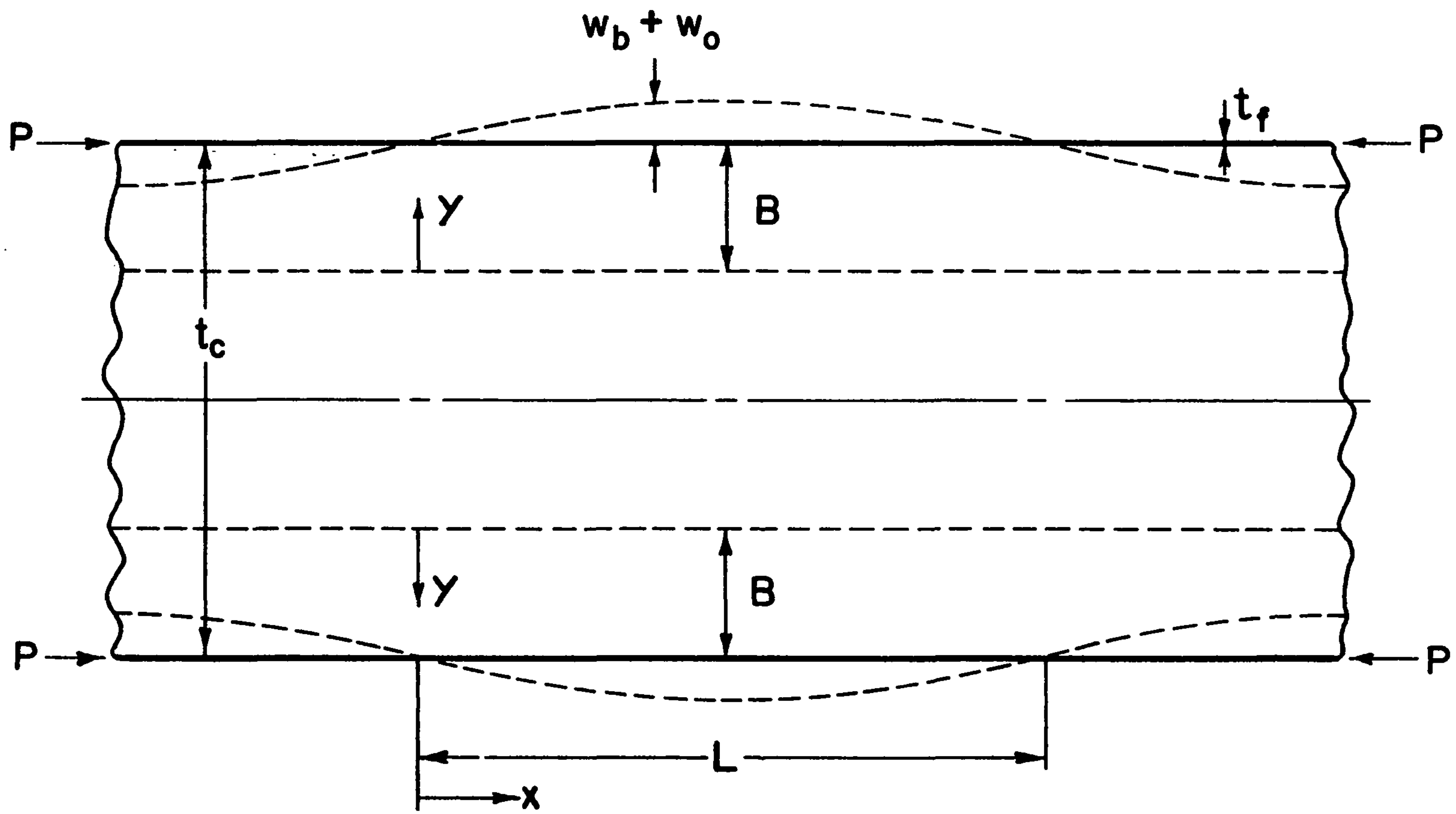

Figure 5-2. Wrinkling Deflection Shape Showing Marginal Zone.

is given by

$$\gamma = \frac{\partial w}{\partial x} = \frac{A\pi y}{L\,B} \cos \frac{\pi x}{L} \tag{5-19}$$

Thus the shear strain energy within a half wave length in one-half the core is

$$U_\gamma = \frac{1}{2} G_c \int_0^L \int_0^B \gamma^2 \, dy \, dx$$

$$= \frac{A^2 \pi^2 \, G_c \, B}{12 \, L} \tag{5-20}$$

where $\underline{G_c}$ is the shear modulus of the core.

The core is now regarded as a spring type support for the facings. It is recalled that the spring modulus, $\underline{k}$, or as it is called in soil mechanics, subgrade modulus, has units of pounds reaction per inch deflection per unit area. The energy stored in a deflected spring system over a half wave length is

$$U_k = \int_0^L \frac{1}{2} k \, w^2 \, (1) \, dx$$

$$= \frac{1}{2} k \int_0^L A^2 \sin^2 \frac{\pi x}{L} \, dx$$

$$= \frac{1}{4} k \, A^2 \, L \tag{5-21}$$

Next, the core system is assumed replaced by an equivalent spring system with a spring modulus, $\underline{k}$, determined by equating the core strain energy to that stored in an equivalent spring. That is,

$$U_k = U_\epsilon + U_\gamma$$

$$\frac{1}{4} k A^2 L = \frac{A^2 E_c L}{4 B} + \frac{A^2 \pi^2 G_c B}{12 L}$$

From which

$$k = \frac{E_c}{B} + \frac{\pi^2 G_c B}{3 L^2} \tag{5-22}$$

This equivalent spring modulus may now be substituted back into the buckling equation, (5-14).

$$P_b = (\frac{\pi}{L})^2 E_f I_f + \frac{E_c}{B}(\frac{L}{\pi})^2 + \frac{\pi^2 G_c B}{3 L^2}(\frac{L}{\pi})^2 \tag{5-23}$$

Critical load will be determined by minimizing $\underline{P_b}$ with respect to the two variables in (5-23), $\underline{B}$ and $\underline{L}$.

$$\frac{\partial P_b}{\partial B} = -(\frac{L}{\pi})^2 \frac{E_c}{B^2} + \frac{G_c}{3} \underset{=}{\underline{\text{set}}} 0$$

$$\frac{L_{cr}^2}{B^2} = \frac{\pi^2 G_c}{3 E_c} \tag{5-24}$$

$$\frac{\partial P_b}{\partial L} = -\frac{\pi^2}{L^4} E_f I_f + \frac{E_c}{\pi^2 B} \underset{=}{\underline{\text{set}}} 0$$

$$B = \frac{E_c L_{cr}^4}{E_f I_f \pi^4} \tag{5-25}$$

From (5-24) and (5-25) B may be eliminated and the following result is obtained for wave length

$$L_{cr} = \left[\frac{3\pi^6 \; E_f^2 \; I_f^2}{E_c \; G_c}\right]^{1/6} \tag{5-26}$$

Moment of inertia, I_f, is

$$I_f = \frac{1}{12} t_f^3 \tag{5-27}$$

where t_f = facing thickness

Substituting (5-27) into (5-26) and reducing, we obtain

$$L_{cr} = 1.647 \; t_f \left[\frac{E_f^2}{E_c \; G_c}\right]^{1/6} \tag{5-28}$$

From (5-25), (5-27), and (5-28) we obtain the expression for the marginal zone thickness

$$B = 0.905 \; t_f \left[\frac{E_f \; E_c}{G_c^2}\right]^{1/3} \tag{5-29}$$

Sandwich cores are classed as "thick" or "thin," depending on the thickness of the theoretical marginal zone given by (5-29). If marginal zone B is calculated from (5-29) to be less than one-half the core thickness, then the core is said to be "thick." If B calculated from (5-29) is greater than one-half the core thickness, then the core is said to be "thin" and the marginal zone is then taken as 0.5 t_c.

If the core is "thick," then the substitution of (5-28) and (5-29) back into the buckling equation (5-23) leads to the "thick core" critical symmetrical wrinkling instability equation

$$P_{cr} = 0.909\ t_f\ [E_f\ E_c\ G_c]^{1/3} \tag{5-30}$$

If the core is "thin," use $B = 0.5\ t_c$. This alters the critical wave length to

$$L_{cr} = 1.42\ t_f \left[\frac{E_f\ t_c}{E_c\ t_f}\right]^{1/4} \tag{5-31}$$

With these expressions for marginal zone thickness and critical wave length, the "thin core" symmetrical wrinkling instability equation becomes

$$P_{cr} = 0.815\ t_f \sqrt{E_f\ E_c\ \frac{t_f}{t_c}} + \frac{1}{6}\ G_c\ t_c \tag{5-32}$$

The Yusuff equations[45,46] for symmetrical wrinkling are incorrect because minimization derivatives were taken improperly. Yusuff minimized equivalent spring modulus $\underline{k}$ with respect to marginal zone thickness $\underline{B}$. This was done erroneously since $\underline{k}$ was also dependent on wave length $\underline{L}$. Likewise, when Yusuff minimized buckling load $\underline{P_b}$ with respect to wave length $\underline{L}$, he treated $\underline{k}$ as a constant when it was actually a function of $\underline{L}$.

D. Development of Anti-Symmetrical Wrinkling

Anti-symmetrical wrinkling is illustrated by the anti-symmetrical deflection pattern in Figure 5-2. A similar procedure is followed in the anti-symmetrical case as previously in the development of the symmetrical case. The major difference is in the expression for core strain energy. As stated in the introduction of this chapter, Hoff and Mautner developed strain energy equations for an anti-symmetrically deformed core. This development is quite lengthy; therefore, the details are omitted for the sake of clarity and brevity.

One-half the extensional and shear strain energy stored in a half wave length of the core is given by

$$\frac{1}{2} U_c = \frac{(2\pi - 3)}{8\pi B} A^2 E_c L + \frac{\pi A^2 G_c}{48 L} [3(\pi + 1)t_c + 2(\pi - 1)B] \quad (5\text{-}33)$$

Equating strain energy to an equivalent spring energy

$$U_k = \frac{1}{2} U_c$$

$$k = \frac{(2\pi - 3)E_c}{2\pi B} + \frac{\pi G_c}{12 L^2} [3(\pi + 1)t_c + 2(\pi - 1)B] \quad (5\text{-}34)$$

Substituting (5-34) back into the buckling equation (5-14) yields

$$P_b = (\frac{\pi}{L})^2 E_f I_f + (\frac{L}{\pi})^2 \frac{(2\pi - 3)}{2\pi} \frac{E_c}{B} + \frac{G_c}{12\pi} [3(\pi + 1)t_c + 2(\pi - 1)B] \quad (5\text{-}35)$$

Minimizing $\underline{P_b}$ with respect to $\underline{L}$ and $\underline{B}$,

$$\frac{\partial P_b}{\partial L^2} = -\frac{\pi^2}{L^4} E_f I_f + (\frac{2\pi - 3}{2\pi}) \frac{E_c}{\pi^2 B} \underline{\underline{\text{set}}} \; 0$$

$$B = (\frac{2\pi - 3}{2\pi}) \frac{L^4 E_c}{\pi^4 E_f I_f} \quad (5\text{-}36)$$

$$\frac{\partial P_b}{\partial B} = -\left(\frac{2\pi - 3}{2\pi}\right)\left(\frac{L}{\pi}\right)^2 \frac{E_c}{B^2} + \frac{G_c}{6\pi}(\pi - 1) \underset{=}{\text{set}} 0$$

$$B = \frac{L}{\pi}\left[\left(\frac{2\pi - 3}{2\pi}\right)\frac{6\pi E_c}{(\pi - 1) G_c}\right]^{1/2} \qquad (5\text{-}37)$$

Equating (5-36) and (5-37), and substituting $t_f^3/12$ for I_f, leads to the critical wave length,

$$L_{cr} = 2.20\, t_f \left[\frac{E_f^2}{E_c\, G_c}\right]^{1/6} \qquad (5\text{-}38)$$

Substituting (5-38) into (5-37) yields the critical marginal zone

$$B = 1.499\, t_f \left[\frac{E_f\, E_c}{G_c^2}\right]^{1/3} \qquad (5\text{-}39)$$

The test on marginal zone thickness to determine if the core is "thick" or "thin" is the same as for the symmetrical case.

If the core is "thick" ($2B \leq t_c$), then the substitution of (5-38) and (5-39) back into the buckling equation (5-35) leads to the critical anti-symmetrical wrinkling instability equation.

$$P_{cr} = 0.5109\, t_f\, [E_f E_c G_c]^{1/3} + 0.3296\, G_c\, t_c \qquad (5\text{-}40)$$

If the core is "thin," use $B = 0.5\, t_c$. This alters the critical wave length to

$$L_{cr} = 1.670\, t_f \left[\frac{E_f\, t_c}{E_c\, t_f}\right]^{1/4} \qquad (5\text{-}41)$$

With these expressions for marginal zone thickness and critical wave length, the "thin core" anti-symmetrical wrinkling instability equation becomes

$$P_{cr} = 0.5902\ t_f \sqrt{E_f\ E_c\ \frac{t_f}{t_c}} + 0.3864\ G_c\ t_c \qquad (5\text{-}42)$$

The critical load may be converted to stress by simply dividing by facing thickness. That is,

$$p_{cr} = \frac{P_{cr}}{t_f} \qquad (5\text{-}43)$$

E. Early Wrinkling Due to Core Failure

When any initial variation of the facing surface exists, facing deflections will amplify upon load application. This will create extensional (compression and tension) and shear strains within the marginal zones of the core. The core may experience strains which will exceed strength limits in tension, compression, or shear. The tension limit would be the lower of the facing bond strength or the core material tensile strength.

Strain relationships were developed earlier in this chapter. Repeating,

$$\epsilon_y = \frac{\partial w}{\partial y} = \frac{A}{B} \sin \frac{\pi x}{L} \qquad (5\text{-}17)$$

$$\gamma = \frac{\partial w}{\partial x} = \frac{A\pi y}{L\ B} \cos \frac{\pi x}{L} \qquad (5\text{-}19)$$

From the basic strain equations come the maximum core strains

$$\epsilon_{max} = \frac{A}{B} \qquad (5\text{-}44)$$

$$\gamma_{max} = \frac{A\pi}{L} \tag{5-45}$$

If it is assumed that the core is unstrained in the unloaded condition then A_b could be substituted for A in (5-17) and (5-19) which would give

$$\epsilon_{max} = \frac{A_b}{B} \tag{5-46}$$

$$\gamma_{max} = \frac{A_b \pi}{L} \tag{5-47}$$

From the one-dimensional form of Hooke's Law,

$$\epsilon_{max} = \frac{F_e}{E_c} \tag{5-48}$$

where F_e is the smallest core compression, core tension, or bond strength. Similarly,

$$\gamma_{max} = \frac{F_s}{G_c} \tag{5-49}$$

where F_s is core shear strength. Equating (5-46) and (5-48)

$$A_b = \frac{F_e\ B}{E_c} \tag{5-50}$$

Equating (5-47) and (5-49)

$$A_b = \frac{F_s\ L}{\pi G_c} \tag{5-51}$$

The smallest value of A_b as determined from (5-50) and (5-51) would produce the lowest wrinkling failure stress.

If A_b is controlled by tension or compression of the core then the sandwich wrinkling stress is

$$p = \frac{p_{cr}}{1 + \frac{A_o}{A_b}} \tag{5-15}$$

$$= \frac{p_{cr}}{1 + \frac{E_c\ A_o}{B\ F_e}} \tag{5-52}$$

where p_{cr} is the critical wrinkling instability stress.

If A_b is controlled by shear of the core then the sandwich wrinkling stress is

$$p = \frac{p_{cr}}{1 + \frac{\pi\ G_c\ A_o}{L\ F_s}} \tag{5-53}$$

F. Experimental Correlations

In Chapter IV it was shown that sandwich composites made up of plastic foam cores and typical construction products for facings (plywood, pressedwood, and cement asbestos), exhibited marked increases in facing strength over individual facing material tests. This results in yield strength and compressive modulus values much higher than expected. It was first suspected that the foam core might be carrying a sizable portion of the load; however, calculations showed that the core would transmit less than one percent of the total load. This phenomenon is certainly caused by an unexpected contribution to compressive strength by the adhesive interacting within the foam cell structure at the interface. Similar behavior has been noted in aircraft honeycomb type sandwiches. Fan[53] suggested that relatively rigid adhesives can aid the facings in resisting in-plane stresses. The writer has shown in reference 10, page 108, that many face wrinkling tests from three different laboratories[42,49,54] have exceeded predicted yield strengths by very sizeable amounts.

If independent facing material data of stress-strain does not coincide with composite test data then the use of the tangent modulus, or some other form of reduced modulus, is wasted effort. After careful consideration of the problem it was found feasible to use linear elastic modulus values obtained from independent facing and core material tests, and to assume that composite strength increases, along with reduced modulus requirements and initial imperfections, could be lumped experimentally into the initial waviness parameter. The waviness parameter is physically defined in the buckling equation as $\underline{A_o}$ divided by $\underline{F}$, the smallest of the core strengths, $\underline{F_e}$, of $\underline{F_s}$. This method is very desirable from the designer's viewpoint. He may take elastic constants available from manufacturer's data rather than having to construct a sample sandwich and subject it to short column tests to determine stress-strain curves. The success of this method rests on the validity of the hypothesis that the waviness parameter is predictable from sandwich geometric and elastic physical properties.

The writer has previously applied the above suggestion to use linear elastic constants and the waviness parameter with most gratifying results.[10] An amazing experimental correlation was discovered between initial waviness parameter (A_o/F) and core moduli product, E_cG_c. As reported by the writer in reference 55, this relationship between A_o/F and E_cG_c is exactly linear on a log-log plot. The resulting equation obtained was

$$\frac{A_o}{F} = \frac{0.316}{\sqrt{E_c\ G_c}} \tag{5-54}$$

To further appreciate this semi-empirical relationship, it is noted that the test data used in this study came from five independent laboratories. The following table lists the sources and the sandwich materials tested:

Data Source	Ref.	Face Mat'l/Core Mat'l
Okla. Univ.	10	Fiberglas/Alum. Honeycomb
Lockheed Missiles	56	Fiberglas/Alum. Honeycomb
Forest Products Lab	49	Steel & Alum./Alum. Honeycomb
Hexcel Inc.	54	Alum./Alum. & Foam Honeycomb
Martin Company	42	Alum./Impreg. Cotton

The initial waviness semi-empirical factor has been examined by sandwich structures authorities at Lockheed Missiles and Space Company, Sunnyvale, California. These researchers include B. O. Almroth and A. B. Burns, considered within Lockheed to be specialists in this field. Both of these researchers have since used the above cited waviness parameter. Almroth stated,[57] "Harris found a relation which gives considerably better correlation with test results than was obtained in previous attempts. It therefore appears that Reference___ (same as reference 10 in this dissertation) would at least give a reasonably close estimate of the face wrinkling stress." Burns extensively referenced the wrinkling equations and waviness parameter in his work on sandwich optimization.[58]

Even though the core moduli product, E_cG_c, for low density foam is four orders of magnitude smaller than that found in moderately strong aluminum honeycomb sandwiches, the waviness parameter given by

(5-54) still yields reasonable results for the foam tests conducted. After investigating all conceivable combinations of parameters, it was found that the initial waviness parameter, for architectural type foam-filled sandwiches, is best represented as a function of critical wave length.

In correlation efforts the foamed-in-place beaded polystyrene panels did not appear consistent with other composite tests. This is believed due to the extreme variation in physical properties of the core within a given panel. Increased densities near the plywood interface contributed to increased strength of the panels. Core test data were taken from samples cut near the center of a large panel. It is believed that the foamed-in-place samples are subject to such large variation in core strengths that they should not be included with the extruded core sandwiches when drawing conclusions about the waviness parameter. The extruded polystyrene was manufactured under very carefully controlled conditions at Dow Chemical Company to produce board stock of uniform, orthotropic strength. The extruded boards were carefully mated with facing materials and glued uniformly under repeatable pressures to form sandwich test specimens.

The majority of the sandwich tests failed in obvious wrinkle modes. The remainder failed in visually indistinguishable modes which could have been compressive failures; however, they were always preceded by recorded small deflections which gives substance to probable wrinkling. The difficulty in distinguishing between wrinkling and compressive failure lies in the fact that ultimate strength is unknown in the facing materials when in a composite structure. The question is really unimportant in these tests since obvious anti-symmetrical wrinkling occurred in many tests at the same stress levels as in the indistinguishable cases.

Before presenting test results, specimen identification is discussed. Specimen groups are identified in code form, best explained by example. A typical specimen group is labelled

4D - 1F

The first term identifies the facing, the second term identifies the core. In sequence, the characters represent:

4 = facing nominal thickness in sixteenths of an inch

D = facing material

D = Douglas fir plywood
A = ash plywood
S = Masonite standard pressedwood
T = Masonite tempered pressedwood
C = cement asbestos

1 = core nominal thickness, inches

F = type of core foam

V = Dorvon board, 1 pcf
L = Dylite foamed-in-place, 1 pcf
F = Styrofoam FR board, 1.9 pcf
R = Styrofoam RM board, 2.5 pcf
H = Styrofoam HD-300 board, 3.3 pcf

A specimen number would be identified by a specimen group followed by a test sequence number. An example would be

4D - 1F - 1

This specimen identification will now be used in presenting test results with wrinkling calculations.

TABLE 5-1

SANDWICH TEST RESULTS AND WRINKLING CALCULATIONS

Specimen Group	Avg. Failure Stress (psi)	Classical Wrinkling (psi)	Critical Wave Length (in)	Parameter $A_o/F \times 10^3$ (in^3/lb)
4D-1F	5360	13210	2.74	0.436
4D-2F	5852	11406	3.26	1.035
4D-3F	5084	11328	3.06	1.260
4D-4F	6203	10769	3.30	0.814
4D-1V	2888	7814	3.51	1.377
4D-2V	4493	6500	4.18	0.720
4D-3V	4460	6342	4.63	1.020
4D-4V	4417	6176	4.22	1.188
4D-3R	4987	12647	3.14	1.358
4D-3H	5541	17484	2.81	1.005
3T-3F	7158	9715	2.50	0.299
3T-3V	4440	5578	3.21	0.580
2T-3F	6027	9578	1.96	0.386
2T-3V	4767	5370	2.56	0.228
4S-3F	4116	8768	2.55	0.967
4S-3V	4020	5039	3.28	0.586
3S-3F	4828	8593	2.12	0.555
3S-3V	4005	4855	2.72	0.408
2S-3F	4765	7700	1.48	0.306
4A-3F	2126	5450	0.91	0.472
4A-3V	2103	3043	2.50	0.791
2A-3F	3781	8317	1.78	0.715
2A-3V	2995	4649	2.03	0.794
2C-3F	7601	13207	2.41	0.596
2C-3V	5830	7558	3.10	0.648
4D-3F*	5705	11328	3.06	1.015
4D-3F**	5120	11328	3.06	1.244

Specimen length = 12 inches unless specified otherwise.

*Length = 6 inches.

**Length = 18 inches.

Treating all of the glued sandwiches as wrinkling failures, an analysis was conducted to determine critical wave lengths and waviness parameters. Results are listed in Table 5-1. Average failure stresses were determined and listed for each specimen group. The column labelled classical wrinkling refers to a theoretical calculation assuming initially perfectly straight columns. Waviness parameter, $\underline{A_o/F}$ was calculated using theoretical equations coupled with experimental results. Waviness parameter is plotted versus critical wave length in Figure 5-3 for all specimen groups.

Experimentally determined waviness correlations must be submitted to a statistical evaluation which will reveal meaningful variance information to the designer. The scatter of data is assumed to follow a normal distribution. A linear least-squares technique[59] was applied to determine the relationship of waviness parameter $\underline{A_o/F}$ to critical wave length, $\underline{L_{cr}}$. The procedure used is summarized as follows: Assume

$$y_i = A_o/F \text{ for test } i$$

$$x_i = L_{cr} \text{ for test } i$$

Let $\underline{A_o/F}$ and $\underline{L_{cr}}$ be related by a linear equation of the form

$$\frac{A_o}{F} = m\,L_{cr} + b \tag{5-55}$$

where

$$m = \frac{N\sum x_i y_i - (\sum x_i)(\sum y_i)}{N\sum x_i^2 - (\sum x_i)^2} \tag{5-56}$$

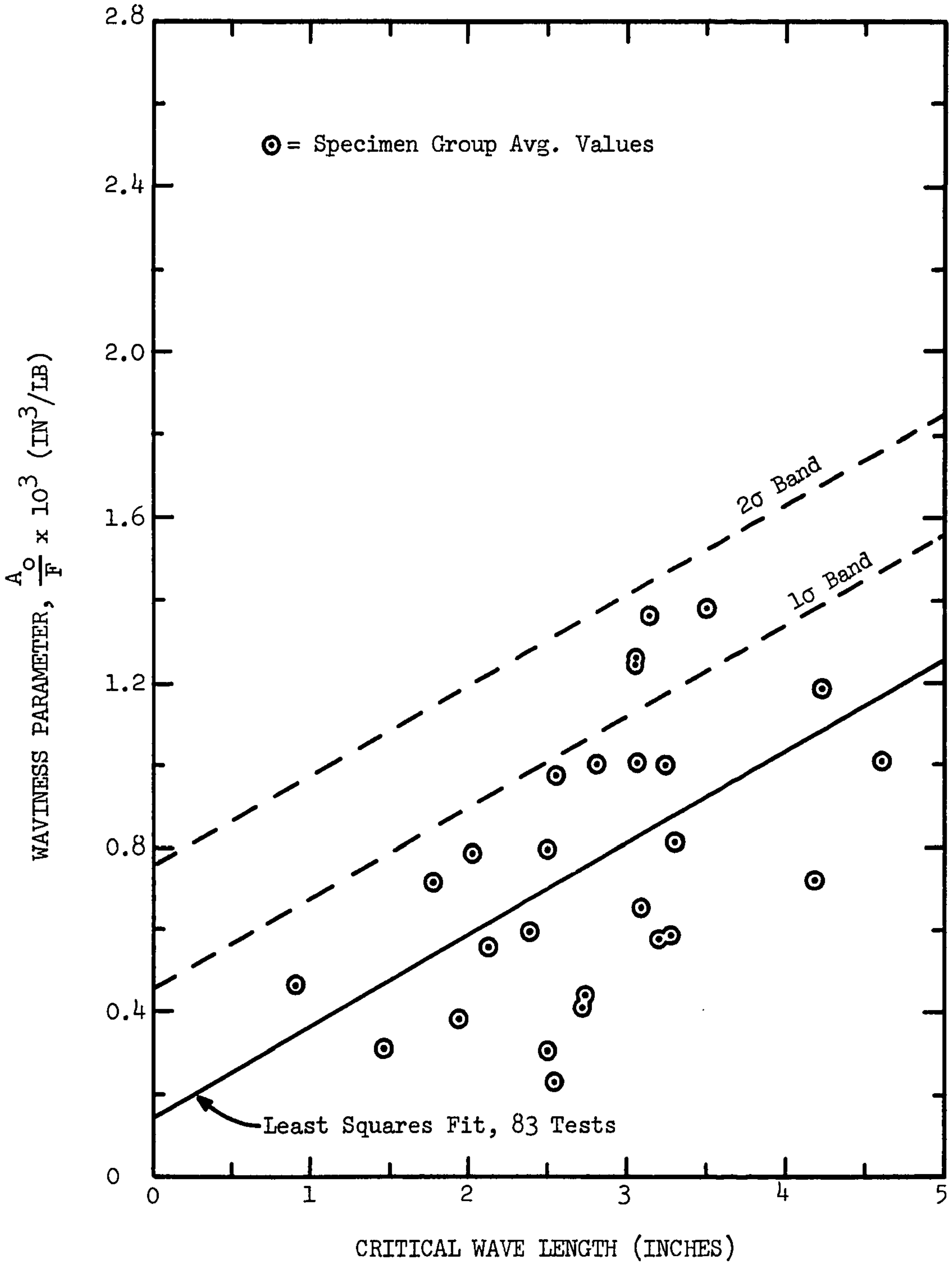

Figure 5-3. - Variation of Waviness Parameter with Critical Wave Length

$$b = \frac{(\sum y_i)(\sum x_i^2) - (\sum x_i y_i)(\sum x_i)}{N\sum x_i^2 - (\sum x_i)^2} \tag{5-57}$$

N = total number of tests = 83

The maximum likelihood estimate of the sample variance is assumed to be determined by[60]

$$\sigma^2 = \frac{1}{N}\sum(\bar{y}_i - y_i)^2$$

$$= \frac{1}{N}\sum(mx_i + b - y_i)^2 \tag{5-58}$$

The sample regression line of A_o/F on independent parameter L_{cr} was determined for 83 tests by calculating m and b from equations (5-56) and (5-57) and then inserting these values of m and b into (5-55). This linear equation, shown in Figure 5-3, is expressed as

$$\frac{A_o}{F} = (0.2191\ L_{cr} + 0.1645)10^{-3} \tag{5-59}$$

Variance was calculated from equation (5-58) and found to be

$$\sigma^2 = 8.7812 \times 10^{-8}$$

A significant limit in evaluating experimental data is the one sigma line (square root of variance). The probability is approximately 68.3 percent that a sample point would fall within a $\pm$ one sigma band about the sample mean for normal distributions. The probability is

95.4 percent for two sigma. The equation of the upper one and two sigma lines are

$$\frac{A_o}{F} + \sigma = (0.2191\ L_{cr} + 0.4608)10^{-3} \qquad (5\text{-}60)$$

$$\frac{A_o}{F} + 2\sigma = (0.2191\ L_{cr} + 0.7571) \times 10^{-3} \qquad (5.61)$$

These equations will be discussed in the application summary of Chapter VII.

After this face wrinkling study was completed the writer was made aware of a paper by Eringen[68] in which he treated local instability as a boundary value problem. The solution of Eringen is quite rigorous but very complex compared with that of the beam-on-elastic foundation concept. It is suggested that a more mathematical approach to the problem of initial waviness might employ the classical solution presented by Eringen and possibly lead to a better understanding of the characteristics of the initial waviness parameter.

CHAPTER VI

GENERAL INSTABILITY AND CORE SHEAR FAILURE

A. Introduction

As was stated in Chapter II, the usual understanding of general instability of a column is that buckling results when compressive loads exceed theoretical limits predicted by Euler's column formulas which are functions of facing material properties only. It is assumed that, at failure, the internal restoring moment of the column is exceeded by the external applied moment at some critical point in the column and the column becomes an unstable mechanism.

When the shearing rigidity of the core is small, the overall buckling load is reduced due to increased lateral deflections brought on by shear deformations. The Engesser equation, (2-1), is used in homogeneous columns where shear deformations are assumed small; however, the extension of the Engesser equation to shear-flexible core sandwiches may lead to substantial errors in predicted buckling stresses. A more accurate treatment of the general instability equation, in a manner suggested by Timoshenko and Gere,[52] is presented in the next section, the results of which are quite different from those based on Engesser's equation. Stresses were determined by the improved method which were, in extreme cases, an order of magnitude different from stresses predicted by the Engesser equation. Fortunately, the Engesser equation predicts conservatively low stresses.

Other methods are available for analyzing sandwich columns. Hoff[61,62] developed a highly mathematical solution based on a variational calculus minimization of the total potential of the system. His method is useful for sandwiches with very thin cores but has the disadvantage of including the same inaccurate shear approximation as found in the Engesser equation. Plantema[63] outlined the Bijlaard method of split rigidities. In this method, the problem is broken into separate solutions of bending and shear effects; however, this does not appear to offer any advantages over the method presented herein.

The general instability developments presented herein assume linear, unlimited core strains until failure results from large deflections. However, failure of the core under transverse shear load could occur prematurely in situations where the panel has initial bowing or if the ends are displaced laterally with respect to the load plane.

In the following sections, general instability equations will be developed specifically applicable to plastic foam cores. Also presented are the developments of theories for sandwich columns under eccentric loads, and for core shear failures.

B. Development of General Instability Theory for Large Core Shear Deformations

The basic equations for the analysis of sandwich columns can be derived in the most general sense by considering the sandwich as a beam-column. The lateral load, q, will be carried through the development of the governing differential equation. In applications to sandwiches with no lateral load, the $\underline{q}$ terms will be omitted.

A beam-column loading system is shown in Figure 6-1(a). The beam is subjected to an axial compressive force $\underline{P}$ and to a distributed lateral load of intensity $\underline{q}$ which varies with the distance $\underline{x}$ along the beam. An element of length $\underline{dx}$ with sides normal to the deflected axis of the beam is shown in Figure 6-1(b) where

Q = shearing force on the deflected element

M = bending moment acting on the element

P_L = axial force normal to the left face of the element ($\approx P$)

P_R = axial force normal to the right face of the element ($\approx P$)

y = total deflection of beam at $\underline{x}$

y_o = initial deflection of beam at $\underline{x}$

γ = shear deformation of element, inducing no rotation of faces

θ = angle between the initial normal to the beam axis at $\underline{x}$ and the normal to the deflected axis at $\underline{x}$ when load P is applied

$d\theta$ = rotation of the differential element due to bending moment

The assumption is made that the initial deflection $\underline{y_o}$ of the beam axis is small compared with the magnitude of the bending deflections. In the ensuing development the initial deflections are superfluous to the derivation of the general instability equations and its omission would simplify matters; however, small initial deflections will later be shown to be very important when considering core shear failures. Initial deflections would also be important when considering facing stress limitations, common to short columns.

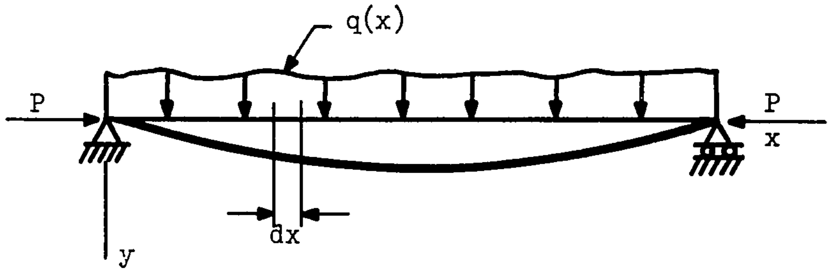

(a)

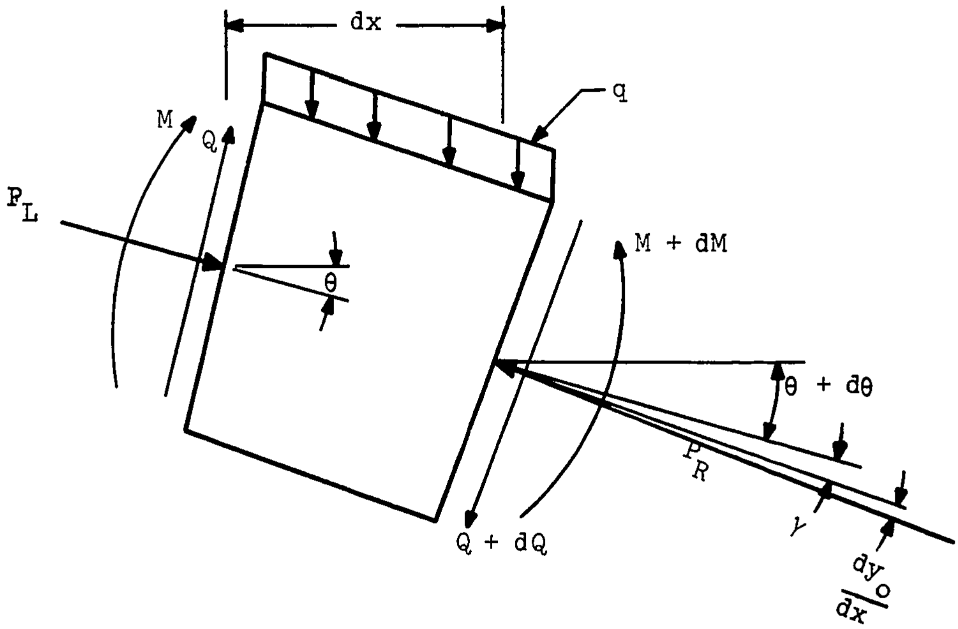

(b)

Figure 6-1. (a) Beam-column Loading System,
(b) Typical Differential Element Showing Bending and Shear Deformations.

The assumption that the initial deflection is small compared with the bending deflection allows the angle θ to be approximated in trigonometric functions as the angle between the x axis and the normal to the deflected axis at x. This becomes an important simplification in determining normal shear force Q.

The shearing force Q differs from the conventional shearing force V taken on a cross section normal to the x axis. The relationship between these two shearing forces is assumed to be

$$Q = V \cos \theta + P \sin \theta \tag{6-1}$$

Assuming small beam deflections compared with beam depth, $\cos \theta \approx 1$, $\sin \theta \approx \theta$, and equation (6-1) becomes

$$Q = V + P\theta \tag{6-2}$$

The shear deformation in shear-flexible core sandwiches, where shear stress is practically constant across the core, is defined as

$$\gamma = \frac{Q}{A_c G_c} \tag{6-3}$$

where A_c is the core cross sectional area and G_c is the core shear modulus.

The assumption of a shear-flexible core means that the core transmits all transverse shear force but has negligible bending resistance compared with the facings. On this assumption the bending moment induced curvature is written

$$\frac{d\theta}{dx} = -\frac{M}{E_f I_b} \tag{6-4}$$

where E_f is the average of the facing tension and compression moduli and I_b is the moment of inertia of the facings about the elastic axis. The shifting of the neutral axis due to the use of an average modulus E_f is neglected.

The slope of the deflected axis at $x + dx$ is expressed as

$$\frac{dy}{dx} = \theta + \gamma + \frac{dy_o}{dx} \tag{6-5}$$

Substituting (6-3) for γ in (6-5),

$$\frac{dy}{dx} = \theta + \frac{Q}{A_cG_c} + \frac{dy_o}{dx} \tag{6-6}$$

If shearing force Q is rewritten as in (6-2), then (6-6) becomes

$$\frac{dy}{dx} = \theta + \frac{V}{A_cG_c} + \frac{P\,\theta}{A_cG_c} + \frac{dy_o}{dx} \tag{6-7}$$

Differentiating,

$$\frac{d^2y}{dx^2} = \frac{d\theta}{dx} + \frac{1}{A_cG_c}\frac{dV}{dx} + \frac{P}{A_cG_c}\frac{d\theta}{dx} + \frac{d^2y_o}{dx^2} \tag{6-8}$$

But $\frac{dV}{dx} = -q$ and $\frac{d\theta}{dx}$ may be written in terms of bending moment (see (6-4)) which, when substituted into (6-8), gives

$$\frac{d^2y}{dx^2} = -\frac{M}{E_fI_b}\left[1.0 + \frac{P}{A_cG_c}\right] - \frac{q}{A_cG_c} + \frac{d^2y_o}{dx^2} \tag{6-9}$$

Rearranging (6-9),

$$M = \frac{E_f I_b}{1 + \frac{P}{A_c G_c}} \left[\frac{d^2 y_o}{d\,x^2} - \frac{q}{A_c G_c} - \frac{d^2 y}{dx^2} \right] \tag{6-10}$$

Differentiating (6-10)

$$\frac{dM}{dx} = \frac{E_f I_b}{1 + \frac{P}{A_c G_c}} \left[-\frac{d^3 y}{dx^3} + \frac{d^3 y_o}{dx^3} - \frac{1}{A_c G_c} \frac{dq}{dx} \right] \tag{6-11}$$

From equilibrium (see Timoshenko,[52] page 2)

$$V = \frac{dM}{dx} - P \frac{dy}{dx} \tag{6-12}$$

Differentiating (6-12), and recalling that $\frac{dV}{dx} = -q$,

$$\frac{dV}{dx} = \frac{d^2 M}{dx^2} - P \frac{d^2 y}{dx^2} = -q \tag{6-13}$$

Differentiating (6-11) and substituting into (6-13) we obtain

$$\frac{E_f I_b}{1 + \frac{P}{A_c G}} \left[-\frac{d^4 y}{dx^4} + \frac{d^4 y_o}{dx^4} - \frac{1}{A_c G_c} \frac{d^2 q}{dx^2} \right] - P \frac{d^2 y}{dx^2} = -q \tag{6-14}$$

After rearranging (6-14) the governing differential equation is obtained. That is,

$$\frac{d^4 y}{dx^4} + \frac{P}{E_f I_b} \left[1 + \frac{P}{A_c G_c} \right] \frac{d^2 y}{dx^2} = \frac{\left[1 + \frac{P}{A_c G_c} \right]}{E_f I_b} q + \frac{d^4 y_o}{dx^4} - \frac{1}{A_c G_c} \frac{d^2 q}{dx^2} \tag{6-15}$$

Let

$$k^2 = \frac{P}{E_f I_b}\left[1 + \frac{P}{A_c G_c}\right] \qquad (6\text{-}16)$$

Equation (6-15) may then be reduced to its final form, using superscripts to represent derivatives taken with respect to the independent variable x,

$$y^{iv} + k^2 y'' = k^2\frac{q}{P} + y_o^{iv} - \frac{1}{AG}q'' \qquad (6\text{-}17)$$

Equation (6-17) is considered by the writer to be the most accurate equation available from which general instabilities may be determined for weak core sandwich columns. In addition to shear deformations, the equation allows any form of small initial surface deflections to be included.

Specific solutions for (6-17) will now be presented for selected combinations of end conditions and initial deflections.

Pinned Ends, Initial Deflections.--This case is illustrated in the following sketch:

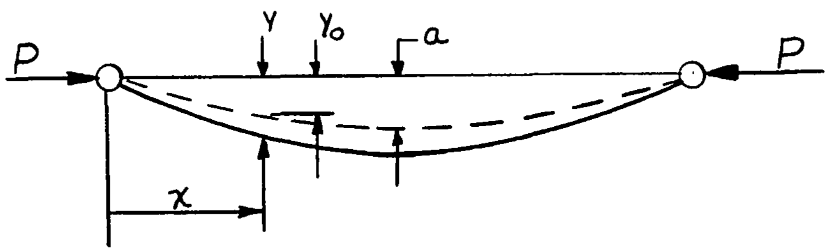

The initial deflection is assumed

$$y_o = a \sin\frac{\pi x}{\ell} \qquad (a)$$

where a is midspan amplitude and ℓ is the column length. For this particular case, equation (6-17) reduces to

$$y^{iv} + k^2 y'' = y_o^{iv} \qquad \text{(b)}$$

Substituting (a) into (b) gives

$$y^{iv} + k^2 y'' = a(\tfrac{\pi}{\ell})^4 \sin\tfrac{\pi x}{\ell} \qquad \text{(c)}$$

recalling that

$$k^2 = \frac{P}{E_f I_b}\left[1 + \frac{P}{A_c G_c}\right] \qquad \text{(d)}$$

The complimentary solution of (c) may be expressed in the form

$$y_c = A_1 + A_2 x + A_3 \sin kx + A_4 \cos kx \qquad \text{(e)}$$

The particular solution takes the form

$$y_p = B_1 \sin\tfrac{\pi x}{\ell} + B_2 \cos\tfrac{\pi x}{\ell} \qquad \text{(f)}$$

Substituting (f) back into (c) leads to the solution of the coefficients

$$B_1 = 0$$

$$B_2 = \frac{a}{1 - k^2(\frac{\ell}{\pi})^2}$$

The deflection equation then becomes

$$\begin{aligned} y &= y_c + y_p \\ &= A_1 + A_2 x + A_3 \sin kx + A_4 \cos kx \\ &\quad + \frac{a}{1 - k^2(\frac{\ell}{\pi})^2} \sin\frac{\pi x}{\ell} \end{aligned} \qquad \text{(g)}$$

The deflection derivatives are

$$y' = A_2 + A_3\, k \cos kx - A_4\, k \sin kx$$

$$+ \frac{a(\frac{\pi}{\ell})}{1 - k^2(\frac{\ell}{\pi})^2} \cos \frac{\pi x}{\ell} \qquad \text{(h)}$$

$$y'' = -A_3\, k^2 \sin kx - A_4\, k^2 \cos kx$$

$$- \frac{a(\frac{\pi}{\ell})^2}{1 - k^2(\frac{\ell}{\pi})^2} \sin \frac{\pi x}{\ell} \qquad \text{(i)}$$

The following boundary conditions were assumed:

(a) At $x = 0$, $y = 0$ and $y'' = 0$

(b) At $x = \ell$, $y = 0$ and $y'' = 0$

Applying the above boundary conditions produces four boundary equations,

$$A_1 + A_4 = 0 \qquad \text{(j)}$$

$$A_4\, k^2 = 0 \qquad \text{(k)}$$

$$A_1 + A_2\ell + A_3 \sin k\ell + A_4 \cos k\ell = 0 \qquad \text{(l)}$$

$$A_3\, k^2 \sin k\ell + A_4\, k^2 \cos k\ell = 0 \qquad \text{(m)}$$

From equations (j) and (k), $A_1 = A_4 = 0$. Since $\underline{A_4}$ is zero, equation (m) reduces to

$$A_3\, k^2 \sin k\ell = 0 \qquad \text{(n)}$$

If $\underline{A_3}$ is taken as zero in (n), then $\underline{A_2}$ would be zero from (l) and a trivial solution would result for deflection $\underline{y}$. However, if $\sin k\ell$

is set equal to zero in equation (n), a non-trivial solution may be determined.

If $\sin k\ell = 0$, then

$$k\ell = n\pi, \quad n = 1,2,\ldots$$

$$k^2 = \frac{n^2\pi^2}{\ell^2} \tag{o}$$

But

$$k^2 = \frac{P}{E_f I_b}\left[1 + \frac{P}{A_c G_c}\right] \tag{d}$$

By equating (o) and (d), we obtain

$$\frac{P}{E_f I_b}\left[1 + \frac{P}{A_c G_c}\right] = \frac{n^2\pi^2}{\ell^2} \tag{p}$$

Let $P_e = \pi^2 E_f I_b/\ell^2$ which corresponds to the Euler equation for pinned end columns neglecting shear deformations.[52] Equation (p) may then be rewritten in terms of $\underline{P_e}$. That is,

$$P^2 + A_c G_c\, P - n^2 A_c G_c\, P_e = 0 \tag{q}$$

Solving (q) for $\underline{P}$,

$$P = -\frac{A_c G_c}{2} + \frac{A_c G_c}{2}\sqrt{1 + 4n^2\frac{P_e}{A_c G_c}} \tag{r}$$

The critical buckling load $\underline{P_{cr}}$ is the minimum value of $\underline{P}$. This is obtained by taking the fundamental buckling mode shape where $n = 1$. Then,

$$P_{cr} = \frac{A_c G_c}{2}\left[\sqrt{1 + \frac{4P_e}{A_c G_c}} - 1\right] \qquad (6\text{-}18)$$

Note that the buckling load is independent of the initial deflection y_o. Note also that the buckling load approaches an indeterminate form as the core thickness approaches zero. This limits the use of the equation to cores of finite thickness but of course this presents no problem since sandwich structures would be expected to have thick cores when compared with their facing thickness.

Fixed Ends--The next case to be considered is the case where both ends are fixed.

There are reactive moments that prevent the ends of the column from rotating during buckling. These end moments and the axial compressive forces are equivalent to forces P applied eccentrically as shown below,

From Timoshenko,[52] the Euler buckling load for a column with fixed ends is

$$P_e = \frac{4\pi^2 E_f I_b}{\ell^2} \tag{6-19}$$

In the previous pinned end case it was shown that initial deflection did not enter into the buckling load, which was based on bending failure; therefore, initial deflections are omitted in the development of the fixed end case.

The buckling equation for the case of a column with fixed ends is developed in exactly the same manner as for the pinned end case. Repetitive details are not given; however, an important point arose in the solution of the boundary equation which is worthy of further discussion.

The basic differential equation for this case is

$$y^{iv} + k^2 y'' = 0 \tag{a}$$

The complimentary and particular solutions for (a) are identical in form to the previous pinned end case, except that $y_o = 0$. The assumed boundary conditions are:

(a) At $x = 0$, $y = 0$ and $y' = 0$

(b) At $x = \ell$, $y = 0$ and $y' = 0$

These boundary conditions, when applied in the complimentary and particular solutions for deflection, lead to the boundary equations,

$$A_1 + A_4 = 0 \tag{b}$$

$$A_2 + A_3 k = 0 \tag{c}$$

$$A_1 + A_2\ell + A_3 \sin k\ell + A_4 \cos k\ell = 0 \qquad \text{(d)}$$

$$A_2 + A_3 k \cos k\ell - A_4 k \sin k\ell = 0 \qquad \text{(e)}$$

Written in matrix form,

$$\begin{bmatrix} 1 & 0 & 0 & 1 \\ 0 & 1 & k & 0 \\ 1 & \ell & \sin k\ell & \cos k\ell \\ 0 & 1 & k \cos k\ell & -k \sin k\ell \end{bmatrix} \begin{bmatrix} A_1 \\ A_2 \\ A_3 \\ A_4 \end{bmatrix} = 0 \qquad \text{(f)}$$

In seeking solutions to homogeneous linear equations a mathematical tool which appears attractive is the theorem (see Kreyszig,[64] p. 421) which states that for a non-trivial solution to exist the determinant of the coefficient matrix must be zero. It must be pointed out that this technique is often used in obtaining natural frequencies of dynamic systems but must be used with caution when attempting to determine lowest buckling modes. In the case under discussion, columns with fixed ends, it will be shown that the solution of the determinant does not provide the critical buckling load.

The determinant of the coefficient matrix in (f) is

$$-k \sin^2 k\ell \qquad \text{(g)}$$

which is set equal to zero. To obtain a non-trivial solution,

$$\sin k\ell = 0 \qquad \text{(h)}$$

which is satisfied if

$$k\ell = n\pi, \quad n = 1,2,3,\cdots$$

or

$$k^2 = \frac{n^2\pi^2}{\ell^2} \tag{i}$$

recalling that

$$k^2 = \frac{P}{E_f I_b}\left[1 + \frac{P}{A_c G_c}\right] \tag{j}$$

Equating (i) and (j),

$$\frac{P}{E_f I_b}\left[1 + \frac{P}{A_c G_c}\right] = \frac{n^2\pi^2}{\ell^2} \tag{k}$$

Solving this quadratic for P and setting $n = 1$ to obtain the lowest mode,

$$P = \frac{A_c G_c}{2}\left[\sqrt{1 + \frac{4\pi^2}{\ell^2}\frac{E_f I_b}{A_c G_c}} - 1\right] \tag{l}$$

This solution for the buckling load is identical to equation (6-18) for the previous pinned end case. Obviously, the fixed end case has a much shorter effective length and would buckle at a higher load than would the pinned end case. Equation (l) is incorrect and points out the danger of using the determinant method.

This takes us back to solving the original boundary equations (b), (c), (d), and (e). Omitting the detailed steps, a non-trivial solution to the boundary equations is obtained if the following relationship is satisfied,

$$\left(\sin \frac{k\ell}{2}\right) \left(2 \sin \frac{k\ell}{2} - k\ell \cos \frac{k\ell}{2}\right) = 0 \qquad \text{(m)}$$

One solution to (m) is

$$2 \sin \frac{k\ell}{2} - k\ell \cos \frac{k\ell}{2} = 0 \qquad \text{(n)}$$

From which

$$\tan \frac{k\ell}{2} = \frac{k\ell}{2} \qquad \text{(o)}$$

The smallest root of this transcendental function, from Jahnke and Emde,[65] is

$$\frac{k\ell}{2} = 4.4934$$

The resulting buckling load is found to be

$$P = \frac{A_c G_c}{2} \left[\sqrt{1 + \frac{4}{A_c G_c} (2.045 \; P_e)} - 1 \right] \qquad \text{(p)}$$

Recalling from (6-19) that $\underline{P_e}$ for the fixed end case is

$$P_e = \frac{4 \pi^2 E_f I_b}{\ell^2}$$

The second solution to (m) is

$$\sin \frac{k\ell}{2} = 0 \qquad \text{(q)}$$

which is satisfied when

$$k\ell = 2 n\pi, \quad n = 1,2,3,\cdots$$

Again, the lowest buckling load is obtained when $n = 1$, and

$$k^2 = \frac{4\pi^2}{\ell^2} \qquad \text{(r)}$$

The resulting buckling load from this value of $\underline{k^2}$ is found to be

$$P = \frac{A_c G_c}{2}\left[\sqrt{1 + \frac{4\,P_e}{A_c G_c}} - 1\right] \qquad \text{(s)}$$

The lowest buckling load determined was that given by equation (s), therefore, the critical buckling load for the column with fixed ends is

$$P_{cr} = \frac{A_c G_c}{2}\left[\sqrt{1 + \frac{4\,P_e}{A_c G_c}} - 1\right] \qquad \text{(6-20)}$$

<u>One End Fixed, Other End Pinned</u>--This case was solved in exactly the same manner as the previous cases. Initial deflections were included for completeness since the end conditions in this case were identical to the short column tests in the experimental program.

The resulting deflection equation obtained is

$$y = \frac{\alpha\pi}{k\ell - \tan k\ell}\left[-\sin k\,x + (\tan k\ell)(\cos kx - 1)\right]$$

$$- \alpha\left(\frac{\pi}{\ell}\right)x + \alpha\sin\frac{\pi x}{\ell} \qquad \text{(6-21)}$$

where

$$\alpha = \frac{a}{1 - (\frac{\ell}{\pi})^2 k^2}$$

a = initial deflection at midspan

Instability occurs when

$$\tan k\ell = k\ell$$

The smallest, non-trivial, root was found (same as in previous case) to be

$$k\ell = 4.4934$$

The resulting buckling equation is then

$$P = \frac{A_c G_c}{2}\left[\sqrt{1 + \frac{4}{A_c G_c}\left[\frac{\pi^2 E_f I_b}{(0.699\ell)^2}\right]} - 1\right]$$

From Timoshenko,[52] the Euler buckling equation for this case is given by

$$P_e = \frac{\pi^2 E_f I_b}{(0.699\ell)^2} \qquad (6\text{-}22)$$

The critical buckling equation can then be written as

$$P_{cr} = \frac{A_c G_c}{2}\left[\sqrt{1 + \frac{4 P_e}{A_c G_c}} - 1\right] \qquad (6\text{-}23)$$

<u>One End Fixed, Other End Free</u>--This case was solved by Timoshenko.[52] He showed in a slightly different manner that the critical buckling equation for this case was

$$P_{cr} = \frac{A_c G_c}{2}\left[\sqrt{1 + \frac{4\ P_e}{A_c G_c}} - 1\right] \tag{6-24}$$

where

$$P_e = \frac{\pi^2\ E_f I_b}{4\,\ell^2} \tag{6-25}$$

General Cases--All four cases just discussed were shown to have buckling equations identical in form. It is concluded that the general instability mode may be determined for any set of end conditions by the equation

$$P_{cr} = \frac{A_c G_c}{2}\left[\sqrt{1 + \frac{4\ P_e}{A_c G_c}} - 1\right] \tag{6-26}$$

where P_e is the classic Euler column buckling equation of the form

$$P_e = \frac{C\ \pi^2\ E_f I_b}{\ell^2} \tag{6-27}$$

Constant C is a function of the end conditions.

Engesser Equations--The Engesser equations are developed for particular cases by Timoshenko and Gere[52] and Boller and Norris.[66] The equations from each source may be reduced to the form

$$P_{cr} = \frac{P_e}{1 + \frac{P_e}{A_c G_c}} \tag{6-28}$$

where P_e is the Euler buckling equation discussed earlier in this section. In the development of the Engesser equations, the normal shearing force equation used is

$$Q = V + P \frac{dy}{dx} \qquad (6\text{-}29)$$

Differentiating (6-29),

$$\frac{dQ}{dx} = \frac{dV}{dx} + P \frac{d^2y}{dx^2} \qquad (6\text{-}30)$$

Herein lies the difference between the general instability equations developed in this chapter and by the Engesser method. From (6-2) and (6-5) we obtain

$$\frac{dQ}{dx} = \frac{dV}{dx} + P \left(\frac{d^2y}{dx^2} - \frac{d\gamma}{dx} - \frac{d^2y_o}{dx^2}\right) \qquad (6\text{-}31)$$

In the Engesser development the normal shearing force derivative, (6-30), is expressed in terms of the total curvature. In equation (6-31) we see that the normal shearing force derivative used in this research is given in terms of curvature due to bending only. This rather subtle difference can lead to sizeable differences in buckling stresses predicted by the two methods.

A comparison of this improved shear method and the Engesser method is given in Table 6-1.

Table 6-1 becomes more meaningful when it is realized that a typical sandwich having 1/4 inch Douglas fir facings and 4 inch Dorvon core would have values of parameter $\frac{P_e}{A_c G_c}$ for lengths of 12 and 96 inches as follows:

Length in.	$\frac{P_e}{A_c G_c}$ (Pinned ends)	$\frac{P_e}{A_c G_c}$ (Fixed ends)
12	116	464
96	1.81	7.24

In the 96 inch case the more accurate method, which is termed the improved method, would predict failure at loads 45 and 164 percent higher than would the Engesser method for the pinned and fixed end conditions, respectively.

TABLE 6-1

COMPARISON OF ENGESSER AND IMPROVED SHEAR METHODS

$\frac{P_e}{A_c G_c}$	Engesser Method P_{cr}/P_e	Improved Method P_{cr}/P_e	Ratio: $\frac{\text{Improved}}{\text{Engesser}}$
0	1.0000	1.0000	1.000
1	0.5000	0.6180	1.235
2	0.3333	0.5000	1.502
6	0.1429	0.3333	2.430
10	0.0909	0.2702	2.970
100	0.0099	0.0951	9.610

Displaced Ends--If one end is assumed fixed and the other end pinned, but displaced a fixed distance δ from the x axis, as shown in the following sketch,

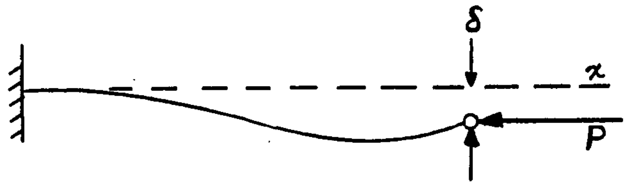

the solution still follows the same procedure as for all previous cases.

The boundary conditions for this case are:

(a) At $x = 0$, $y = 0$ and $y' = 0$

(b) At $x = \ell$, $y = \delta$ and $y'' = 0$

The resulting deflection equation is

$$y = \left[\frac{\delta}{k\ell \cot k\ell - 1}\right]\left[-\cot k\ell \sin k x + \cos k x + k x \cot k\ell - 1\right] \tag{6-32}$$

General instability is determined by equation (6-26), in exactly the same manner as for the previous cases.

Core shear is induced by end displacement and will be discussed in the last section of this chapter under core shear failures.

C. Sandwich Columns Under Eccentric Loads

A column is assumed eccentrically loaded a distance e at each end as shown in the following sketch

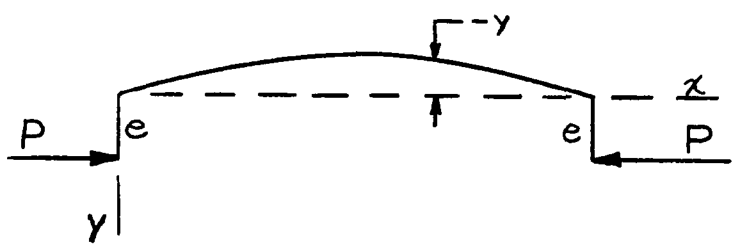

The local bending moment is

$$M = P(y - e) \tag{a}$$

From equation (6-10) we see that the bending moment for this case can also be written as

$$M = \frac{E_f I_b}{1 + \frac{P}{A_c G_c}} (- y'') \tag{b}$$

Equating (a) and (b),

$$y'' + k^2 y = k^2 e \tag{c}$$

where, as before,

$$k^2 = \frac{P}{E_f I_b} (1 + \frac{P}{A_c G_c})$$

Taking the two boundary conditions that deflection is zero at each end, the general solution of (c) is found to be

$$y = \frac{e}{\sin (k\ell)} [\sin (kx - k\ell) - \sin kx + \sin k\ell] \tag{6-33}$$

At midspan, the deflection equation (6-33) reduces to the well known secant formula,

$$y = e\left[1 - \sec \frac{k\ell}{2}\right] \tag{6-33a}$$

The general instability equation, determined from (6-33a), was found to be the same as for the previous fixed end case.

The core shear stress induced by the eccentric load is discussed in the last section on core shear failures.

D. Sandwich Column Failure by Core Shear

Failure of sandwich columns may occur before general instability loads are reached if induced core shear stresses should exceed their ultimate limits. Core shear may be induced by initial bow, end displacements, or eccentric loads. This section develops the basic equations for maximum shear stress under each of these three influencing factors.

Initial Bow--The effect on core stress due to initial bow will be determined for the case of one end fixed, other end pinned. This case is most representative of typical one-story load-bearing walls. The fixed end moment may be simulated by displacing the reactive axial end load a distance d. The local bending moment is then

$$M = P(y - d) \tag{a}$$

Differentiating,

$$\frac{dM}{dx} = P\frac{dy}{dx} \tag{b}$$

The shearing force N, normal to the deflected axis, may be assumed as

$$N = \frac{dM}{dx} \tag{c}$$

Equating (b) and (c),

$$N = P\frac{dy}{dx} \tag{d}$$

Recall from (6-21) that the deflection equation for this case is

$$y = \frac{\alpha \pi}{k\ell - \tan k\ell}\left[-\sin kx + (\tan k\ell)(\cos kx - 1)\right]$$

$$- \alpha\left(\frac{\pi}{\ell}\right)x + \alpha \sin \frac{\pi x}{\ell} \qquad (6\text{-}21)$$

where

$$\alpha = \frac{a}{1 - \left(\frac{\ell}{\pi}\right)^2 k^2} \qquad (e)$$

a = initial deflection at midspan

$$k^2 = \frac{P}{E_f I_b}\left[1 + \frac{P}{A_c G_c}\right]$$

Differentiating (6-21) and then substituting into (d) gives

$$\frac{N}{\pi \alpha P} = \frac{k}{k\ell - \tan k\ell}\left[-\cos kx - \tan k\ell \sin kx + 1\right]$$

$$- \frac{1}{\ell} + \frac{1}{\ell}\cos\frac{\pi x}{\ell} \qquad (f)$$

Maximum shearing force is obtained by setting the derivative of $\underline{N}$ equal to zero, that is

$$\frac{\partial N}{\partial x} = 0 \qquad (g)$$

From (g) it is found that maximum shear occurs at the ends, as expected. The maximum shear is then found to be

$$\frac{N_{max}}{\pi \alpha P} = \frac{k}{k\ell - \tan k\ell}\left[-\cos k\ell - \tan k\ell \sin k\ell + 1\right] - \frac{2}{\ell} \qquad (6\text{-}34)$$

Let us now convert to shear stress, $\underline{\tau}$. As previously given

$$N = \tau A_c \qquad (h)$$

or

$$N_{max} = \tau_{max} A_c \qquad (i)$$

The substitution of N_{max} from (i) back into (6-34) leads to the final equation for maximum shear stress induced by initial bowing. That is,

$$\tau_{max} = \frac{a\,P}{A_c \ell} C_a \qquad (6\text{-}35)$$

where

$$C_a = \frac{\pi\alpha}{a} \left[\frac{k\ell}{k\ell - \tan k\ell} (1 - \cos k\ell - \tan k\ell \sin k\ell) - 2.0 \right] \qquad (6\text{-}36)$$

The core shear coefficient $\underline{C_a}$ is plotted versus load parameter $k\ell$ in Figure 6-2. It is shown to be asymptotic to the critical buckling value of $k\ell$, 4.493.

It was found that for the class of sandwiches considered in this research that core shear failure due to bowing is highly unlikely at normal wall heights. If the sandwich is used as a column with a height of approximately three feet or less then this type of failure could occur. For example, a 3 foot column having 1/4 inch Douglas fir plywood faces and 2 inch Dorvon core would fail in core shear under a facing load of 3000 psi for an initial panel bow of 0.2 inches. For this same case the experimental value of face wrinkling stress was 4493 psi.

End Displacements--A physical description with accompanying sketch was given earlier in this chapter for the condition where a column had one end in a fixed displacement $\underline{\delta}$ from the $\underline{x}$ axis.

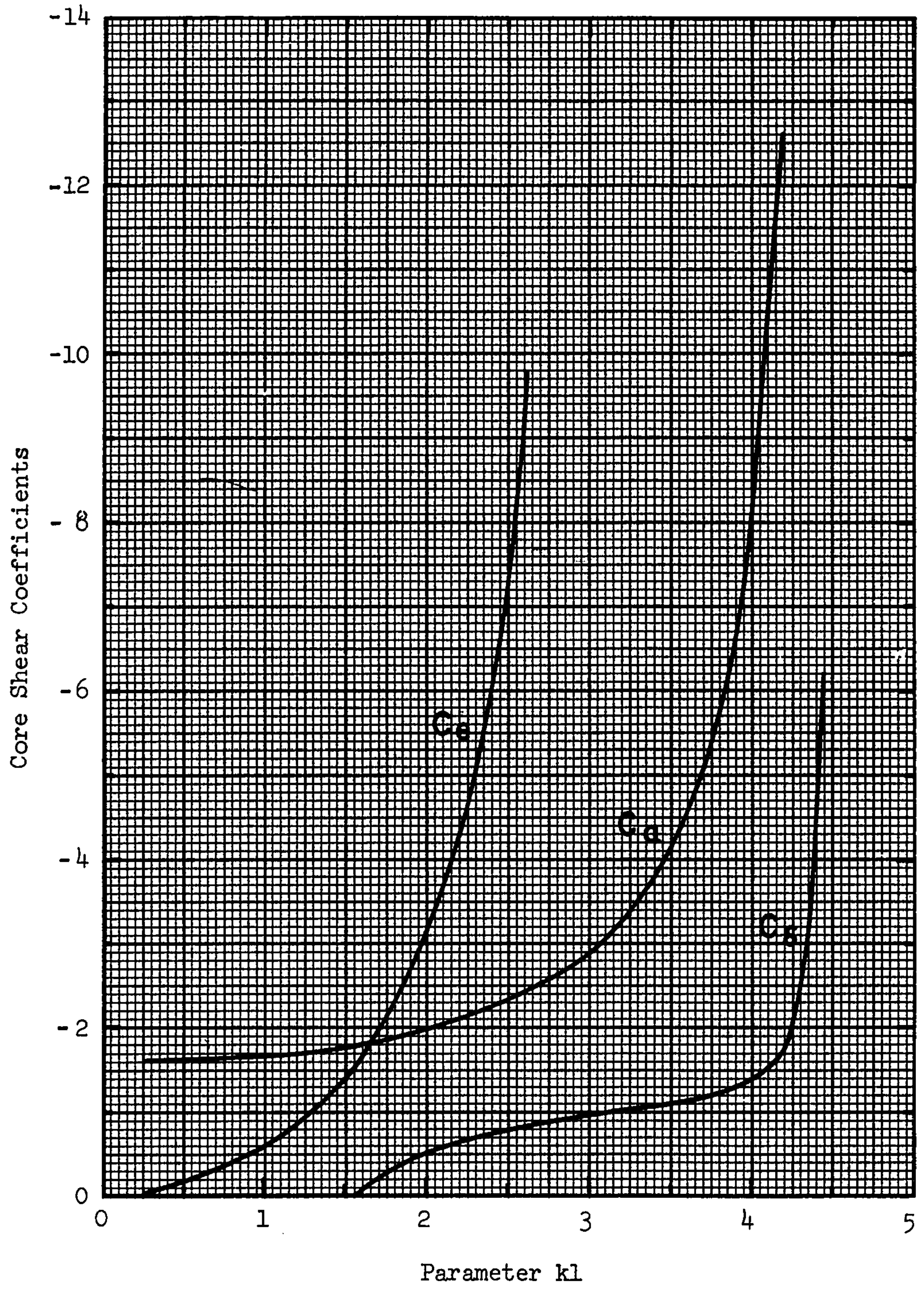

Figure 6-2. Core Shear Coefficients Versus Load Parameter kl.

The shearing forces are not as easily determined in this case as for the previous case with initial bowing. From (6-12),

$$V = \frac{dM}{dx} - P\frac{dy}{dx} \tag{6-12}$$

Substituting $\frac{dM}{dx}$ from (6-11) into (6-12)

$$V = \frac{E_f I_b}{1 + \frac{P}{A_c G_c}}\left[-\frac{d^3y}{dx^3}\right] - P\frac{dy}{dx} \tag{6-37}$$

The deflection equation, from (6-32), is then substituted into (6-37) from which one obtains

$$V = \frac{\delta}{k\ell \cot k\ell - 1}\left[\frac{E_f I_b}{1 + \frac{P}{A_c G_c}}(-k^3 \cot k\ell \cos kx - k^3 \sin kx) - P(-k \cot k\ell \cos kx - k \sin kx + k \cot k\ell)\right] \tag{6-38}$$

By maximizing (6-38), shear was found to be a maximum at the ends, as expected. By substituting either $x = 0$ or $x = \ell$ into (6-38) the maximum shear force is found to be

$$V_{max} = \frac{\delta P k}{\tan k\ell - k\ell} \tag{6-39}$$

Setting $V_{max} = \tau_{max} A_c$, the maximum stress is obtained from (6-39). That is,

$$\tau_{max} = \frac{P\delta}{A_c \ell} C_\delta \tag{6-40}$$

where

$$C_\delta = \frac{k}{\tan k\ell - k\ell} \tag{6-41}$$

The core shear coefficient $\underline{C_\delta}$ is plotted versus load parameter $k\ell$ in Figure 6-2. The effect of end displacement is most pronounced for relatively short columns. The example given in the previous bowing case of a 3 foot column of 1/4 inch Douglas fir plywood and 2 inch Dorvon core also is a good case to demonstrate end displacement effects. At a facing stress level of 3000 psi the core would fail in shear if one end is displaced a distance of 0.57 inches.

Eccentric Loads--The effects of eccentric end loads on core shear is more critical in practical areas of application than either bowing or end displacement. In contrast, the eccentric loading case grows progressively worse as column length increases. The development of core shear due to eccentric loads follows the same development as for the bowed case. The only difference is in the deflection equations used. In this case, equation (6-33) was used.

The equation for maximum shear stress due to eccentric loads was found to be

$$\tau_{max} = \frac{P\,e}{A_c \ell} C_e$$

where

$$C_e = \frac{k\ell\,(\cos k\ell - 1)}{\sin k\ell}$$

Core shear coefficient $\underline{C_e}$ is plotted versus load parameter $k\ell$ in Figure 6-2.

In the design of wall panels for building construction, an accepted method for evaluating panels under axial loads is ASTM Standard E 72-61.[67] This standard specifies that the axial load shall be applied eccentrically a distance equal to one-sixth of the total sandwich thickness.

A sandwich having 1/4 inch Douglas fir plywood faces and a 3 inch Dorvon foam core would fail in shear (11 psi) at the axial facing stresses given below for several column lengths:

Column Length	Facing Stress at Core Shear Failure
1 ft.	3620 psi
3	2570
6	1640
10	900

The effect of eccentric loads on core shear is shown to be quite significant. This points out the necessity for always checking this potential failure mode.

CHAPTER VII

UNIFIED SANDWICH COLUMN ANALYSIS

A. Introduction

Once a designer has selected a trial sandwich column for his particular application it is then necessary to subject this design to a column analysis to see if it is stable in all modes and does not fail in core shear or face crushing. The instability modes are the overall column buckling, including shear instability, and the localized face wrinkling instability. It is not practical to define the regions of "short" or "long" columns by a simple parameter such as the ratio of length to radius of gyration (ℓ/r), commonly used in homogeneous columns.

The analysis consists of checking the critical buckling stresses and core shear stresses to see if allowable facing and core stresses are exceeded. If allowable limits are not set by standards or codes it is common practice to assume one-half of the yield stresses as the allowable working stresses for many applications.

Analysis of the sandwich column requires the values, or estimates, of the following sandwich physical and geometric properties:

E_c = Core average elastic extensional modulus

G_c = Core average elastic shear modulus

E_f = Facing elastic compression modulus

t_c = Core thickness

t_f = Facing thickness (each face)

ℓ = Column length

C = Euler column constant for given end conditions

A_c = Core area (= t_c, assuming unit width)

I_b = Moment of inertia of facings about middle plane

The following sections summarize the analysis for each of the possible failure mechanisms. Note that in all cases the analysis is for a section of unit width.

B. General Instability Analysis

Overall buckling and shear instability are checked through the use of the classical Euler column buckling equation for given end conditions and the improved shear method developed in Chapter VI. Euler and critical loads are

$$P_e = \frac{C\,\pi^2\,E_f I_b}{\ell^2} \tag{7-1}$$

$$P_{cr} = \frac{A_c G_c}{2}\left[\sqrt{1 + \frac{4\,P_e}{A_c G_c}} - 1\right] \tag{7-2}$$

Buckling stress is then

$$p_{cr} = \frac{P_{cr}}{t_f} \tag{7-3}$$

C. Core Shear Stresses

Premature core failure in shear is a potential failure mechanism if the sandwich is subjected to bowing, end displacement, or eccentric loading. Maximum shear stress is determined by the following general equation:

$$_{\max} = \frac{P\,\Delta}{A_c \ell}\, C_\Delta \qquad (7\text{-}4)$$

where $\underline{\Delta}$ is either the initial bowing deflection $\underline{a}$, the end displacement $\underline{\delta}$, or the off-set distance $\underline{e}$ in an eccentrically loaded column. Coefficient C_Δ is the coefficient corresponding to the particular displacement (a, δ, or e) under consideration. The coefficients $\underline{C_a}$, $\underline{C_\delta}$, and $\underline{C_e}$ are obtained from Figure 6-2 for a given value of $k\ell$. It is recalled that

$$k^2 = \frac{P}{E_f I_b}\left[1 + \frac{P}{A_c G_c}\right] \qquad (7\text{-}5)$$

It is necessary to solve for the limiting load by an iterative procedure. It might prove best to make several calculations and plot compressive load $\underline{P}$ versus $\underline{\tau_{max}}$. From this graph, one could then select the limiting load $\underline{P}$.

D. Face Wrinkling Analysis

It is suggested that the designer read and understand the theory and experimental correlations employed in face wrinkling analysis. The procedure is somewhat complex and must be carefully followed.

Therefore, the following procedure goes into more detail than for the other failure modes.

The first part of this section outlines the procedure for determining the classical upper bound of face wrinkling buckling load. The last part deals with the lower bound problem of initial waviness. Let

$$\alpha = \left(\frac{t_f}{t_c}\right)^3 \frac{E_f E_c}{G_c^2}$$

The wrinkling mode is always anti-symmetrical if $\alpha \geq 0.9551$. If $\alpha \geq 0.9551$, the marginal zone for the anti-symmetrical case is

$$B = 1.499\ t_f \left[\frac{E_f E_c}{G_c^2}\right]^{1/3} \qquad (7\text{-}6)$$

The wrinkling mode is always symmetrical if $\alpha \leq 0.5674$. The marginal zone for the symmetric case is

$$B = 0.905\ t_f \left[\frac{E_f E_c}{G_c^2}\right]^{1/3} \qquad (7\text{-}7)$$

If the wrinkling mode is identified, the next step is to compare marginal zone thickness with core half-thickness. This will further classify the mode as to whether "thick" or "thin." This will dictate the proper buckling equation to use. If $0.5674 < \alpha < 0.9551$ then the mode is not readily identified. The following procedure will cover all ranges of α.

Classical Wrinkling Procedure:

1. <u>If $\alpha \geq 0.9551$</u> buckle = Anti-symmetrical.

   a. Calculate B from Eq. (7-6)

   b. If $B \leq t_c/2$, core is thick

$$P_{cr} = 0.5109\ t_f\ [E_f E_c G_c]^{1/3} + 0.3296\ G_c t_c \tag{7-8}$$

   c. If $B > t_c/2$, core is thin

$$P_{cr} = 0.5902\ t_f \sqrt{E_f E_c \frac{t_f}{t_c}} + 0.3864\ G_c t_c \tag{7-9}$$

2. <u>If $\alpha \leq 0.5674$</u> buckle = symmetrical

   a. Calculate B from Eq. (7-7)

   b. If $B \leq t_c/2$, core is thick

$$P_{cr} = 0.909\ t_f \left[E_f E_c G_c\right]^{1/3} \tag{7-10}$$

   c. If $B > t_c/2$, core is thin

$$P_{cr} = 0.815\ t_f \sqrt{E_f E_c \frac{t_f}{t_c}} + \frac{1}{6}\ G_c t_c \tag{7-11}$$

3. <u>If $0.5674 < \alpha < 0.9551$</u>

   a. Calculate $B_a = 1.5\ t_f \left[\frac{E_f E_c}{G_c^2}\right]^{1/3}$

   b. If $B_a \leq t_c/2$, buckle is anti-symmetrical, thick core. Use Eq. (7-8) for P_{cr}.

3. c. If $B_a > t_c/2$, buckle is sym. Check B_s from Eq. (7-7).
If $B_s \leq t_c/2$, core is thick. Use Eq. (7-10) for P_{cr}.
If $B_s > t_c/2$, core is thin. Use Eq. (7-11) for P_{cr}.

The classical wrinkling stress determined by the above procedure is the upper stress limit. As previously discussed, true wrinkling stress is reduced due to initial imperfections represented in the waviness parameter A_o/F. The initial waviness parameter prediction equations must be considered accurate, or conservative, to within some accepted probability. It would not be uncommon to see expectation probabilities of 95 percent. Some aircraft applications might accept expectation probabilities associated with one sigma variations. More conservative groups might require three sigma limits which carry expectation probabilities of 99.9 percent. In the absence of set standards, the writer suggests the use of the two sigma criteria which would provide a confidence level of 95.4 percent.

In conclusion of this section, the procedure recommended for determining lower bound wrinkling stresses is summarized as follows:

1. Determine classical wrinkling stress from the procedure given in this section.
2. Set expectation probability (E.P.) for determination of waviness parameter, A_o/F, in terms of one sigma multiplies,

$$E.P. = n\sigma$$

3. Calculate L_{cr} and A_o/F.

$$\frac{A_o}{F} = (0.2191\ L_{cr} + 0.2963\ n + 0.1645) \times 10^{-3} \qquad (7\text{-}12)$$

4. Calculate expected wrinkling stress

   a. If $\frac{E_c}{B} \geq \frac{\pi G_c}{L_{cr}}$, failure is controlled by core tension or compression failure and

$$p = \frac{p_{cr}}{1 + \frac{E_c}{B}\frac{A_o}{F}} \tag{7-13}$$

   b. If $\frac{E_c}{B} < \frac{\pi G_c}{L_{cr}}$, failure is controlled by core shear failure and

$$p = \frac{p_{cr}}{1 + \frac{\pi G_c}{L_{cr}}\frac{A_o}{F}} \tag{7-14}$$

E. Failure by Face Crushing

This is likely to be a problem only in relatively short columns. It is also difficult to predict the yield strength of a facing material when in a composite state with adhesion to a core material. This was discussed in Chapter V on face wrinkling. Until this problem is resolved it is suggested that the raw yield strength of the facing material be taken as the sandwich facing yield strength.

Face crushing should be checked after all other instability and failure mechanisms have been investigated. The procedure is to first find the lowest buckling load <u>P</u> for other modes, secondly obtain the proper deflection equation from Chapter VI for the given end conditions, next take the second derivative of the deflections, and then obtain the facing compression stress from the following equation:

$$f = \left[\frac{E_f(0.5\ t_c + t_f)}{1 + \frac{P}{A_c G_c}}\right]\left(\frac{d^2y}{dx^2}\right)_{max} + \frac{P}{t_f} \tag{7-15}$$

CHAPTER VIII

SUMMARY AND CONCLUSIONS

A. Summary

A theoretical and experimental investigation has been presented on the structural behavior of axially loaded architectural sandwich columns having plastic foam cores. This research was concentrated on establishing rational analysis formulas for localized modes of instability. This objective was accomplished through the development of face wrinkling theories, which, for the first time, allow the unified analysis of face wrinkling with initial waviness for anti-symmetrical mode shapes. The success of the face wrinkling analysis procedure is based on the semi-empirically determined correlation factor for initial waviness.

The experimental program on foam-filled sandwiches with promising facing materials revealed that with respect to local instabilities face wrinkling could be assumed to be the controlling failure mechanism. The experimental program also provided a statistical base for establishing the initial waviness correlation factor.

Strain gage studies of facing strains revealed that sizeable increases in the effective facing strength were realized when the facings were tested in the composite sandwich configuration as compared with independent facing tests. Until this unknown phenomenon is explained, the suggestion was made that in design analysis the elastic properties of the raw facing material be used rather than properties from composite tests.

The effects of unbonded regions were studied experimentally and it was revealed that surprisingly large "debonded" areas had little effect on buckling.

The second major area of research was the analytical investigation of general instabilities of sandwich columns. Here it was revealed that present theories are not adequate for foam-filled sandwich columns. A basic development of general instability equations was presented which introduced a more accurate method of treating shear deformations. Solutions were presented for end conditions most likely to be encountered, including displaced ends and eccentric loads.

Column failure is likely to occur at loads less than critical buckling if initial bowing, end displacements, or load eccentricity is present. This problem was treated in depth and useful analysis equations were developed.

An underlying motivation in this research was the desire to provide the structural designer with a practical guide for accurately analyzing sandwich columns. An attempt was made to satisfy this requirement through the presentation of a chapter on the unified analysis of sandwich columns.

It is hoped that the practical design information put forth in this dissertation will speed the day when plastic foam-filled architectural sandwich panels will be used to carry heavy bearing loads, thereby fulfilling their total potential as the most efficient structural element available to the building construction industry.

B. Conclusions and Recommendations

1. In local instability tests, face wrinkling appeared to be the controlling failure mode for all sandwiches with 1.0 pcf foam densities, and could be reasonably expected to occur in sandwiches with 1.9, 2.5, and 3.3 pcf foam densities.
2. Measurements of facing strain revealed sizeable increases in effective facing material strength when tested in the composite configuration as compared with tests on independent facing material specimens.
3. The effects on buckling strength of small unbonded areas of less than 2 inches across would be negligible; 4 inch strips would decrease face wrinkling strength by 10 percent.
4. The Engesser equation, used in calculating general instability loads, was found to be inaccurate for use with highly shear-flexible sandwich columns, such as foam-filled ones. An improved method was developed and suggested for use.
5. Anti-symmetrical face wrinkling was found to be critical in many cases. It was concluded that a face wrinkling analysis is valid only if it can account for both anti-symmetrical and symmetrical modes of face wrinkling.
6. The Yusuff method of face wrinkling analysis is invalid for the cases considered due to minimization errors and the inability to handle anti-symmetrical wrinkling.

7. Initial waviness was determined experimentally to be a function of critical wave length.
8. Analysis of sandwich columns should follow a unified procedure such as given in Chapter VII since so many potential modes of failure exist. It is recommended that the designer carefully check (a) the general instability mode with the proper equations including shear, (b) for possible core shear failures, (c) face wrinkling in both modes plus initial waviness, and (d) for possible facing crushing.

C. Suggestions for Further Research

1. Research is needed to study the strengthening effect of facing materials in composite configurations as compared with raw facing sheets.
2. The general buckling of foam-filled architectural sandwiches by minimization of the total potential based on the element distortion geometry given in Chapter VI (Reference Hoff,[62] p. 180) needs further study.
3. Experiments to confirm the improved shear method of determining instability loads which was given in Chapter VI should be conducted.

REFERENCES

1. Dietz, A. G. H. "Keynote Address," Sandwich Panel Design Criteria. Publication NAS-NRC 793, Washington, D. C.: Building Research Institute, 1960.

2. Kuenzi, E. W. "Structural Sandwich Design Criteria," Report No. 2161, U. S. Forest Products Laboratory, Madison, Wis., 1959.

3. American Society for Testing Materials, "Structural Sandwich Construction," ASTM Standard C274-53, 1953.

4. Parkinson, R. E. "Selection of Materials for Architectural Sandwich Panels," Symposium on Structural Sandwich Constructions. American Society for Testing Materials Special Technical Publication No. 201., 1956.

5. Ferrigno, T. H. Rigid Plastic Foams. New York: Reinhold Publishing Co., 1963.

6. Koppers, Inc., Dylite Panels-Engineering Manual. Plastics Division, Koppers Inc., Detroit, Mich., 1958.

7. Chalker, R. L. "Load-Bearing Plywood Sandwich Panels," American Plywood Association Lab. Report No. 93, Tacoma, Wash., 1962.

8. Engesser, F. "Die Knickfestigkeit Gerader Stäbe," Zentr. Bauverwaltung, Vol. 11, 1891, p. 483.

9. Kuenzi, E. W. Private Communication to B. J. Harris, Sept. 9, 1966.

10. Harris, B. J., and Crisman, W. C. "Face-Wrinkling Mode of Buckling of Sandwich Panels," Journal of the Engineering Mechanics Division, Proceedings of the American Society of Civil Engineers, Vol. 91, No. EM3, June, 1965, pp. 93-111.

11. Nordby, G. M., and Crisman, W. C. "Strength Properties and Relationships Associated with Various Types of Fiberglass-Reinforced Facing Sandwich Structure," U. S. Army Aviation Materiel Laboratories Tech. Report 65-15, Fort Eustis, Virginia, Aug., 1965.

12. Kuenzi, E. W. Private Communication to B. J. Harris, September 10, 1964.

13. Boller, K. H. and Norris, C. B. "Effect of Shear Strength on Maximum Loads of Sandwich Columns," Report No. 1815, U. S. Forest Products Laboratory, Madison, Wis., 1955.

14. Norris, C. B. "Short-Column Compressive Strength of Sandwich Construction as Affected by Size of Cells of Honeycomb Core Materials," Report No. FPL-206, U. S. Forest Products Laboratory, Madison, Wis., 1964.

15. Warren, T. B. "Strength Properties and Relationships Associated with Various Types of Fiberglass Reinforced Facing Sandwich Structure Progress Report No. 16," Report No. 1386-19, University of Oklahoma Research Inst., Norman, Oklahoma, May, 1964.

16. "Workshop on Sandwich Panel Design Criteria for Exterior Load-Bearing Walls," Sandwich Panel Design Criteria. Publication NAS-NRC 798, Washington, D. C.: Building Research Institute, 1960.

17. Perkins, N. W. Plywood: Properties, Design and Construction. Tacoma, Wash.: The Douglas Fir Plywood Association, 1962.

18. Miller, G. D. and Countryman, D. "Performance of Sandwich Constructions with Styrofoam Cores and Douglas Fir Plywood Faces under Accelerated Exposure Conditions," Laboratory Report No. 86, Douglas Fir Plywood Association, Tacoma, Wash., 1960.

19. Forest Products Laboratory, Wood Handbook. U. S. Department of Agriculture Handbook No. 72, Washington, D. C.: U. S. Government Printing Office, 1955.

20. "Asbestos-Cement," New Horizons in Construction Materials, Vol. 1. Los Altos, Calif.: Hudson Publishing Co., 1962.

21. Plastics in Building. Edited by Modern Plastics, New York: McGraw-Hill, Inc., 1966.

22. "Foamed Plastics," Modern Plastics Encyclopedia 1967. New York: McGraw-Hill, Inc., 1966.

23. "Styrofoam Sandwich Construction," Bulletin 171-144, Dow Chemical Co., Midland, Mich., 1960.

24. "Coro-Foam," Technical Data Information, Cook Paint and Varnish Co., Kansas City, Mo., December, 1965.

25. U. S. Plastics in Building and Construction. Stamford, Conn.: Technomic Publishing Co., 1965.

26. "Adhesives and Coatings for Dow Foam Plastics," Bulletin 171-177C, Dow Chemical Co., Midland, Mich.

27. "Bending Strength and Stiffness of Plywood," Research Note FPL-059, U.S. Forest Products Laboratory, Madison, Wis., 1964.

28. "Building Components," Internal Interim Report, Project No. A 10-2, Masonite Corp., St. Charles, Ill., Jan. 25, 1961.

29. "Styrofoam (Expanded Polystyrene)," Bulletin 171-262, Dow Chemical Co., Midland, Mich., 1965.

30. "Stress-Strain Curve for Dorvon FR 100," Internal Laboratory Report, Dow Chemical Co., Midland, Mich., August, 1966.

31. "Sandwich Constructions and Core Materials; General Test Methods," Military Standard MIL-STD 401A, Dept. of Defense, Washington, D. C.: U. S. Government Printing Office, 1956.

32. O'Dell, Jr., W. W. and Graham, D. L. "Structural Behavior of Sandwich Panels with Foamed-Plastic Cores," Paper No. 30, Conference on Plastics in Building Structures, The Plastics Institute, London, June, 1965.

33. Engel, H. C., Hemming, C. B., and Merriman, H. R. Structural Plastics. New York: McGraw-Hill Book Co., Inc., 1950.

34. Borg, S. F., and Gennaro, J. J. Advanced Structural Analysis. Princeton, N. J.: D. Van Nostrand Co., Inc., 1960.

35. "Fabrication of Dow Foam Plastics," Bulletin 171-175B, Dow Chemical Co., Midland, Mich.

36. "Weldwood Waterproof Resorcinol Glue," Technical Data Sheets, United States Plywood Corporation, Kalamazoo, Mich.

37. Youngquist, W. G. "Performance of Bonded Wire Strain Gages on Wood," Report No. 2087, U. S. Forest Products Laboratory, Madison, Wis., 1957 (Reaffirmed 1965).

38. Hoff, N. J., and Mautner, S. E. "The Buckling of Sandwich-Type Panels," Journal of the Aeronautical Sciences, Vol. 12, No. 3, July, 1945, pp. 285-297.

39. Gough, C. S., Elam, C. F., and de Bruyne, N. A. "The Stabilization of a Thin Sheet by a Continuous Supporting Medium," Journal of the Royal Aeronautical Society, Vol. 44, January, 1940, pp. 12-43.

40. Williams, D. "Sandwich Construction - A Practical Approach for the Use of Designers," Royal Aircraft Establishment, Farnborough, England, Structures Report No. 2, 1947.

41. Wan, C. C. "Face Buckling and Core Strength Requirements in Sandwich Construction," Journal of the Aeronautical Sciences, Vol. 14, No. 9, September 1947, pp. 531-539.

42. Troxell, W. W., and Engel, H. C. "Column Characteristics of Sandwich Panels Having Honeycomb Cores," Journal of the Aeronautical Sciences, Vol. 14, No. 7, July, 1947, pp. 413-421.

43. Norris, C. B., Ericksen, W. S., March, H. W., Smith, C. B., and Boller, K. H. "Wrinkling of the Facings of Sandwich Construction Subjected to Edgewise Compression," Report No. 1810, U. S. Forest Products Laboratory, Madison, Wis., 1949.

44. Sandwich Construction for Aircraft - Part II, Second Edition, Dept. of Defense, Bulletin ANC-23, Washington, D. C.: U. S. Government Printing Office, 1955.

45. Yusuff, S. "Theory of Wrinkling in Sandwich Construction," Journal of the Royal Aeronautical Society, Vol. 59, January, 1955, pp. 30-36.

46. Yusuff, S. "Face Wrinkling and Core Strength in Sandwich Construction," Journal of the Royal Aeronautical Society, Vol. 64, March, 1960, pp. 164-167.

47. Habip, L. M. "A Survey of Modern Developments in the Analysis of Sandwich Structures," Applied Mechanics Surveys. edited by H. N. Abramson, et al., Washington, D. C.: Spartan Books, Inc., 1966.

48. Norris, C. B., Boller, K. H., and Voss, A. W. "Wrinkling of the Facings of Sandwich Construction Subjected to Edgewise Compression," Report No. 1810A, U. S. Forest Products Laboratory, Madison, Wis., 1953.

49. Jenkinson, P. M., and Kuenzi, E. W. "Wrinkling of the Facings of Aluminum and Stainless Steel Sandwich Subjected to Edgewise Compression," Report No. 2171, U. S. Forest Products Laboratory, Madison, Wis., 1959.

50. Harris, B. J. "Strength Properties and Relationships Associated with Various Types of Fiberglass Reinforced Facing Sandwich Structures Progress Report No. 1386-16," University of Oklahoma Research Inst., Norman, Oklahoma, for USATRECOM, February, 1964.

51. Matonis, V. A. "Elastic Behavior of Low Density Rigid Foams in Structural Applications," Society of Plastics Engineers Journal, Vol. 20, September, 1964, pp. 1024-1030.

52. Timoshenko, S. P., and Gere, J. M. Theory of Elastic Stability. Second Edition, New York: McGraw-Hill Book Co., Inc., 1961.

53. Fan, T. C. Discussion of "Face Wrinkling Mode of Buckling of Sandwich Panels," Journal of the Engineering Mechanics Division, Proceedings of the American Society of Civil Engineers, Vol. 91, No. EM 6, December, 1965, pp. 191-193.

54. Jackson, W. T. "Application of Composite Constructions with Honeycomb and Foam Cores," WADD Technical Report 60-874, by Hexcel, Inc., for Aeronautical Systems Div., Air Force Systems Command, June, 1961.

55. Harris, B. J., and Crisman, W. C. Closure Discussion of "Face-Wrinkling Mode of Buckling of Sandwich Panels," Journal of the Engineering Mechanics Division, Proceedings of the American Society of Civil Engineers, Vol. 92, No. EM 3, June, 1966, pp. 103-104.

56. Hendra, D. "Test Results on Mariner C Shroud Honeycomb Material Evaluation," (Internal Report), Lockheed Missiles and Space Co., Sunnyvale, Calif., October, 1963.

57. Almroth, B. O. "Evaluation of Sandwich Cylinder Tests," Interdepartmental Communication to H. D. Anderson, Dept. 52-20, Lockheed Missiles and Space Co., Sunnyvale, Calif., December 18, 1964.

58. Burns, A. B. "Structural Optimization of Foam-Core and Honeycomb-Core Sandwich Cylinders Under Axial Compression," Technical Report 6-62-64-17, Lockheed Missiles and Space Co., Sunnyvale, Calif., December, 1964.

59. Young, H. D. Statistical Treatment of Experimental Data. New York: McGraw-Hill Book Co., Inc., 1962.

60. Mood, A. M., and Graybill, F. A. Introduction to the Theory of Statistics. Second Edition, New York: McGraw-Hill Book Co., Inc., 1963.

61. Hoff, N. J. "The Strength of Laminates and Sandwich Structural Elements," Engineering Laminates. edited by A. G. H. Dietz, New York: John Wiley & Sons, Inc., 1949.

62. Hoff, N. J. The Analysis of Structures. New York: John Wiley & Sons, Inc., 1956.

63. Plantema, F. J. Sandwich Construction. New York: John Wiley & Sons, Inc., 1966.

64. Kreyszig, E. Advanced Engineering Mathematics. New York: John Wiley and Sons, Inc., 1962.

65. Jahnke, E. and Emde, F. Tables of Functions. 4th edition, New York: Dover Publications, 1945.

66. Boller, K. H. and Norris, C. B. "Effect of Shear Strength on Maximum Loads of Sandwich Columns," Report No. 1815, U. S. Forest Products Laboratory, Madison, Wis., 1950 (reviewed and reaffirmed in 1960).

67. "Conducting Strength Tests of Panels for Building Construction," Standard E 72-61, American Society for Testing and Materials, 1961.

68. Eringen, A. C. "Ripple-Type Buckling of Sandwich Columns," Journal of the Aeronautical Sciences, Vol. 19, No. 6, June, 1952, pp. 409-417.

69. Reissner, E. "The Effect of Transverse Shear Deformation on the Bending of Elastic Plates," Journal of Applied Mechanics 12, Transactions of the American Society of Mechanical Engineers 67, 1945, A 69-A77.

70. Timoshenko, S. P. Vibration Problems in Engineering. Third edition, Princeton, N. J.: D. Van Nostrand Company, Inc., 1955.

APPENDIX A

DEVELOPMENT OF SHEAR STRAIN ENERGY FORM FACTOR

APPENDIX A

DEVELOPMENT OF SHEAR STRAIN FORM FACTOR

By arbitrarily choosing an axis system one may depict a shear deformed element as shown in the following sketch.

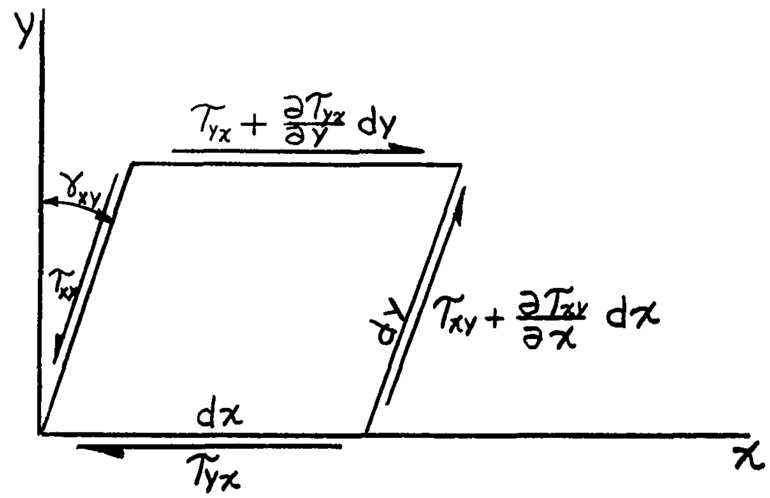

Shear stresses are also indicated in this sketch. From equilibrium considerations

$$\tau_{xy} = \tau_{yx} \tag{A-1}$$

In deforming the element as shown, the shear force on the positive y face of the element does work in moving through the distance γ_{xy} dy. This average shear force on the differential element has a magnitude of

$$dS = \frac{1}{2} (\tau_{yx} + \frac{\partial \tau_{yx}}{\partial y} dy) (dx) (dz) \qquad (A-2)$$

noting that the positive z axis would come outward from the sketch. The work done by the shearing force dS is

$$dW = \frac{1}{2}\left[\tau_{xy} \, dx \, dz + \frac{\partial \tau_{xy}}{\partial y} dy \, (dx \, dz)\right] (\gamma_{xy} \, dy) \qquad (A-3)$$

Neglecting the second term on the right as a higher order term,

$$dW = \frac{1}{2} \tau_{xy} \gamma_{xy} \, dx \, dy \, dz \qquad (A-4)$$

From Hooke's Law,

$$\gamma_{xy} = \frac{1}{2} \tau_{xy} \qquad (A-5)$$

$$G = \frac{E}{2(1 + \nu)} \qquad (A-6)$$

where G is the shear modulus, E is Young's modulus, and ν is Poisson's ratio.

Next, internal strain energy is equated to external work. That is,

$$d U = d W \qquad (A-7)$$

Substituting equations (A-4) and (A-5) into (A-7),

$$d U = \frac{1}{2G} \tau_{xy}^2 \, dx \, dy \, dz \qquad (A-8)$$

Integrating over the entire beam, total shear strain energy is

$$U = \iiint \frac{1}{2G} \tau_{xy}^2 \, dx \, dy \, dz \qquad (A-9)$$

Equation (A-9) may be integrated readily if the mathematical description of the shear stress distribution is known. A solution is presented for the simple parabolic shear stress distribution typical in rectangular beams.

It is assumed that a parabolic distribution of shear in the x-y plane (constant along z) is symmetrical about the mid depth. Local transverse shear force, V_x, can then be written as

$$V_x = \int_{-d_1}^{d_1} \tau_{xy} \, b \, dy \tag{A-10}$$

where d_1 is one-half the beam depth, and b is the local beam width. From the shear distribution assumption,

$$\tau_{xy} = (\tau_{xy})_{max} \left(1 - \frac{y^2}{d_1^2}\right) \tag{A-11}$$

Substituting (A-11) into (A-10) and integrating,

$$V_x = (\tau_{xy})_{max} \left(A_t - \frac{I_o}{d_1}\right) \tag{A-12}$$

where A_t is the total cross-sectional area and I_o is the moment of inertia of the cross-section about a mid depth lateral axis.

Rearranging equation (A-12)

$$(\tau_{xy})_{max} = \frac{V_x \, d_1^2}{d_1^2 \, A_t - I_o} \tag{A-13}$$

The shear strain may then be determined by substituting (A-13) into (A-11) and reducing to obtain

$$\tau_{xy} = V_x \left[\frac{d_1^2 - y^2}{d_1^2 A_t - I_o} \right] \tag{A-14}$$

Next the shear strain energy (A-9) may be rewritten as

$$U = \int_o^{\ell} \int_{-d_1}^{d_1} \frac{V_x^2}{2 G B^2} (d_1^4 - 2d_1^2 y^2 + y^4) b \, dy \, dx \tag{A-15}$$

where

$B = d_1 A_t - I_o$

ℓ = beam length

Finally, the shear strain energy from (A-15) may be written in an abbreviated form where $\underline{C_F}$ is defined as the shear strain form factor. That is,

$$U = \int_o^{\ell} \frac{C_F V_x^2}{2 A_t G} dx \tag{A-16}$$

$$C_F = \frac{A_t(d_1^4 A_t - 2d_1^2 I_o + \int_{-d_1}^{d_1} y^4 b \, dy)}{(d_1^2 A_t - I_o)^2} \tag{A-17}$$

Equation (A-17) gives a $\underline{C_F}$ value of 1.20 for a rectangular section. This is in agreement with the transverse shear coefficient recommended by Reissner[69] and Timoshenko.[70]

APPENDIX B

TABULATION OF RAW DATA FROM CORE SHEAR TESTS

TABLE B-1

RAW CORE SHEAR DATA

Shear Test No.	Foam I.D.	Beam Length (in)	Cross Section Area (in^2)	Moment of Inertia (in^4)	Load P (lbs)	End Deflection (10^{-3} in)
1	Dylite	1.08	2.00	0.67	0	0
					5.8	25.5
					9.3	40.0
					11.1	46.5
					13.5	65.0
					18.3	-
2	Dylite	1.08	1.93	0.63	0	0
					6.4	17.5
					10.6	42.0
					13.8	82.0+
3	Dylite	1.00	2.14	0.70	0	0
					3.4	8.0
					5.0	12.5
					6.6	19.5
					7.7	28.0
					9.5	40.5
					11.4	55.5
					13.8	88.0+
4	Dorvon	0.98	2.97	0.97	0	0
					6.6	5.2
					9.0	9.1
					12.6	14.7
					16.3	19.3
					21.9	27.0
					24.3	32.9
					28.8	41.5
					31.2	51.0
					33.2	-
5	Dorvon	0.95	2.87	0.90	0	0
					6.3	5.8
					10.8	11.0
					15.9	19.3
					19.0	24.8
					22.2	31.8

TABLE B-1--(Continued)

Shear Test No.	Foam I.D.	Beam Length (in)	Cross Section Area (in^2)	Moment of Inertia (in^4)	Load P (lbs)	End Deflection (10^{-3} in)
5	(continued)				25.4	42.9
					28.8	58.0
					34.1	-
6	Dorvon	0.95	2.87	0.91	0	0
					5.5	7.2
					8.2	13.7
					13.2	22.3
					16.9	29.5
					19.8	38.2
					23.0	51.9+
7	Dorvon	1.00	2.85	0.90	0	0
					6.6	4.7
					10.6	10.2
					15.3	17.1
					18.8	23.7
					22.5	43.0
					25.9	71.6
					28.1	93.0
					31.7	-
8	Styro FR	1.00	2.00	0.67	0	0
					5.3	4.5
					10.6	10.5
					15.1	16.5
9	Styro FR	1.00	2.00	0.67	0	0
					5.3	8.5
					8.5	13.0
					10.9	16.5
					13.5	20.0
					15.4	23.5
					17.2	28.5
					17.8	-
10	Styro FR	1.00	2.00	0.67	0	0
					5.3	5.5
					10.9	12.5
					13.0	15.0
					15.4	19.0
					17.5	21.0
					19.6	24.0

TABLE B-1--(Continued)

Shear Test No.	Foam I. D.	Beam Length (in)	Cross Section Area (in^2)	Moment of Inertia (in^4)	Load P (lbs)	End Deflection (10^{-3} in)
11	Styro RM	1.00	2.00	0.67	0	0
					11.3	7.5
					18.8	19.0
12	Styro RM	1.00	2.00	0.67	0	0
					6.1	3.5
					10.6	7.0
					15.6	11.5
					20.4	15.5
					24.6	20.0
13	Styro RM	1.00	2.00	0.67	0	0
					6.1	2.5
					10.9	5.5
					15.9	10.0
					18.6	12.0
					20.9	14.5
					23.6	18.0
					24.7	-
14	Styro HD	1.00	2.00	0.67	0	0
					5.8	3.5
					10.3	8.5
					15.1	13.5
					18.8	17.5
					24.6	23.5
					28.9	28.0
					33.4	33.5
					37.6	39.0
					38.7	41.0
15	Styro HD	1.00	2.00	0.67	0	0
					10.1	4.0
					15.4	9.5
					19.4	12.5
					23.6	16.0
					28.6	20.5
					32.1	24.5
					35.8	28.0
					38.4	31.0
					40.5	-

TABLE B-1--(Continued)

Shear Test No.	Foam I.D.	Beam Length (in)	Cross Section Area (in^2)	Moment of Inertia (in^4)	Load P (lbs)	End Deflection (10^{-3} in)
16	Styro HD	1.00	2.00	0.67	0	0
					10.6	8.0
					15.9	13.0
					20.7	18.0
					25.4	27.0
					29.7	31.5
					34.2	36.5
					37.9	41.5

67

413